SCUOLA DI DOTTORATO
UNIVERSITÀ DEGLI STUDI DI MILANO-BICOCCA

School of Medicine and Surgery

PhD program in Neuroscience, Cycle XXXIV

Curriculum in Experimental Neuroscience

Preliminary characterization of CR13626, a novel tyrosine kinase inhibitor for the treatment of glioblastoma.

Surname: Galimberti Name: Chiara

Registration number 067954

Tutor: Dr. Caselli Gianfranco

Coordinator: Prof. Moresco Rosa Maria

ACADEMIC YEAR 2020/2021

Table of contents

1. List of abbreviations

2-HG	2-hydroxyglutaric acid
ABC	ATP binding cassette
ADCs	Antibody drug conjugates
AGC	Protein A/G/C-related
AP-1	Activator protein 1
AREG	Amphiregulin
ATCC	American type culture collection
ATRX	Alpha thalassemia/mental retardation syndrome X-linked
BBB	Blood brain barrier
BBTB	Blood brain tumor barrier
BCRP	Breast cancer resistance protein
BDNF	Brain-derived neurotrophic factor
BLI	Bioluminescence
BRAF	v-raf murine sarcoma viral oncogene homolog B1
BSA	Bovine serum albumin
BTC	Betacellulin
CAMK	Ca2+/calmodulin-dependent kinases
CAR-T	Chimeric antigen receptor T
CDK4	Cyclin dependent kinase 4
CDKN2A/2B	Cyclin dependent kinase inhibitor 2A and 2B
cIMPACT-NOW	the Consortium to Inform Molecular and Practical Approaches to CNS Tumor Taxonomy — Not Officially WHO
CK1	Casein kinases
CL	Classical GBM subgroup
CMGC	CDK/MAPK/GSK-3/CDK-like kinases
CNS	Central nervous system
CSCs	Cancer stem cells
CSF1	Colony-stimulating factor1
CTK	**I**ntracellular tyrosine kinases
CTLA-4	Cytotoxic T lymphocyte antigen 4

CTLs	Cytotoxic T-cell lymphocytes
DC	Dendritic cells
DDRs	Discoidin domain receptors
DMEM	Dulbecco's Modified Eagle's Medium
EANO	European Association of Neuro- Oncology
ECACC	European collection of authenticated cell cultures
ECGS	Endothelial cell growth supplement
ECM	Extracellular matrix
EGF	Epidermal growth factor
EGFR	Epidermal growth factor receptor
EGFRvIII	Epidermal growth factor receptor variant III
EMA	European Medicines Agency
EPCs	Endothelial progenitor cells
EPGN	Epigen
Eph	Erythropoietin-producing hepatocellular
EREG	Epiregulin
F12K	Ham's F-12K (Kaighn's) Medium
FasL	Fas ligand
FBS	Fetal bovine serum
FDA	Food and Drug Administration
FGF	Fibroblast growth factor
FLT3	Fms-like tyrosine kinase 3
G-CIMP	Glioma-CpG island methylator phenotype
GAPs	GTPase activating proteins
GBM	Glioblastoma multiforme
GDNF	Glial cell line-derived neurotrophic factor
GEF	Guanine-nucleotide exchange factor
GI50	Growth inhibition 50
GPCRs	G-protein-coupled receptors
GSK3β	Glycogen synthase kinase 3-β

HB-EGF	Heparin-binding EGF-like growth factor
HEK-293	Human embryonic kidney 293
HIF-1α	Hypoxia-inducible factor 1-alpha
HGF	Hepatocyte growth factor
HGFR	Hepatocyte growth factor receptor
HPLC	High-performance liquid chromatography
HPMC	Hydroxypropyl methylcellulose
HRP	Horseradish peroxidase
HSCs	Hematopoietic stem cells
HUVEC-C	Human umbilical vein endothelial cells
IC50	Half maximal inhibitory concentration
ICIs	Immune checkpoint inhibitors
IDH1/2	Isocitrate dehydrogenase 1 and 2
IDO	Indoleamine 2,3-dioxygenase
IFP	Interstitial fluid pressure
IGF	Insulin-like growth factor
IGF1R	Insulin-like growth factor 1 receptor
IL-1	Interleukin-1
IL-6	Interleukin-6
IL-8	Interleukin-8
IL-10	Interleukin-10
INSR	Insulin receptor
INSRR	Insulin receptor-related receptor
IP_3R	Inositol 1,4,5-trisphosphate receptor
JAK	Janus kinase
LC-MS/MS	Liquid chromatography-tandem mass spectrometry
MAPK	Mitogen-activated protein kinase
MDM2	Murine double minute 2
MDRPs	Multidrug resistance proteins
MDSCs	Myeloid-derived suppressor cells

ME	Mesenchymal GBM subgroup
MEM	Minimum essential media
MGMT	O^6-methylguanine-DNA methyltransferase
MMP2	Matrix metalloprotease 2
M-PER	Mammalian protein extraction reagent
MSCs	Mesenchymal stem cells
mTORC2	Mammalian target of rapamycin complex 2
MRI	Magnetic resonance imaging
NE	Neural GBM subgroup
NF1	Neurofibromin 1
NGF	Nerve growth factor
NK	Natural killer
nGBM	Newly diagnosed GBM
NTRK	Neurotrophic tropomyosin receptor kinase
OS	Overall survival
PBS	Phosphate buffered saline
PBST	Phosphate buffered saline with 0.05% (v/v) Tween20
P-gP	P-glycoprotein
PD-1	Programmed death 1
PD-L1	Programmed death-ligand 1
PET	Positron emission tomography
PDGFα	Platelet-derived growth factor α
PDGFRα/β	Platelet-derived growth factor receptor α/β
PDK1	Phosphoinositide-dependent protein kinase-1
PDL	Poly-D-lysine hydrobromide
PFS	Progression free survival
PFS6	6-month progression free survival
PI3K	Phosphatidylinositol 3-kinase
PIGF	Placenta growth factor
PIP2	Phosphatidylinositol 4,5-bisphosphate

PIP3	Phosphatidylinositol (3,4,5)-trisphosphate
PMA	Phorbol 12-myristate 13-acetate
PN	Proneural GBM subgroup
PTB	Phosphotyrosine binding
PTEN	Tensin homolog
PTPS	Protein tyrosine phosphatases
PVDF	Polyvinylidene fluoride
RB1	RB Transcriptional Corepressor 1
rGBM	Recurrent GBM
RGC	Receptor guanylate cyclases
RT	Radiotherapy
RTKs	Receptor tyrosine kinases
SCF	Stem cell factor
SD	Standard deviation
SEM	Standard error of the mean
SFKs	Src-family kinases
SH2	Src homology 2
SHP2	SRC homology 2 domain PTP
SNHG12	Small nuclear RNA host gene 12
SoC	Standard of care
SOS	Son of Sevenless
SOX2	SRY-Box transcription factor 2
SPECT	Single-photon emission computed tomography
STAT3	Signal transducers and activators of transcription 3
STE	Sterile serine/threonine kinases
TAMs	Tumor associated macrophages
TERT	Telomerase reverse transcriptase
TCGA	The Cancer Genome Atlas
TSAD	T cell-specific adaptor
TIM-3	T cell immunoglobulin mucin 3

TGFα/β	Transforming growth factor α/β
TKIs	Tyrosine kinase inhibitor
TKL	Tyrosine kinase-like
TMB	3,3′,5,5′-tetramethylbenzidine
TME	Tumor microenvironment
TMZ	Temozolomide
Treg	Regulatory T-cells
Trk	Tropomyosin receptor kinase
TTFs	Tumor Treating Fields
VCAM-1	Vasculature cell adhesion molecule-1
VEGF	Vascular endothelial growth factor
VEGFR2	Vascular endothelial growth factor receptor 2
VEPTP	Vascular endothelial PTP
VRAP	VEGFR2-associated protein
WHO	World Health Organization

2. Abstract

Glioblastoma multiforme (GBM) is the most malignant type of primary brain cancer. To date, there is no cure for glioblastoma, and the prognosis and survival rates remain poor. The first-line treatment options are limited, and recurrence of the tumor is almost universal. Thus, the unmet medical needs for GBM are extremely high and many efforts are ongoing to find a more effective therapy that provides survival benefit.

The high grades of cellular proliferation, invasiveness, cellular atypia, and angiogenesis of the tumor contribute to its poor prognosis and depend largely upon the activity of the receptor tyrosine kinases (RTKs), such as EGFR (epidermal growth factor receptor) and VEGFR2 (vascular endothelial growth factor receptor 2). Upon activation of the receptors, members of Src-family kinases (SFKs) are recruited and involved in the intracellular signal transmission, contributing to malignant transformation and tumor progression. Thus, RTKs, their ligands and intracellular effectors still represent promising targets for GBM treatment.

CR13626 has emerged as a novel tyrosine kinase inhibitor with a good tropism for the brain and the ability to inhibit EGFR, VEGR2, Fyn, Yes, Lck, HGK and RET kinases relevant for GBM development. In addition, CR13626 resulted to be not a substrate of multidrug transporters involved in tumor resistance. Thus, the aim of my project is to characterize the activity of the compound, both in vitro and in vivo, to investigate the potential of CR13626 for glioblastoma therapy.

To this purpose, I firstly investigated the ability of CR13626 to inhibit the ligand-induced activation of EGFR and VEGFR2 receptors in U87MG glioblastoma cells and HUVEC-C cells, respectively, through western blot experiments. Indeed, upon activation of tyrosine kinase receptors, several residues located in the intracellular domain of the receptors were phosphorylated, leading to the recruitment of downstream effectors that mediate signal into the cell and activate specific biological pathways. To better define the potency of CR13626 on Fyn kinase in a cellular model, I exploited the Fyn-mediated phosphorylation levels of Tau in Fyn/Tau co-transfected HEK-293 cells through a customized indirect-ELISA.

Because of VEGFR2 is largely involved in promoting the angiogenesis process, which contributes to tumor sustenance, I evaluated the ability of CR13626 to reduce the formation of new vessel-like structures in a HUVEC-C tube formation assay, as an indication of its antiangiogenic properties.

Then I verified the effect of CR13626 on cellular proliferation in different 2D human glioblastoma cell lines such as U87MG, U373, U87MG vIII and T98G, each harboring some of the genetic alterations/mutations present in GBM tumor cells. I also evaluated the activity of CR13626 on HEK-

293 cells to assess the effect of the compound on a non-tumoral human cell line and to exclude a potential toxicity on healthy cells.

Since 3D cell spheroids are more representative of the complexity of tumor environment with respect to 2D cultures, they constitute a more reliable model to assess cellular response to a drug treatment; for this reason, I also investigated the efficacy of CR13626 in reducing cellular proliferation in U87MG glioblastoma cells cultured as 3D spheroids.

Finally, an appropriate model to assess the in vivo antitumor activity of CR13626 has been selected. The orthotopic xenograft mouse model of GBM based on the injection of U87MG-Luciferase cells (U87MG-Luc) in nude mice was chosen and the experiment was performed at Accelera Srl, Nerviano, Italy. Animals were orally treated with CR13626 (50 mg/kg/daily) or vehicle for 10 days, starting on day 9 post-implantation. Tumor progression was evaluated through the measurement of bioluminescence (BLI) at the end of dosing (day 19) and during follow-up (days 26 and 33). The survival of animals was also evaluated. In addition, the plasma and brain concentrations of CR13626 in tumor-bearing mice were determined in a satellite group of animals orally treated for 5 days with CR13626 (50 mg/kg/daily).

My results showed that CR13626 was able to inhibit the ligand-induced receptor activation in cells by reducing the phosphorylation levels at specific residues. In human GBM U87MG cell line, CR13626 inhibited the EGF-induced EGFR activation at residue Y1068 in a concentration dependent fashion, with an IC_{50} value of 3 µM. In HUVEC-C cells, CR13626 inhibited the VEGF-induced VEGFR2 activation at residue Y1175 in a concentration dependent manner, reaching a total signal inhibition at 1 µM. In the same samples, CR13626 also inhibited the phosphorylation of the downstream VEGFR2 effectors Fyn/Src, suggesting a potential stronger impact on the intracellular signal transmission upon receptor activation. The evidence of the inhibitory activity of CR13626 on Fyn kinase was confirmed in Fyn/Tau co-transfected HEK-293 cells, since CR13626 was able to inhibit the Fyn-mediated phosphorylation of Tau at Y18 residue, with an IC_{50} value of 401 nM.

The HUVEC-C tube formation assay showed that CR13626 decreased the PMA-induced tube formation in a dose-dependent manner, indicating a potential effect of the compound on the angiogenic process.

CR13626 reduced the proliferation of the U87MG human GBM cells reaching more than 50% decrease of the viability of cells at 1 µM concentration and at 24 hours of incubation. Conversely, when CR13626 has been tested in the same conditions on a non-tumoral human HEK-293 cell line,

it did not show any effects on cellular proliferation. Moreover, in U87MG human GBM cells CR13626 showed a higher efficacy than erlotinib (EGFR inhibitor), while saracatinib (Src family inhibitor) resulted inactive after 6-7 days of treatment.

In addition to U87MG cells, CR13626 reduced the proliferation of U373, U87MG vIII and T98G cells, being more effective than comparators. The effect of CR13626 resulted still present after 7 days of treatment.

CR13626 decreased the proliferation of U87MG glioblastoma cells cultured as 3D spheroids in a dose-dependent fashion, showing an GI_{50} value of 4.5 µM. In the same culture conditions, the standard of care temozolomide (TMZ) was also able to reduce U87MG spheroids proliferation, even if at higher concentrations with respect to CR13626.

In the orthotopic xenograft mouse model of GBM, the oral treatment with CR13626 50 mg/kg/daily for 10 days led to a time-dependent reduction of tumor growth, reaching 60% on the last BLI evaluation, 33 days post-implantation (i.e., 15 days after the end of dosing). Tumor growth inhibition translated into an increase of 25% of the median survival time of animals treated with CR13626 compared to the vehicle group ($p<0.05$). The observed antitumor effects agreed with the exposure of tumor-bearing mice to CR13626, which was above the TKs in-vitro IC_{50} values.

The brain tropism of CR13626 was confirmed in the satellite group of tumor-bearing mice. Indeed, upon the oral treatment of CR13626 50 mg/kg/daily for 5 days, CR13626 preferentially accumulates in the right brain hemisphere, where the U87MG-Luc cells were injected, and tumor developed. This evidence confirmed the ability of CR13626 to cross the blood brain barrier (BBB) and penetrate the brain, suggesting the potential of CR13626 to reach the tumor and remain at the tumor site.

In conclusion, the combined abilities of CR13626 to inhibit the activity of tyrosine kinases (TKs) involved in GBM development, to cross the BBB without being a substrate of the multidrug transporters involved in tumor resistance, and to reduce tumor growth in-vivo leading to increased survival, warrant its further development as a drug candidate in GBM.

3. Introduction

GBM: disease definition

Glioblastoma multiforme (GBM) is the most malignant type of primary brain cancer. It represents half of all new diagnoses of gliomas, the most common tumors of the central nervous system (CNS) [Paolillo et al., 2018; Anjum et al., 2017; Ostrom et al., 2020].

Gliomas originate from the non-neuronal or glial portion of the brain, namely astrocytes, oligodendroglial, microglial, or ependymal cells [Tilak et al., 2021].

According to the 2021 fifth edition of the WHO (World Health Organization) Classification of Tumors of the Central Nervous System (WHO CNS5), GBM belongs to the "adult-type diffuse gliomas" family, together with the "astrocytoma, IDH-mutant" and "oligodendroglioma, IDH-mutant and 1p/19q-codeleted" tumor types and is defined as "Glioblastoma, IDH-wildtype". Specifically, GBM should be diagnosed "in the setting of an IDH-wildtype diffuse and astrocytic glioma in adults if there is microvascular proliferation or necrosis or TERT (telomerase reverse transcriptase) promoter mutation or EGFR gene amplification or +7/−10 chromosome copy number changes" and is associated to the highest WHO grade (grade 4) [Louis et al., 2021].

As implied by the term "multiforme", GBMs are characterized by high intratumoral heterogeneity due to the sequential accumulation of genetic alterations and abnormal regulation of signaling pathways that result in malignant transformation. The high mitotic activity, the microvascular proliferation, the resistance to apoptosis, the necrosis, the invasion into adjacent brain tissue, and the presence of cancer stem cells that are the most responsible of tumor recurrence, are all features rendering GBM as one of the most aggressive and difficult-to-treat tumors [Tilak et al., 2021].

GBM classification over the years and patient segmentation

Historically, GBMs were categorized into two groups, "primary" and "secondary", based on clinical presentation (if arising de novo or progressing from lower grade gliomas, respectively). Primary GBM had been described to account the 90% of diagnosed cases and to occur in older patients (mean age 60 years), whereas secondary GBM had been reported in younger cohort (mean age 45 years) [Kleihues et al., 1999]. Primary and secondary GBMs were not distinguishable histologically but some differences in genetic and epigenetic profiles were highlighted. Primary GBMs were associated with amplification or mutations of epidermal growth factor receptor (EGFR), mutations

of phosphatase and tensin homolog (PTEN), amplification of murine double minute 2 (MDM2, encoding for an inhibitor of p53), and homozygous deletions of cyclin dependent kinase inhibitor 2A (CDKN2A). Conversely, secondary GBMs were associated with the overexpression of platelet-derived growth factor α (PDGFα), mutations of p53 and isocitrate dehydrogenase 1 and 2 (IDH1/2) and inactivation of the retinoblastoma gene (RB Transcriptional Corepressor 1, RB1) [Kleihues et al., 1999; Alifieris et al., 2015]. Although widely used over the years, the division of glioblastomas into primary and secondary tumors is not more utilized, since a more precise tumor categorization has been provided thanks to the development of technology and classification algorithms.

Before publication of the revised WHO classification of tumors of the CNS in 2016 [Louis et al., 2016], gliomas were classified according to the histological criteria defined in the 2007 WHO classification [Louis et al., 2007]. Moreover, a histological grade was assigned to each tumor based on the degree of anaplasia, from WHO grade I to IV, where grade I was assigned to a slow-growing lesion and was associated with a favorable prognosis and grade IV indicated a highly malignant tumor characterized by a dismal prognosis. Despite of these categorization, a considerable interobserver variability was observed, particularly in the context of diffusely infiltrating gliomas, posing challenges to GBM diagnosis, prognosis, and treatment. The advances in molecular understanding of gliomas showed that molecular classification of gliomas better correlates with clinical outcome than histological classification. Thus, an “integrated diagnosis” model for disease categorization, based on a multilayered approach incorporating both histological and molecular information, was introduced by the 2016 WHO classification of tumors of the CNS, aimed at improving patient clinical management and clinical trial design [Reifenberger et al., 2017].

The 2016 WHO classification of gliomas incorporated IDH1/2 mutations, 1p/19q codeletion, histone H3-K27M mutation and C11orf95–RELA fusion as diagnostic biomarkers defining distinct glioma entities [Louis et al., 2016; Reifenberger et al., 2017]. Other biomarkers were taken into consideration for additional diagnostic information, including loss of nuclear ATRX expression (a transcriptional regulator involved in chromatin remodeling and telomere length regulation), TERT promoter mutation (leading to an aberrant expression of telomerase reverse transcriptase), BRAF mutation or fusion, and histone H3-G34 mutation [Reifenberger et al., 2017]. Regarding the IDH gene mutation status, three main groups had been defined: IDH-wild type, IDH-mutant, and not-otherwise specified (NOS, if the full IDH evaluation cannot be assessed) [Louis et al., 2016]. IDH1/2 mutations had been identified as strong positive prognostic factors, and IDH-mutant glioblastoma patients showed greater likelihood of long-term survival than IDH-wild type glioblastoma patients

[Parsons et al., 2008; Reifenberger et al., 2017]. According to the current WHO CNS5 classification, all IDH-mutant diffuse astrocytic tumors are considered a single type (Astrocytoma, IDH-mutant) and glioblastoma is not defined as IDH1/2-mutated tumor anymore, as described below [Louis et al., 2021].

Given the rapid advancement in the biological sciences, the Consortium to Inform Molecular and Practical Approaches to CNS Tumor Taxonomy — Not Officially WHO (cIMPACT-NOW) was created in 2017 to convey timely updates and provide recommendations for the further WHO publications [Rushing EJ, 2021]. Thus, the latest WHO CNS5 builds on the previous 2016 fourth edition, on the developments in the field following the previous classification, and on the recommendations of cIMPACT-NOW, and provides a new integrated histological and molecular classification system that enables a more accurate classification of CNS neoplasms. In the WHO CNS5, classification names have been simplified as much as possible, and two specific aspects of CNS tumor grading have changed: Arabic numerals have been employed (rather than Roman numerals) and neoplasms have been graded within types (rather than across different tumor types) [Louis et al., 2021]. The figures below are intended to provide a quick overview focused on gliomas of the WHO CNS5 classification of CNS tumors respect to the previous fourth edition (Figure 1A-B).

As displayed in Figure 1B, according to the current WHO CNS5 classification system, the gliomas, glioneuronal, and neuronal tumors are divided into 6 different families: (1) adult-type diffuse gliomas, that primarily occur in adults; (2) pediatric-type diffuse low-grade gliomas, which occur primarily in children; (3) pediatric-type diffuse high-grade gliomas; (4) circumscribed astrocytic gliomas; (5) glioneuronal and neuronal tumors (a diverse group of tumors, featuring neuronal differentiation); and (6) ependymomas [Louis et al., 2021]. Each family further contains different types and subtypes of tumors, which are defined by a combination of histological features, molecular alterations of key genes and proteins and specific tumor grading. With the change to grading within tumor type, terms like “anaplastic” are not included anymore (Figure 1A-B). By combining histological and molecular evidence, molecular parameters sometimes add value to histological findings in assigning a grade, allowing for example the designation of glioblastoma, IDH-wildtype CNS WHO grade 4 even in cases that result histologically of lower grades. Respect to the fourth edition CNS classification from 2016, where the common diffuse gliomas of adults were divided into 15 entities, WHO CNS5 includes only 3 types: “Astrocytoma, IDH-mutant”, “Oligodendroglioma, IDH-mutant and 1p/19q-codeleted”, and “Glioblastoma, IDH-wildtype”, as already mentioned above and displayed in Figure 1A-B [Louis et al., 2021].

A

Tumour classification	WHO grade
Diffuse astrocytic and oligodendroglial tumours	
Diffuse astrocytoma, IDH-mutant • Gemistocytic astrocytoma, IDH-mutant	II
Diffuse astrocytoma, IDH-wild-type*	II
Diffuse astrocytoma, NOS	II
Anaplastic astrocytoma, IDH-mutant	III
Anaplastic astrocytoma, IDH-wild-type*	III
Anaplastic astrocytoma, NOS	III
Glioblastoma, IDH-wild-type • Giant-cell glioblastoma • Gliosarcoma • Epithelioid glioblastoma*	IV
Glioblastoma, IDH-mutant	IV
Glioblastoma, NOS	IV
Diffuse midline glioma, H3-K27M-mutant	IV
Oligodendroglioma, IDH-mutant and 1p/19q-codeleted	II
Oligodendroglioma, NOS	II
Anaplastic oligodendroglioma, IDH-mutant and 1p/19q-codeleted	III
Anaplastic oligodendroglioma, NOS	III
Oligoastrocytoma, NOS†	II
Anaplastic oligoastrocytoma, NOS†	III
Other astrocytic tumours	
Pilocytic astrocytoma • Pilomyxoid astrocytoma§	I
Subependymal giant-cell astrocytoma	I
Pleomorphic xanthoastrocytoma	II
Anaplastic pleomorphic xanthoastrocytoma	III
Ependymal tumours	
Subependymoma	I
Myxopapillary ependymoma	I
Ependymoma • Clear-cell ependymoma • Papillary ependymoma • Tanicytic ependymoma	II
Ependymoma, *RELA*-fusion-positive	II or III
Anaplastic ependymoma	III
Other gliomas	
Chordoid glioma of the third ventricle	II
Angiocentric glioma	I
Astroblastoma	–

B

World Health Organization Classification of Tumors of the Central Nervous System, fifth edition
Gliomas, glioneuronal tumors, and neuronal tumors
Adult-type diffuse gliomas
Astrocytoma, IDH-mutant
Oligodendroglioma, IDH-mutant, and 1p/19q-codeleted
Glioblastoma, IDH-wildtype
Pediatric-type diffuse low-grade gliomas
Diffuse astrocytoma, *MYB*- or *MYBL1*-altered
Angiocentric glioma
Polymorphous low-grade neuroepithelial tumor of the young
Diffuse low-grade glioma, MAPK pathway-altered
Pediatric-type diffuse high-grade gliomas
Diffuse midline glioma, H3 K27-altered
Diffuse hemispheric glioma, H3 G34-mutant
Diffuse pediatric-type high-grade glioma, H3-wildtype and IDH-wildtype
Infant-type hemispheric glioma
Circumscribed astrocytic gliomas
Pilocytic astrocytoma
High-grade astrocytoma with piloid features
Pleomorphic xanthoastrocytoma
Subependymal giant cell astrocytoma
Chordoid glioma
Astroblastoma, *MN1*-altered
Glioneuronal and neuronal tumors
Ganglioglioma
Desmoplastic infantile ganglioglioma / desmoplastic infantile astrocytoma
Dysembryoplastic neuroepithelial tumor
Diffuse glioneuronal tumor with oligodendroglioma-like features and nuclear clusters
Papillary glioneuronal tumor
Rosette-forming glioneuronal tumor
Myxoid glioneuronal tumor
Diffuse leptomeningeal glioneuronal tumor
Gangliocytoma
Multinodular and vacuolating neuronal tumor
Dysplastic cerebellar gangliocytoma (Lhermitte-Duclos disease)
Central neurocytoma
Extraventricular neurocytoma
Cerebellar liponeurocytoma
Ependymal tumors
Supratentorial ependymoma
Supratentorial ependymoma, *ZFTA* fusion-positive
Supratentorial ependymoma, *YAP1* fusion-positive
Posterior fossa ependymoma
Posterior fossa ependymoma, group PFA
Posterior fossa ependymoma, group PFB
Spinal ependymoma
Spinal ependymoma, *MYCN*-amplified
Myxopapillary ependymoma
Subependymoma

C

CNS WHO Grades of Selected Types	
Astrocytoma, IDH-mutant	2, 3, 4
Oligodendroglioma, IDH-mutant, and 1p/19q-codeleted	2, 3
Glioblastoma, IDH-wildtype	4
Diffuse astrocytoma, *MYB*- or *MYBL1*-altered	1
Polymorphous low-grade neuroepithelial tumor of the young	1
Diffuse hemispheric glioma, H3 G34-mutant	4
Pleomorphic xanthoastrocytoma	2, 3
Multinodular and vacuolating neuronal tumor	1
Supratentorial ependymoma[a]	2, 3
Posterior fossa ependymoma[a]	2, 3
Myxopapillary ependymoma	2
Meningioma	1, 2, 3
Solitary fibrous tumor	1, 2, 3

Figure 1. A comparison between (A) the 2016 WHO classification of gliomas [Reifenberger et al., 2017] and (B) the current WHO classification of the gliomas, glioneuronal, and neuronal tumors. (C) Grades of selected types of tumors, according to the WHO CNS 5 classification. (B-C) are from [Louis et al., 2021].

As mentioned above, IDH1/2 mutations were included in the 2016 WHO classification as diagnostic biomarkers defining distinct glioma entities. According to this classification and in the context of the diffuse astrocytic tumors, “IDH-mutant” specification was assigned to 3 different tumor types (Diffuse astrocytoma, Anaplastic astrocytoma, and Glioblastoma) depending on histological parameters. In the current WHO CNS5 classification, all IDH-mutant diffuse astrocytic tumors are considered a single type (Astrocytoma, IDH-mutant) and are graded as CNS WHO grade 2, 3, or 4 (Figure 1C) [Louis et al., 2021]. Thus, the term “IDH-mutant glioblastoma” is currently discontinued and now is referred to as IDH-mutant astrocytoma, WHO grade 4 (Figure 2). Moreover, the term “glioblastoma” is no longer used in the setting of pediatric-type neoplasm and “oligoastrocytomas” are no longer considered as a distinct glioma subtype [Louis et al., 2021; Weller et al., 2021]. In addition, the use of the terms NOS (not otherwise specified) and NEC (not elsewhere classified) has been clarified: NOS suffix is applied when diagnostic information (histological or molecular) needed for a specific WHO diagnosis is not available, whereas NEC can be applied when there is a mismatch between histological features and molecular results or when diagnostic tests show noncanonical results, suggesting the emerging of a potential new tumor type [Rushing EJ, 2021].

In response to the major changes in diagnostic algorithms, the European Association of Neuro-Oncology (EANO) provides updated guidelines aimed at facilitating the diagnosis and management of adult patients with diffuse gliomas [Weller et al., 2021]. The diagnostic process should follow the updated WHO classification and should take into consideration the recommendations from cIMPACT-NOW. Grading is no longer entirely histological, as illustrated in Figure 2.

According to Figure 2, the presence of IDH1/2 mutations excludes IDH-wildtype glioblastomas and other IDH-wildtype gliomas from the diagnosis. The loss of nuclear ATRX in an IDH-mutant glioma is diagnostic for astrocytic lineage tumors. The 1p/19q codeletion leads to the inactivation of putative tumor suppressor genes and distinguishes “oligodendroglioma, IDH-mutant and 1p/19q co-deleted” from “astrocytoma, IDH-mutant”. The presence of a homozygous deletion of CDKN2A/CDKN2B is a marker of poor outcome and WHO grade 4 disease in IDH-mutant astrocytoma. The TERT promoter mutation, EGFR amplification and/or +7/-10 cytogenetic signature (gain of chromosome 7, which harbors genes encoding for example PDGFα and EGFR, and loss of chromosome 10, which harbors genes including PTEN and MGMT) are all molecular markers of “glioblastoma, IDH-wildtype, WHO grade 4”. Finally, the presence of mutations in histone H3, K27M or G34V is important for the definitions of the “diffuse midline glioma, H3 K27M mutant” and the “diffuse hemispheric glioma, H3.3 G34-mutant” [Weller et al., 2021].

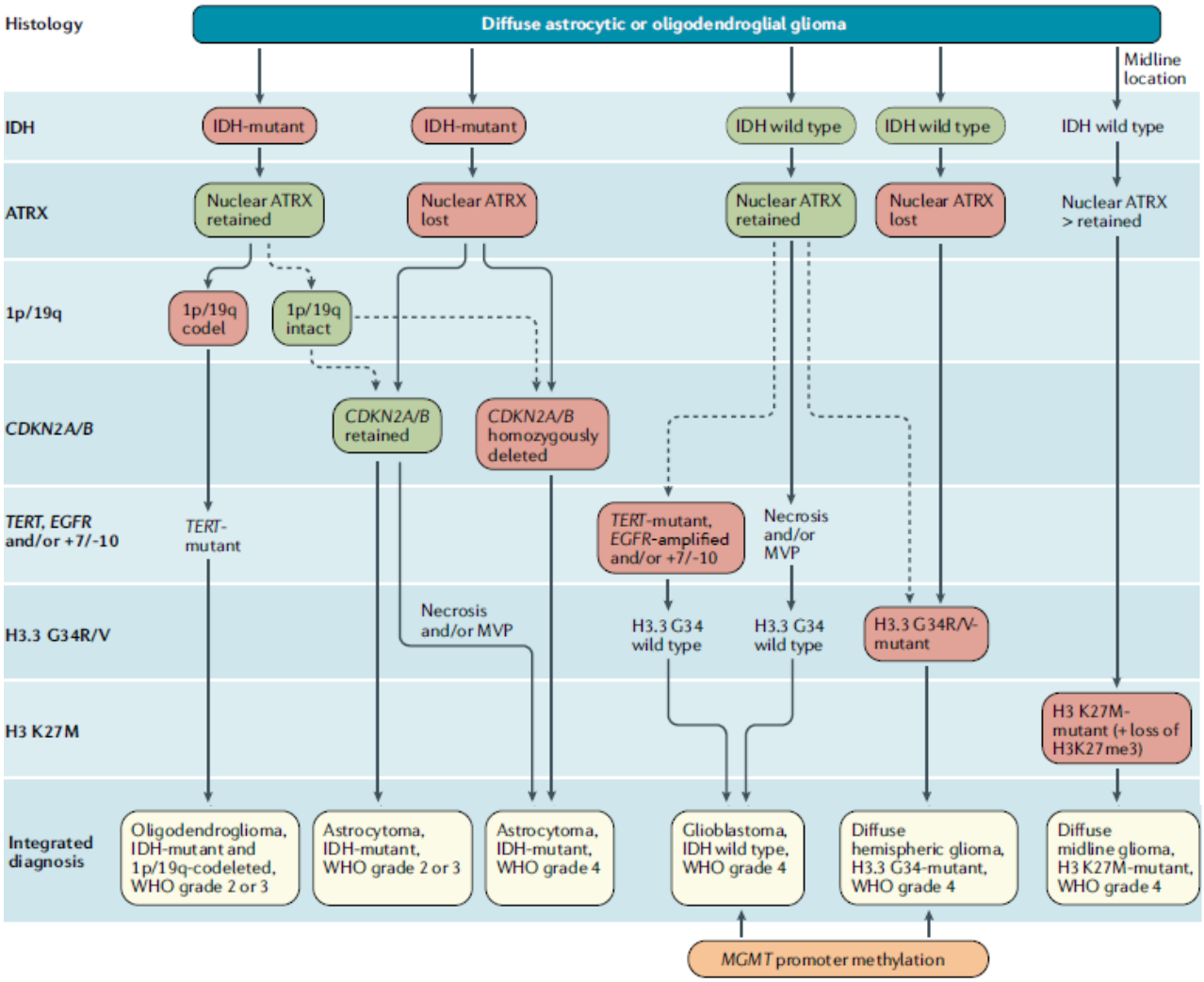

Figure 2. Diagnostic algorithm for the integrated classification of the major diffuse gliomas in adults [Weller et al., 2021].

Thus, as an example, the presence of cyclin-dependent kinase inhibitor 2A/2B (CDKN2A/B) homozygous deletion results in a CNS WHO grade of 4, even in the absence of microvascular proliferation (MVP) or necrosis. Moreover, for IDH-wildtype diffuse astrocytic tumors in adults, the presence of 1 or more of 3 genetic parameters (TERT promoter mutation, EGFR gene amplification, combined gain of entire chromosome 7 and loss of entire chromosome 10 [+7/−10]) is sufficient to assign the highest WHO grade. WHO CNS5 incorporates these 3 genetic parameters as criteria for a diagnosis of “Glioblastoma, IDH-wildtype”. As a result, Glioblastoma, IDH-wildtype should be diagnosed in the setting of an IDH-wildtype diffuse and astrocytic glioma in adults if there is microvascular proliferation or necrosis or TERT promoter mutation or EGFR gene amplification or +7/−10 chromosome copy number changes, Figure 2 [Louis et al., 2021].

Molecular subtypes

Gene expression profiling studies conducted by various groups during the past two decades have helped to further characterize GBM into different subclasses [Tilak et al., 2021]. This classification could help to develop specific targeted treatments and to better design of clinical trials on a molecular basis [El-Khayat et al., 2021].

Through the analysis of 206 GBM tumors, The Cancer Genome Atlas (TCGA) consortium identified common mutations in genes such as TP53 (tumor suppressor), EGFR, IDH1, and PTEN, as well as the frequent and concurrent presence of abnormalities in the p53, RB, and receptor tyrosine kinase (RTKs) pathways [Cancer Genome Atlas Research Network, 2008]. By using the data generated by TCGA the original study conducted by Verhaak et al. classified GBM in four molecular subgroups termed classical (CL), mesenchymal (ME, or MES), proneural (PN) and neural (NE), each displaying distinct gene expression signatures, as shown in Figure 3 [Verhaak et al., 2010].

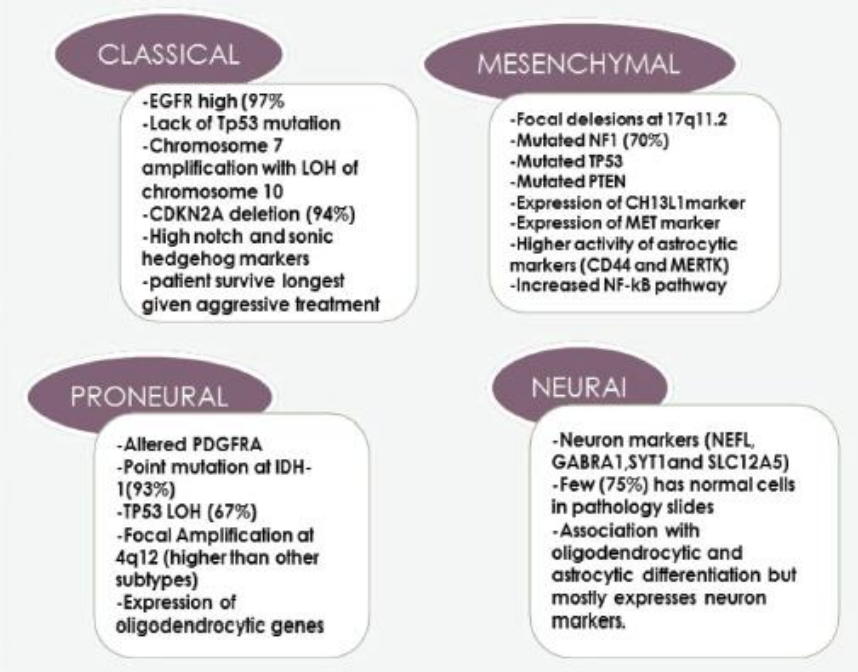

Figure 3. Four subtypes of GBM and the dominant genes and molecular abnormality in each group [El-khayat et al., 2021].

A more recent transcriptomic analysis performed by Wang et al. (2017) on glioma single cells identified a clustering enrichment for only three subtypes, which resulted specific for GBM, and whose genetic signatures overlapping the previously reported classical, mesenchymal and proneural

subtypes. The NE subtype was not confirmed as tumor specific, and the reason of this discrepancy was attributed to a possible contamination with the normal neural tissue, since the NE subtype had previously been related to the tumor margin, where increased normal neural tissue is likely to be detected [Wang et al., 2017]. The expression subtypes were also associated with tumor immune environment, providing potential indications to improve immunotherapy approaches. Indeed, the association of the tumor-intrinsic MES GBM subtype with increased levels of M2 macrophages, which has been demonstrated to be related to NF1 deactivation in glioma cells, suggested as a potential advance for therapies directed against tumor-associated macrophages for this type of tumor. Likewise, the greater activated dendritic cell gene signature found in the CL subtype has been hypothesized to be a potential advantage from dendritic cell vaccines [Wang et al., 2017].

Epigenetic alterations

Since DNA methylation at CpG islands is one of the epigenetic mechanisms that cells use to control gene expression, aberrant DNA methylation states often occur also during tumor transformation and evolution and may reflect the history of cancer cells and their response to the tumor microenvironment (TME) [Kim et al., 2017]. Along with genetic and phenotypic differences in GBM subgroups, ongoing refinements in GBM classification have also revealed distinct epigenetic alterations. Of particular importance is the identification of altered methylation patterns in a cluster of GBM tumors, referred to as the glioma-CpG island methylator phenotype (G-CIMP) [Tilak et al., 2021]. It is noteworthy that such changes are more likely to occur in glioma cancer stem cells of IDH1/2 mutant tumors [Huang et al., 2019]. Indeed, among the consequences of IDH1/2 mutations, the accumulation and secretion of a vast excess of the oncometabolite 2-hydroxyglutaric acid (2-HG) are included. This ultimately leads to the inhibition of the catalytic activity of α-KG-dependent dioxygenase, damaging key steps in histone modification and DNA demethylation, and eventually leading to wide-spread hypermethylation of CpG islands [Huang et al., 2019].

As with IDH mutations, the G-CIMP phenotype is also closely associated with methylation of the O^6-methylguanine-DNA methyltransferase (MGMT) promoter, irrespective of glioma grade [Tilak et al., 2021]. MTMG is a DNA repair enzyme, able to reverse the DNA damage induced by alkylating agents such as temozolomide (TMZ). The methylation of MTMG gene promoter (found in 30-60% of GBM cases) results in gene silencing, thereby leading to an inefficient DNA repair, a more sensitiveness of glioma cells to TMZ treatment and a favorable therapeutic outcome [Alifieris et al., 2015; Hegi et

al., 2005]. Thus, MGMT promoter has been established as a predictive biomarker for benefit from TMZ, although firmly only in newly diagnosed settings, and an overexpression of MGMT has been considered as a determinant in resistance to TMZ therapy [Le Rhun et al., 2019; Tilak et al., 2021].

GBM epidemiology: incidence and risk factors

Datamonitor Healthcare estimates that in 2019 there were 77,000 incident cases of glioblastoma worldwide, and forecasts that the number of incident cases of GBM globally increase by 19.2% between 2019 and 2028 [Informa Pharma Intelligence, 2021]. The incidence of GBM increases steadily with age; the mean age at diagnosis is 64 years, males are approximately 1.7-fold more often affected than females, and it is 2 times more common in whites compared to blacks [Le Rhun et al., 2019; Alifieris et al., 2015].

Etiologically, there are known linked factors associated with an increased risk of developing GBM. The exposure to therapeutic ionizing radiation, and to pesticides and vinyl chloride, as well as working in petroleum refining or synthetic rubber manufacturing facilities have been confirmed as risk factors for GBM [Alifieris et al., 2015; Informa Pharma Intelligence, 2021]. In addition, genetic syndromes such as Turcot syndrome, Li-Fraumeni syndrome, and neurofibromatosis have conclusively been implicated in the development of the disease [Informa Pharma Intelligence, 2021].

GBM symptoms and diagnosis

Clinically, patients with GBM may show generalized symptoms or focal symptoms, depending on the tumor size, and location. Patients with GBM may present with memory loss, headaches, nausea, vomiting, seizures, personality changes and sometimes with motor and neurologic impairments [Alifieris et al., 2015].

Upon presentation of symptoms, magnetic resonance imaging (MRI) is generally used for an initial assessment and the primary diagnosis of GBM typically shows an irregular tumor mass of differing density with surrounding edema [LIoyd, 2017]. Other imaging tests, such as positron emission tomography (PET) and single-photon emission computed tomography (SPECT), can be used to distinguish the cancer cells from normal cells, and a surgical biopsy of affected tissue helps in the

definite diagnosis of GBM [Informa Pharma Intelligence, 2021]. Additional analyses are also performed to identify molecular and genetic alterations that can help in determining patient prognosis and treatment plans [Informa Pharma Intelligence, 2021].

GBM: pathological features

There are several factors contributing to the poor prognosis of GBM. The high grades of cellular proliferation, invasiveness, cellular atypia, and angiogenesis are important features of GBM tumors. In addition, the high intratumoral heterogeneity and the immunosuppressive microenvironment, as well as the presence of cancer stem cells (CSCs), provide to GBM different mechanisms to overcome the activity of therapeutic agents, evade immunosurveillance and promote tumor growth.

Histologically, GBM is characterized by necrotic foci with surrounding cellular pseudopalisades and microvascular hyperplasia [Monteiro et al., 2017]. Pseudopalisades constitute an invasive front created by tumor cells migrating away from a central hypoxic (low oxygenated) region resulted from the increased cell proliferation/tumor growth [Monteiro et al., 2017]. Microvascular hyperplasia occurs in response to hypoxia and is induced by the secretion of proangiogenic factors (e.g., vascular endothelial growth factor, VEGF, and interleukin-8, IL-8,) and the high expression of the hypoxia-inducible factor 1-alpha (HIF-1α) by cells that form pseudopalisades [Monteiro et al., 2017; Gong et al., 2018]. GBM vessels are tortuous, disorganized, highly permeable, and characterized by abnormalities in their endothelial walls due to the lack of pericytes [Monteiro et al., 2017]. The physiological consequences of these vascular abnormalities include spatial heterogeneity in tumor blood flow and oxygenation, and an increase in tumor interstitial fluid pressure, which promotes intratumoral edema, a major cause of morbidity for GBM patients [Clavreul et al., 2019; Monteiro et al., 2017].

GBM treatment

To date, glioblastoma is not curable. Prognosis and survival rates remain poor, with a median patient survival of approximately 15 months from diagnosis and a five-year survival of 5% [Pearson et al., 2017].

According to the current guidelines, the standard of care (SoC) for the first-line treatment consists in the so-called “Stupp regimen”, a multistep treatment including surgery plus radiotherapy with the concurrent and adjuvant alkylating agent TMZ (Temodar, Merck), which acts by methylating guanine residues in DNA, leading to cell death [Stupp et al., 2005; Oronsky et al., 2021]. The EORTC 26981-22981 phase III study of 573 subjects randomized to temozolomide + radiotherapy (n=287) or radiotherapy alone (n=286) demonstrated that temozolomide administered concomitantly with brain radiotherapy (RT), and then as maintenance chemotherapy, significantly improved overall survival (OS) compared with patients receiving radiation therapy alone. Particularly, median survival was 14.6 months (TMZ+RT) versus 12.1 months (RT alone) [Stupp et al., 2005; Cohen et al., 2005].

In addition to TMZ, carmustine (BCNU, included in Gliadel wafer) and lomustine (CCNU) are two alkylating drugs often used as second line treatment of GBM progressed after temozolomide [Alifieris et al., 2015].

Since the approval of TMZ in 2005, no other therapeutic agents have been shown improved OS in GBM patients, except for the Optune portable device (Novocure), also known as Tumor Treating Fields (TTFs), which delivers alternating electric fields of low intensity to the tumor interfering with cell division and causing cell death [Oronsky et al., 2021]. Optune has been approved by the U.S. Food and Drug Administration (FDA) in October 2015 as an adjunct treatment to TMZ in first-line glioblastoma on the basis of the EF-14 Phase III trial results which showed a median OS of 20.9 months for TTFs/TMZ vs. 15.6 months for TMZ alone and a progression free survival (PFS) of 7.1 months for TTFs/TMZ vs. 4.0 months for TMZ alone [Stupp et al., 2015]. In addition, an increase in 5-year survival from 5% to 13% was observed [Oronsky et al., 2021, Stupp et al., 2017]. Nevertheless, Optune’s use has been limited due to cost and patient inconvenience [Oronsky et al., 2021].

Regarding biologics, bevacizumab is the most thoroughly studied anti-vascular endothelial growth factor (VEGF) agent in GBM [Lu-Emerson et al., 2015]. The promising results obtained in the initial phase II studies in recurrent GBM patients (rGBM), showing an improvement of radiographic response rate (5-10%) and of 6-month progression-free survival (PFS6) rate (9%-25%), led to bevacizumab approval by FDA in March 2009, but not to European Medicines Agency (EMA) approval [Lu-Emerson et al., 2015]. However, two subsequent randomized placebo-controlled phase III trials of bevacizumab with chemotherapy in patients with newly diagnosed GBM (nGBM), failed to demonstrate an improvement in overall OS and, on this basis, bevacizumab is not administered in the first line therapy [Lu-Emerson et al., 2015; Oronsky et al., 2021].

However, the approved therapeutic options are never conclusive, the recurrence of the GBM tumor is almost universal, and the management of recurrent GBM remains challenging due to the limited availability of treatment options, reflecting a strong medical need for this dramatic disease [Oronsky et al., 2021].

Challenges in GBM treatment

Many obstacles have been encountered by investigational GBM treatments and several factors have been identified as fundamental elements to be considered for the development of new therapeutical agents for GBM. The major challenging factors in GBM treatment are summarized in Figure 4 and include the intratumoral heterogeneity, the presence of cancer stem cells (CSCs), immunosuppressive microenvironment and blood brain barrier (BBB), the development of drug resistance, the drug diffusion into the brain and drug side effects, and external factors related to previous systemic treatment that can modulate tumor microenvironment [Khaddour et al., 2020; Ganipineni et al., 2018].

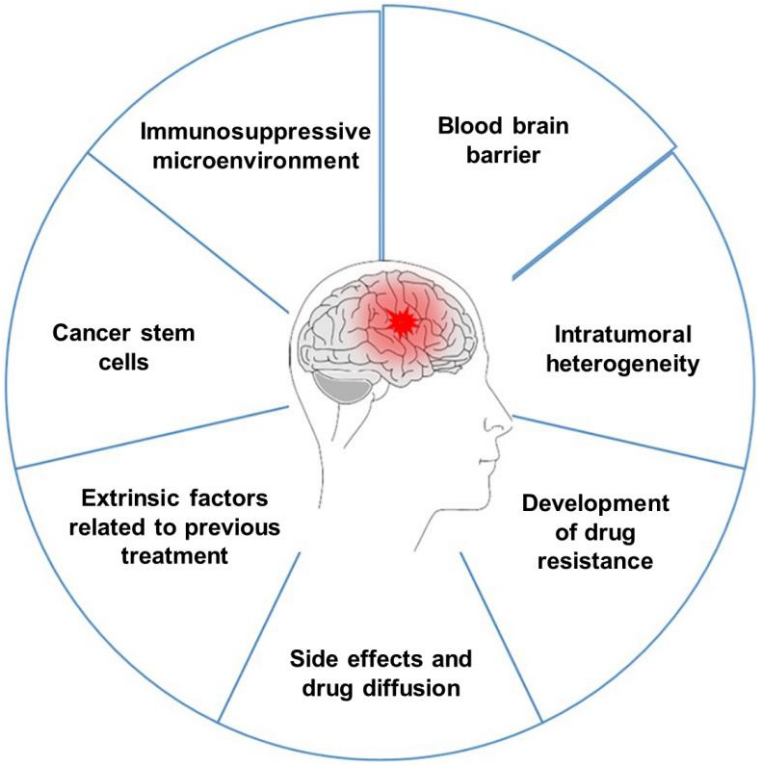

Figure 4. Challenging factors in GBM treatment [modified from Ganipineni et al., 2018].

Intratumoral heterogeneity

GBM displays extensive cellular heterogeneity, which represents a major obstacle for effective treatment [Dirkse et al., 2019]. Although the classification of GBM into four distinct molecular subgroups, it has been demonstrated that GBM tumor consists of a heterogeneous mixture of cells representing all the different subgroups that can co-exist in different regions of the tumor [Qazi et al., 2017; Neftel et al., 2019]. The presence of different subclonal populations of cells allows tumor to evade therapy and generates resistance to specific inhibitors, leading to tumor recurrence [Qazi et al., 2017]. Moreover, it has been demonstrated by Neftel et al. that malignant cells in GBM exist in a limited set of distinct cellular states that recapitulate neural-progenitor-like, oligodendrocyte-progenitor-like, astrocyte-like, and mesenchymal-like states [Neftel et al., 2019]. These four cellular states are influenced by the tumor microenvironment (TME), and exhibit plasticity, which give the potential to each cellular subtypes to change in an another over time and through therapy [Neftel et al., 2019]. The authors observed that, although each GBM sample contains cells in multiple states, the relative frequency of each state varies between different tumor subtypes and they hypothesized that this can be explained by the genetics and/or the microenvironment of individual tumors, favoring particular cellular states over others. It has been demonstrated that the frequencies of cells in each state are influenced by genetic alterations in CDK4, PDGFRα, EGFR, and NF1, which each favor a particular state, suggesting that certain genetic drivers in glioblastoma can not only promote GBM growth, but might also dictate certain transition probabilities and define the steady state distribution. Thus, the targeting of such genetic drivers might modulate the distribution of states and could possibly lead to an alternative distribution driven primarily by the self-renewal of a different state [Neftel et al., 2019]. All these aspects can therefore contribute to the clinical failure of specific inhibitors and suggest the need of combinatorial therapies for GBM [Qazi et al., 2017].

Cancer stem cells

Cancer stem cells (CSCs) constitute a second layer of GBM heterogeneity [Neftel et al., 2019].

CSCs are thought to represent the tumor driving force, due to their tumor-propagating potential and resistance to radiotherapy and chemotherapies [Lathia et al., 2015]. They are involved in GBM invasion and in the modulation of immune system to create an immunosuppressive microenvironment, by inducing regulatory T-cells (Treg), diminishing cytotoxic T-cell lymphocytes

(CTLs) activation, and promoting the M2 immunosuppressive phenotype of macrophages [Lathia et al., 2015]. Moreover, CSCs contribute to angiogenesis process through the release of high levels of VEGF and to vascular structure through the transdifferentiation into pericytes to promote tumor growth [Lathia et al., 2015].

Interestingly, the hierarchical model by which CSCs reside at the apex of a hierarchical organization and recreate intratumoral phenotypic heterogeneity through the generation of differentiated progeny has been challenged in GBM [Dirkse et al., 2019]. Indeed, it has been demonstrated that in GBM tumors CSCs do not constitute a clonal entity defined by distinct functional properties and transcriptomic signatures, but rather a cellular state adapting to microenvironmental cues, being non-hierarchical, reversible, and occurring via state transitions of existing populations [Dirkse et al., 2019]. GBM cells expressing stem cell markers are often attributed to specific tumor niches and a role of microenvironment has been pointed out in shaping the tumor phenotype toward spatial and temporal heterogeneity [Dirkse et al., 2019]. Moreover, it has been demonstrated that the reciprocal crosstalk of CSCs with tumor cells representing more differentiated phenotypes, rather than CSCs alone, creates supportive niches and promotes tumor growth, supporting the evidence that the tumorigenic potential is more linked to intrinsic plasticity rather than to CSC multipotency [Dirkse et al., 2019]. Thus, the intrinsic plasticity of GBM cancer cells has important implications for the design of treatment strategies; indeed, if the CSC state is inducible and transient, the targeting of a small subpopulation of cancer cells can be ineffective, instead the dynamic processes should be tackled [Dirkse et al., 2019].

Immunosuppressive microenvironment

TME plays critical roles in tumor growth and invasion, angiogenesis process, and contributes to therapeutic resistance [Abedalthagafi et al., 2018; Tamura et al., 2019]. The major components of TME are microvasculature and immune cells including tumor associated macrophages (TAMs), Tregs, and myeloid-derived suppressor cells (MDSCs) [Tamura et al., 2019].

Glioblastoma TME is characterized by severe immunosuppression that leads to define GBM as an immunologically “cold” tumor.

GBM cells secrete several factors contributing to immunosuppression such as transforming growth factor β (TGF-β)/interleukin-1 (IL-1), which inhibit lymphocyte activity, and colony-stimulating

factor1 (CSF1)/interleukin-10 (IL-10), which activate and polarize microglia towards an M2 anti-inflammatory phenotype [Abedalthagafi et al., 2018]. The further upregulation of the indoleamine 2,3-dioxygenase (IDO) enzyme involved in the metabolism of tryptophan, leads to the accumulation of the metabolic product kynureurine, which mediates the apoptosis of effector T-cells, the inactivation of natural killer (NK) cells, and the activation of Treg cells [Abedalthagafi et al., 2018]. Moreover, checkpoint receptors expressed by immune cells such as programmed death 1 (PD-1), cytotoxic T lymphocyte antigen 4 (CTLA-4), and T cell immunoglobulin mucin 3 (TIM-3), are used by tumor cells to escape immune surveillance and to create a widespread immunosuppression [Abedalthagafi et al., 2018].

Hypoxia and tumor angiogenesis also exert important role in the establishment of the immunosuppressive TME in GBM, as shown in Figure 5 [Yi et al., 2019]. In particular, the new leaky vessels often lack some adhesion molecules (e.g., vasculature cell adhesion molecule-1, VCAM-1), and cause a high interstitial fluid pressure (IFP) which leads to a greater difference of pressure to be overcome for T cell infiltration [[Yi et al., 2019]. On the other hand, hypoxia upregulates some inhibitory signals for anti-tumor immune response (e.g., programmed death-ligand 1 (PD-L1), IDO, interleukin-6 (IL-6), and IL-10), contributes to the recruitment of Treg cells into tumor, and promotes the polarization of tumor-associated macrophage (TAM) to M2-like phenotype [Yi et al., 2019]. Then, circulating VEGF exerts several functions, including some of the activities already described for hypoxia and the inhibition of the maturation and function of dendritic cells (DC) [Yi et al., 2019; Tamura et al., 2019]. Lastly, the expression of Fas ligand (FasL) on tumor endothelial barrier selectively eliminates effector CD8+ T cells [Yi et al., 2019].

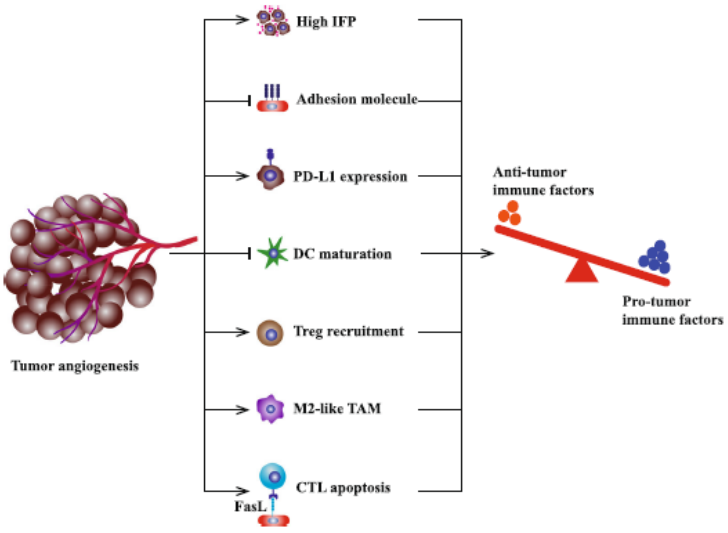

Figure 5. Contribution of the induction of immunosuppressive TME by tumor angiogenesis [Yi et al., 2019].

Blood brain barrier

The blood brain barrier (BBB) is a cellular barrier between the blood compartment and the brain. It consists of endothelial cells and different types of perivascular cells, such as pericytes and astrocytes, as shown in Figure 6 [van Tellingen et al., 2015]. BBB exerts several functions, including the regulation of the ionic composition needed for a proper synaptic signaling, the ensuring of brain nutrition, the prevention of the entrance of macromolecules and unwanted cells into the brain, and the protection of central nervous system (CNS) from neurotoxic substances [van Tellingen et al., 2015]. The entrance of unwanted molecules is countered by the presence of tight junctions between the endothelial cells, which are steadily maintained by astrocytes and pericytes. Moreover, the presence of ATP binding cassette (ABC) transporters, e.g., P-glycoprotein (P-gp) and multidrug resistance proteins (MDRPs), contributes to an efficient efflux of unwanted compounds, and prevents drug accumulation into the brain [van Tellingen et al., 2015; Ganipineni et al., 2018]. For all these reasons, BBB constitutes the main obstacle for the systemic treatment of brain tumors and other CNS disorders.

In GBM, the organization of BBB is affected, leading to the formation of a dysfunctional barrier called blood brain tumor barrier (BBTB), which is clinically visualized by contrast-enhanced MRI [van Tellingen et al., 2015]. BBTB develops through some steps (Figure 6) including the accumulation of GBM cells around the existing blood vessels, the removal of the astrocytic end feet processes and the loss of the contacts between endothelial cells and basement membrane [Ganipineni et al., 2018]. The further degradation by MMPs of the tight junctions between endothelial cells and of the surrounding extracellular matrix (ECM) ultimately leads to the migration of endothelial cells and to the formation of improper blood vessels due to the presence of hypoxia-induced VEGF stimuli [Ganipineni et al., 2018]. The leakage of the disrupted BBB leads to the development of brain edema and to an increased intracranial pressure, which is one of the major clinical complications of GBM [Ganipineni et al., 2018].

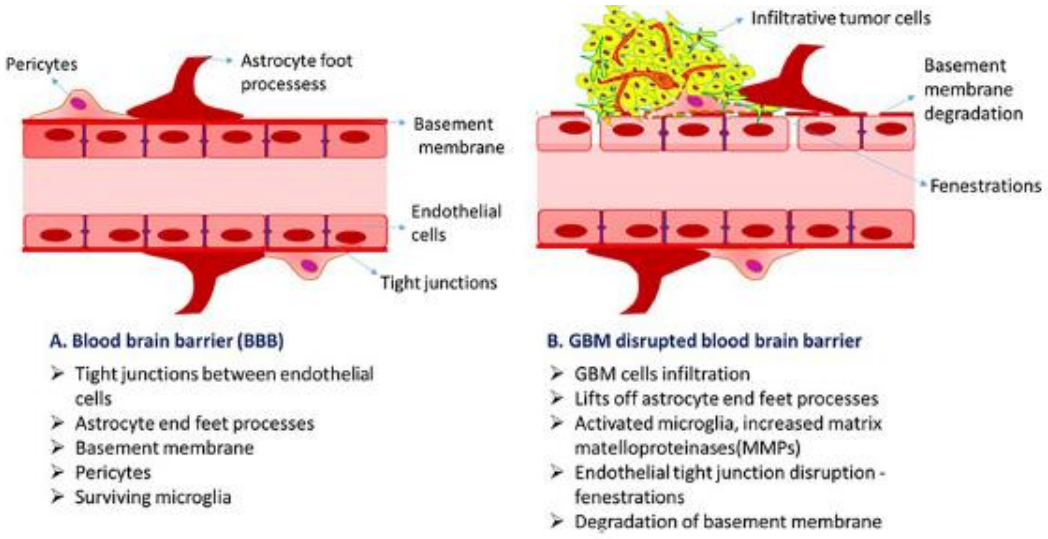

Figure 6. Features of BBB and BBTB [Ganipineni et al., 2018].

The disruption of BBB is observed only at primary site of the tumor but not at infiltrative areas where the intact BBB is maintained, thus limiting the access of therapeutic drugs to tumor cells [Ganipineni et al., 2018]. Moreover, BBB disruption does not necessarily imply the loss of biologic mechanism of drug resistance since drug efflux transporters can also be found in endothelial cells at the BBTB, and some ABC transporters can be expressed also in a subset of tumor cells [van Tellingen et al., 2015]. To date, several methods are under investigation to overcome the BBB and the BBTB [Khaddour et al., 2020].

Drug resistance

The aforementioned factors (i.e., the BBB, the tumoral heterogeneity, the presence of CSCs, and the microenvironment) can be included in the category of innate mechanisms of treatment resistance [Ou et al., 2020]. In addition, adaptive mechanisms can modulate the response of GBM cells to a specific drug treatment, leading to tumor growth and recurrence.

Various mechanisms of resistance have been identified to conventional treatments (e.g., chemotherapy and radiotherapy), as well as to investigational targeted therapies and immunotherapy [Ou et al., 2020]. For example, in case of TMZ treatment, one of the earliest characterized mechanisms of resistance was the upregulation of the DNA repair enzyme MGMT; more recently, the upregulation of the long non-coding RNA small nuclear RNA host gene 12 (SNHG12) in glioma cells has been demonstrated to be related to the epigenetic demethylation of

its promoter, occurring after TMZ treatment, and to be involved in the induction of anti-apoptotic signal [Ou et al., 2020].

Regarding the use of single-agent targeted therapies, the presence of redundant signaling pathways allows tumor to bypass the effect of a drug treatment, and the failure of many single agent therapies supports the idea that combinatorial approaches and/or the use of a multikinase approach, could contribute to the overcoming of these obstacles [Ou et al., 2020; Frantz, 2005].

On the other hand, the immunosuppressive microenvironment, the low expression of PD-1 and CTLA-4 ligands, as well as the loss of class I and/or II histocompatibility complex on tumor cells, and the presence of few tumor associated antigens are some of the obstacles encountered by immunotherapy, which includes monoclonal antibodies (i.e., immune checkpoint inhibitors, ICIs), engineered chimeric antigen receptor T (CAR-T) cells, cancer vaccines, and oncolytic viruses [Ou et al., 2020; Khaddour et al., 2020].

Drug diffusion, side effects and TME changes related to previous treatments

The infiltrative nature of GBM needs larger areas to be covered by current local delivery system; however, at the same time, low drug diffusion rates may result in unwanted high local toxicity at local delivery sites [Ganipineni et al., 2018].

Moreover, the lack of selectivity and specificity for tumor cells limit the efficiency of chemotherapeutics, by exerting toxicity on the surrounding healthy brain tissues, and neurological side effects such as chemotherapy-induced neurodegeneration are common dose-limiting chemotherapy complications [Ganipineni et al., 2018].

In parallel, external factors can induce alteration of GBM on the genomic level as well as TME [Khaddour et al., 2020]. For examples, the standard chemotherapeutic treatment of malignant glioma induces immunosuppression that can interfere with immune-based therapies [Ou et al., 2020]. Moreover, the use of steroids, such as dexamethasone, to manage the tumor associated vasogenic edema can lead to lymphodepletion, favoring a more immunosuppressive environment which could hinder the efficacy of novel drugs such as immunotherapeutic agents [Khaddour et al., 2020]. Thus, highlighting the influence of previous medications on TME of GBM and subsequent treatments is imperative for the evaluation of the efficacy of novel GBM therapeutics [Khaddour et al., 2020].

Molecular mechanisms of GBM development

The pathogenesis of gliomas involves sequential accumulation of genetic alterations and abnormal regulation of growth factor signaling pathways that result in malignant transformation [Alifieris et al., 2015]. In normal cells, processes such as growth, survival, differentiation, and migration are tightly regulated by the activity of the receptor tyrosine kinases (RTKs) and the activation of their downstream signals, which include the mitogen-activated protein kinase (Ras/MAPK) and phosphatidylinositol 3-kinase (PI3K/Akt/mTOR) pathways [Tilak et al., 2021]. RTKs dysregulation through mutations and amplifications often occurs in a wide range of cancers, including GBM [Gong et al., 2018]. Therefore, RTKs constitute attractive targets for therapy [Pearson et al., 2017].

Upon activation of RTKs by ligands, signal propagation requires interaction with intracellular components such as adaptor proteins that function primarily to bridge RTKs and downstream effectors [Tilak et al., 2021]. Adaptor proteins bind to specific receptor phosphorylated residues to activate enzymes such as kinases and GTPases that, in turn, phosphorylate and activate other kinases in well-characterized signaling pathways, which ultimately regulate the expression of target genes in the nucleus [Tilak et al., 2021].

RTKs alterations usually coexist with mutations that activate other core intracellular regulatory pathways [Gong et al., 2018]. Three of the most prominently altered RTK pathways in gliomas include the Ras/MAPK, PI3K/Akt/PTEN, and FAK/Src pathways, all of which rely on adaptor proteins such as Grb2 and Shc to relay the signals from the cell membrane [Tilak et al., 2021]. Figure 7 shows a simplified schematic illustration of common RTK signaling pathways in normal and cancer cells. However, accumulating evidence suggest that other molecular events connected to RTKs can also influence the migration, proliferation, treatment resistance, and/or survival of cancer cells, such as the RTK transactivation by G-protein-coupled receptors (GPCRs) and the inositol 1,4,5-trisphosphate receptor (IP_3R) mediated signaling involved in the maintenance of Ca^{2+} homeostasis [Tilak et al., 2021].

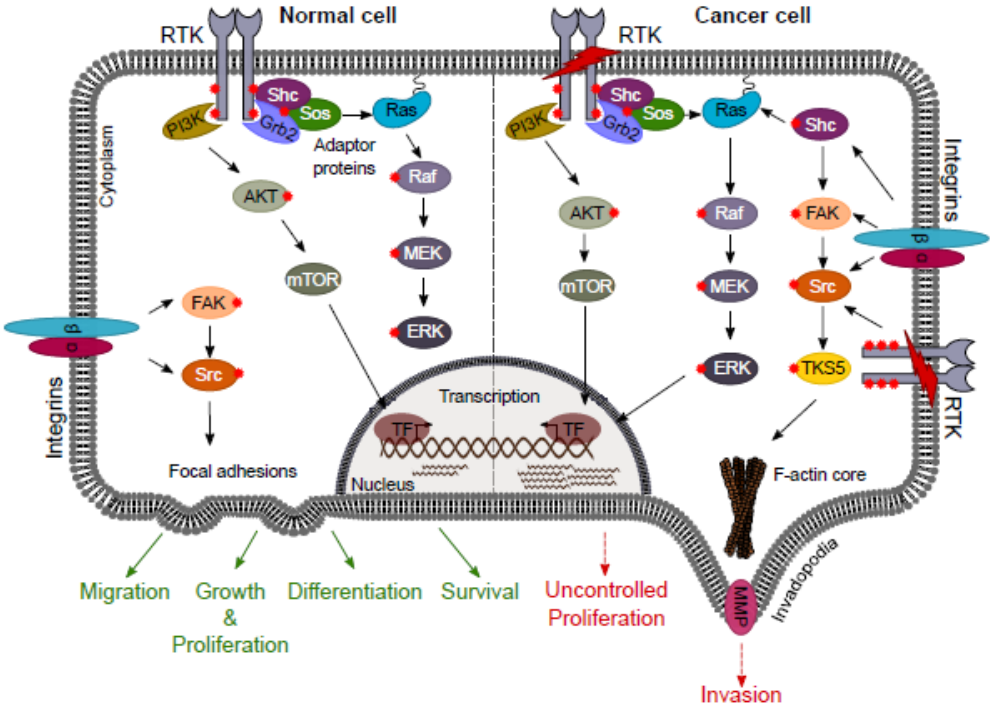

Figure 7. Schematic illustration of common RTK signaling pathways in normal and cancer cells [Tilak et al., 2021].

Receptor tyrosine kinases

In GBM, tumor's growth, progression, proliferation, as well as the angiogenesis process, depend largely upon the activity of cell surface membrane RTKs [Paolillo et al., 2018].

RTKs are transmembrane proteins comprising a unique extracellular ligand-binding domain, a transmembrane helix, an intracellular tyrosine kinase domain, and a series of tyrosine residues which serve as docking sites for cytoplasmic signaling effectors once phosphorylated [Tilak et al., 2021].

In cancer, RTKs are aberrantly activated and contribute to the oncogenic phenotype either by the (1) stimulation of the overproduction of growth factors by cancer cells; (2) overexpression and/or amplification of the RTK itself, enabling hypersensitivity to low ligand concentrations; (3) acquisition of mutations in their ligand-binding or kinase domains; (4) fusion of kinase domains with motifs of other, unrelated proteins; or (5) chromosomal translocation, giving rise to chimeric products with enhanced kinase activity [Tilak et al., 2021].

Within the human kinome, the 58 identified RTKs have been categorized into 20 distinct classes based on sequence and structural similarities in their extracellular regions, as shown in Figure 8A

[Tilak et al., 2021]. Of these, several RTKs are also found in the TCGA-GBM dataset; Tilak et al. assigned disease association scores to the RTKs frequently altered (either in expression, mutation, or copy number changes) in the various subtypes of GBM, as shown in Figure 8B [Tilak et al., 2021]. Thus, it was highlighted that the RTKs showing the higher degree of association with GBM tumors belong to the following 12 classes of receptors, as evidenced in Figure 8B: epidermal growth factor (EGF) receptors, insulin-like growth factor (IGF) receptors, platelet-derived growth factor (PDGF) receptors, vascular endothelial growth factor (VEGF) receptors, fibroblast growth factor (FGF) receptors, neurotrophin receptors, hepatocyte growth factor (HGF) receptor (HGFR, aka MET), erythropoietin-producing hepatocellular (Eph) receptors, Tie receptors, discoidin domain receptors (DDRs), RET receptor, and ROS receptors [Tilak et al., 2021]. Since the EGF and VEGF receptors families are the most extensively studied receptors in the past years, because of their strong involvement in tumor growth and angiogenesis process, they are thoroughly described in separate paragraphs (see Epidermal growth factor receptor (EGFR) and Vascular endothelial growth factor receptors (VEGFRs) sections), whereas a summary of the other receptor families and their contributions in GBM is provided below.

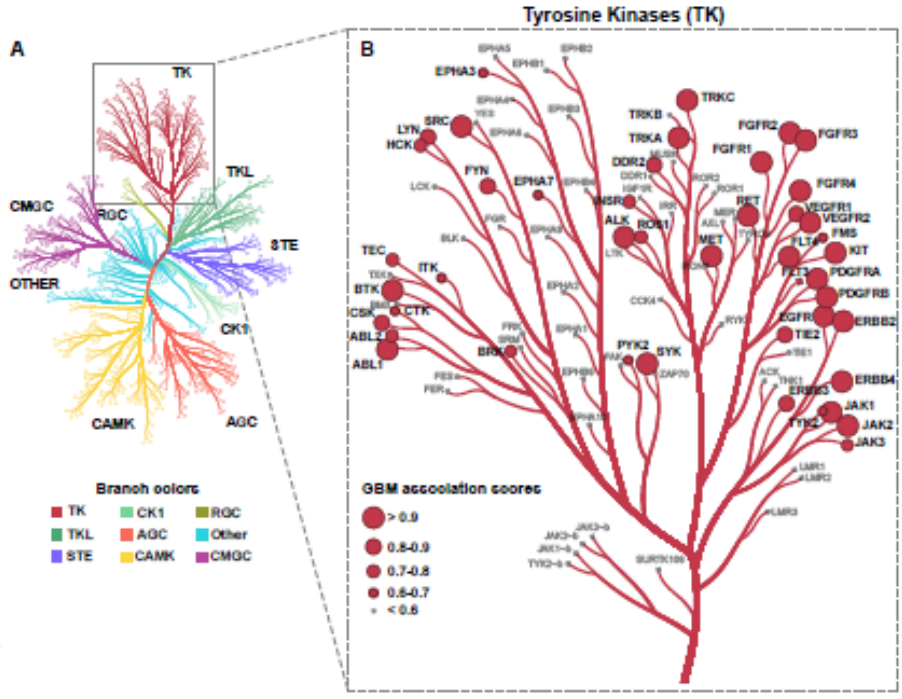

Figure 8. The human kinome and top altered RTKs in GBM. A) Kinome tree of human kinases grouped according to their sequence similarity. B) Tyrosine kinases (TK) group visualized and respective GBM association scores (ranging from 0 to 1, presented as red circles at the end of each branch; larger circles indicate a higher degree of association). Abbreviations: TKL (tyrosine kinase-like); STE (sterile serine/threonine kinases); CK1 (casein kinases); AGC (protein A/G/C-related); CAMK (Ca^{2+}/calmodulin-dependent kinases); RGC (receptor guanylate cyclases); CMGC (CDK/MAPK/GSK-3/CDK-like kinases) [Tilak et al., 2021].

Among the insulin receptors, the insulin-like growth factor 1 receptor (IGF1R) is highly expressed in the developing brain and regulates cell proliferation and differentiation; in GBM, IGF1R is overexpressed compared to normal tissue and is necessary for neoplastic transformation [Tilak et al., 2021]. Moreover, high IGF1R expression is associated with chemoresistance to TMZ as well as reduced survival, suggesting that the receptor may be used as a biomarker [Tilak et al., 2021]. It has been reported that IGF1R mutations are only present in the 2.5% of the CL subtype samples analyzed, whereas deletion of the gene was observed in the 40% of PN subtype samples [Tilak et al., 2021]. Moreover, the insulin receptor (INSR)-related receptor (INSRR), which is physiologically involved in the maintenance of pH homeostasis, was found both mutated and amplified (29.8%) in ME, suggesting a subtype specific role of the receptor in GBM [Tilak et al., 2021].

The PDGF family of receptors comprises several receptors, including the platelet-derived growth factor receptor α and β (PDGFRα and β), c-KIT (also known as stem cell factor (SCF) receptor/CD117) and Fms-like tyrosine kinase 3 (FLT3), all of which implicated in GBM [Tilak et al., 2021]. PDGFRα and PDGFRβ are involved in promoting tumor growth and angiogenesis [Alifieris et al., 2015]. In the TCGA-GBM dataset analyzed by Tilak et al., PDGFRα resulted among the most amplified receptors in GBM, second only to EGFR and preferentially upregulated in proneural GBM, which harbor oligodendrocytic signatures, whereas PDGFRβ is reported to be preferentially expressed in glioma stem cells where regulates levels of stem cell markers such as the SRY-Box transcription factor 2 (SOX2) [Tilak et al., 2021]. Regarding c-KIT, overexpression and amplification has been reported in GBM and in the TCGA-GBM dataset it resulted mutated in the 4.3% of ME glioblastoma samples, whereas its amplification (32%) and mutation (4%), together with an increased protein expression, were detected in the PN subtype [Tilak et al., 2021].

In humans, the FGFR family consists of four receptors (FGFR1-4) which activate signaling cascades crucial for normal CNS development as well as for adult neuron and astrocyte survival [Tilak et al., 2021]. FGFR amplification was identified in 3.2% of the cases studied by TCGA [Pearson et al., 2017]. It has been observed that *FGFR3* mRNA is significantly elevated in the classical GBM subtype, and its expression seems to be five times higher in infiltrating GBM cells at the migrating front compared to the tumor core [Tilak et al., 2021].

The tropomyosin receptor kinase (Trk) A, B, and C are encoded by the neurotrophic tropomyosin receptor kinase (NTRK) 1, 2, and 3 genes, respectively, and exert distinct biological functions through their diverse and variable binding affinities to neurotrophin ligands. For instance, it has been

demonstrated that TrkA binds with high affinity the nerve growth factor (NGF) ligand and activates proliferative pathways in GBM cells. On the other hand, TrkB binds the ligand brain-derived neurotrophic factor (BDNF), plays a pivotal role in neuronal survival, and some evidence supports a role for TrkB signaling in glioma cell growth [Tilak et al., 2021].

MET receptor (also known as HGFR) is a proto-oncogene stimulated by HGF ligand. During embryonic development, MET is important for skeletal muscle growth and epithelial remodeling. In GBM, MET results involved in the maintenance of stemness, in addition to tumoral proliferation, migration, invasion, and angiogenesis process. Moreover, MET can colocalize with the cytoskeletal protein cortactin to invadopodia, contributing to the increase of cortactin phosphorylation in Src kinase independent way. In the TCGA-GBM dataset analyzed by Tilak et al., over 80% of samples within each GBM subtype showed amplification of the *MET* gene, and dysregulation of MET has been demonstrated to be associated with increased invasion and poor prognosis [Tilak et al., 2021].

The Eph receptor family comprises 14 members categorized into two subclasses according to their structures, EphA1-8, and EphB1-6. In contrast to normal brain tissue, GBM cells express elevated levels of EphA2 and EphA3; EphA2 is highly correlated with the tumor propagating potential of GBM cells with stem-like properties, while EphA3 is involved in the maintenance of tumorigenicity in tumor-initiating cells. An altered expression of Eph receptors was observed in all GBM subtypes, with different amplifications and mutations present in the GBM subtypes [Tilak et al., 2021].

The Tie receptor family consists of two members, Tie1 and Tie2, which are regulated by angiopoietin ligands Ang-1 and Ang-2. Some evidence demonstrated that Tie2 signaling may regulate crosstalk between glioma cells and vascular endothelial cells of the tumor microenvironment [Tilak et al., 2021]. In addition, the angiopoietin-Tie receptor signaling has been suggested to be involved in the stimulation of compensatory angiogenesis after the blockade of the VEGF axis [Gacche., 2015]. Ang-2 resulted overexpressed in gliomas, where it promotes tumor invasion through activation of matrix metalloprotease 2 (MMP2) [Tilak et al., 2021].

The discoidin domain receptors DDR1 and DDR2 bind collagen in the surrounding ECM and physiologically orchestrate important cell functions, such as proliferation, migration, adhesion, and ECM remodeling. In glioma, the elevated levels of collagen lead to changes in DDR signaling, as well as alterations in ECM stiffness, which may further influence tumor progression. An enhanced invasion and migration have been observed in cells overexpressing DDR1 and the upregulation of DDR1 has been shown to be associated with poor clinical outcomes [Tilak et al., 2021].

RET is the receptor for glial cell line-derived neurotrophic factor (GDNF) family ligands. It plays an important role as a guidance co-receptor during axon growth and neuronal survival [Tilak et al., 2021]. RET has been shown to be overexpressed in several cancers, including glioma, where RET resulted significantly elevated in the CL GBM subtype [Mulligan, 2019; Tilak et al., 2021]. In addition, although RET overexpression and fusions are well-known mechanisms of EGFR resistance in many tumors, only recently they have been associated also with GBM [Pan et al., 2020].

Finally, ROS receptor is an orphan RTK encoded by the *ROS1* gene. While *ROS1* is expressed at low levels in normal brain tissues, it resulted highly expressed in some GBM cell lines and in surgical GBM samples, where its expression levels correlate with the increase of tumor grade, suggesting a role in tumor initiation rather than in tumor progression [Tilak et al., 2021].

Epidermal growth factor receptor (EGFR)

The epidermal growth factor (EGFR, also known as ErbB1) belongs to a family of RTKs that comprises three other members: ErbB2/HER2, ErbB3/HER3, and ErbB4/HER4, and they are encoded by EGFR, ERBB2, ERBB3, ERBB4 genes, respectively [Talukdar et al., 2020; Tilak et al., 2021].

EGFR (ErbB1) signaling network is crucial in the regulation of cancer cell proliferation, migration, and survival; in GBM, it has been demonstrated to be significantly implicated in the tumor initiation and progression [Azuaje et al., 2015]. ErbB2 is particularly well-characterized in breast cancer, where its expression is considered a prognostic factor, and elevated expression levels of the receptor have been reported also in GBM [Tilak et al., 2021]. ErbB3, which is physiologically involved in cell division and survival, also resulted upregulated in some high-grade gliomas. ErbB4 is crucial in cardiac muscle differentiation, axon guidance, and neuronal migration during development; despite its low mRNA expression in GBM, activation of the receptor is associated with increased proliferation, angiogenesis, tumorigenicity, and decreased sensitivity to anti-EGFR therapy [Tilak et al., 2021].

Among all RTKs, EGFR is the most amplified in GBM [Oprita et al., 2021]. Indeed, EGFR has been shown to be amplified in approximately 40–50% of tumors and overexpressed in over 60% of patients, suggesting a causal role of the receptor in the disease [Tilak et al., 2021]. In the TCGA-GBM dataset analyzed by Tilak et al., overall, 55% of patients presented with EGFR alterations. EGFR amplification frequencies are the highest in CL (97.4%), NE (95.8%), and ME (93.6%), followed by the PN subtype (84%) [Tilak et al., 2021]. Moreover, primary GBMs displays a higher prevalence of

EGFR gene amplification and overexpression than secondary GBMs [Oprita et al., 2021]. In addition to amplification, EGFR can harbor point mutations (such as the substitution of methionine for threonine at position 790, T790M) or deletions. Specifically, mutations were detected in the 44.7% and the 23.4% of samples representing the CL and ME subtypes, respectively [Tilak et al., 2021]. The EGFR gene is located on chromosome 7p11.2 and consists of 28 exons; exons 5–7 and 13–16 encode the ligand binding domain, whereas exons 18–24 encode the tyrosine kinase domain [Oprita et al., 2021]. A notable and commonly occurring mutation in GBM is the in-frame deletion of exon 2-7 in the extracellular domain of the receptor, which leads to the loss of a portion of the extracellular domain resulting in the truncated variant III (EGFRvIII); this variant is constitutively activated, independently of the binding with specific ligand, and it has been found usually co-expressed with EGFR [Thorne et al., 2016; Eskilsson et al., 2018]. Both EGFR and EGFRvIII receptors promote GBM cell proliferation and survival through PI3K/Akt activation but, if wild-type EGFR promotes GBM cell invasion through classical EGFR signaling pathways (e.g., Ras/MAPK), the constitutive active EGFRvIII fosters angiogenesis through activation of different oncogenic pathways (e.g., Src, c-Myc, and NFκB), as shown in Figure 9 [Eskilsson et al., 2018]. Thus, the co-expression of the two forms of receptor allows invasion and angiogenesis to be stimulated in parallel. In particular, Eskilsson et al. described a functional model of EGFR heterogeneity in GMB development according to which the EGFR amplification is acquired early by GBM cells, contributing to invasive processes; then, upon tumor progression, the acquisition of EGFRvIII mutation by GBM cells contributes to the angiogenic switch and a more aggressive tumor growth [Eskilsson et al., 2018]. Moreover, it has been reported that EGFRvIII is also involved in the regulation of stemness in glioma stem cells through MEK/HEK pathway [Talukdar et al., 2020]. Lastly, since EGFRvIII is a specific tumor associated antigen because of is not present in normal tissue, it can represent an attractive target for cancer immunotherapy [Huang et al., 2015].

Regarding the other members of EGF receptor family, in the TCGA-GBM dataset analyzed by Tilak et al. no mutations were detected for the ERBB2-4 genes in any of the four subtypes, while there was notable copy number loss for ERBB2 in ME samples (23.4%) and ERBB3 in NE and PN samples (12.5% and 20.0%, respectively), suggesting that these receptors may play a more secondary role in GBM compared to EGFR [Tilak et al., 2021].

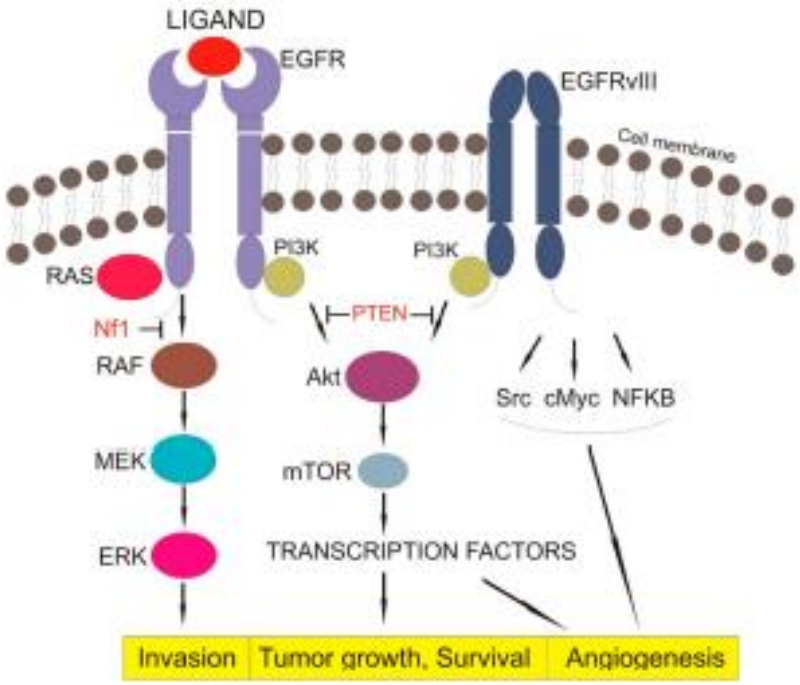

Figure 9. Schematic of EGFR and EGFRvIII signaling pathways [Oprita et al., 2021].

There are more than 40 EGFR ligands that control specific intracellular signaling, which can be divided into high-affinity ligands, such as EGF, heparin-binding EGF-like growth factor (HB-EGF), transforming growth factor α (TGFα), betacellulin (BTC), and low-affinity ligands, such as epiregulin (EREG), amphiregulin (AREG), and epigen (EPGN) [Oprita et al., 2021]. Ligand binding results in an active dimeric conformation of EGFR by forming a complex with another EGFR (homodimerization) or with one of the other ErbB members (heterodimerization) [Azuaje et al., 2015]. Upon dimerization, the catalytic intracellular domain is activated by phosphorylation of tyrosine residues and results in the recruitment of different cytosolic signaling proteins containing Src homology 2 (SH2) or phosphotyrosine binding-(PTB) domains [Oprita et al., 2021]. These proteins bind to specific phosphotyrosine residues in EGFR and initiate intracellular signaling via several pathways, including the RAS/MAPK and the phosphatidylinositide 3 kinase (PI3K)/AKT pathways (Figure 9), the janus kinase (JAK)/signal transducers and activators of transcription 3 (STAT3) pathway, the phospholipase Cγ, and the Src kinase pathway [Huang et al., 2015; Azuaje et al., 2015; Talukdar et al., 2020].

The RAS/MAPK signaling pathway involves the growth-factor-receptor bound-2 (GRB2) protein, which forms a complex with the guanine-nucleotide exchange factor (GEF) called Son of Sevenless (SOS), leading to the activation of the Ras G-protein; the activated Ras in turn triggers a downstream

signaling cascade via mitogen-activated protein kinases (MAPKs) which ultimately phosphorylate the nuclear protein Jun [Oprita et al., 2021; Azuaje et al., 2015]. Jun creates complexes with different nuclear proteins forming the key transcription factor activator protein 1 (AP-1), which is responsible for the translation and transcription of proteins involved in the growth and division of cells [Oprita et al., 2021]. Activated RAS is negatively regulated by GTPase activating proteins (GAPs), such as the tumor suppressor neurofibromin 1 (NF1) [Oprita et al., 2021].

The PI3K/AKT signaling pathway involves PI3K, which is recruited upon EGFR activation and phosphorylation to the cell membrane, where it phosphorylates phosphatidylinositol 4,5-bisphosphate (PIP2) to phosphatidylinositol (3,4,5)-trisphosphate (PIP3) [Oprita et al., 2021]. AKT enzyme interacts with PIP3 and reaches full activity after its phosphorylation at Threonine 308 and Serine 473 by phosphoinositide-dependent protein kinase-1 (PDK1) and the mammalian target of rapamycin complex 2 (mTORC2), respectively [Oprita et al., 2021]. Activated AKT can transduce the signal through the phosphorylation of several downstream substrates, such as the transcription factor FOXO, resulting in the regulation of numerous processes such as proliferation and cell survival [Azuaje et al., 2015]. The phosphatase and tensin homolog (PTEN) tumor suppressor negatively regulates the PI3K/AKT pathway by dephosphorylating and delocalizing PIP3 from the cellular membrane, resulting in the relocalization of AKT in the cytoplasm, where it cannot be activated anymore [Oprita et al., 2021].

Beside alterations in RAS and PI3K enzymes, mutations or deletions of negative regulators, such as NF1 and PTEN, are very common in cancer, resulting in the unterminated EGFR signaling which allows cells to proliferate and survive without restraint [Azuaje et al., 2015].

Because of EGFR can activate different signal transduction pathways in parallel, EGFR can be considered as a hub involved in regulating various cellular processes, including proliferation, migration, differentiation, and in inducing the angiogenesis process through VEGF expression [Alifieris et al.; Oprita et al., 2021]. Thus, considering the importance of EGFR in the GBM tumor pathophysiology, a wide range of targeted treatments have been developed, although with very limited clinical success [Warta et al., 2017]. Three generations of small molecules tyrosine kinase inhibitor (TKIs) have been identified: first-generation TKIs were created to inhibit the receptor by competitive binding with ATP (e.g., erlotinib, gefitinib, lapatinib, and vandetanib), second-generation TKIs were developed to irreversibly inhibit all four ErbB (e.g., afatinib, dacotinib), and third-generation TKI were designed to specifically target the T790M mutation (Osimertinib) [Oprita

et al., 2021]. Besides small molecules, other strategies include the use of monoclonal antibodies (e.g., cetuximab, necitumumab, and panitumumab), antibody drug conjugates (ADCs) (e.g., Depatux-M), toxin-loaded delivery vehicles and vaccines (e.g., rindopepimut, an EGFRvIII-specific peptide vaccine), oncolytic viruses, CAR-T cells, and nanoparticles [Thorne et al., 2016; Eskilsson et al., 2018; Oprita et al., 2021].

Whereas targeted therapy towards mutations responsible for tumor growth and progression showed effectiveness in different tumor types, in case of GBM the responses to EGFR-pathway inhibitors were not as expected, since no satisfactory results have been achieved so far [Oprita et al., 2021]. Reasons why GBM escapes EGFR treatment can be classified into primary and secondary resistance [Warta et al., 2017]. Among the causes of primary resistance there is the BBB, which limits the access of drugs to the tumor site. On the contrary, secondary resistance mechanisms are related to the adoption of adaptive strategies by tumor to overcome drug treatment [Warta et al., 2017]. These include "target independence" mechanisms, such as the acquisition of new resistance mutations (e.g., T790M) and the decrease of EGFR amplification through the elimination of the extrachromosomal DNA, and "target compensation" mechanisms, which concern the activation of alternative compensatory signaling pathways such as IGFR1, PDGFR, and c-MET pathways [Thorne et al., 2016; Westphal et al., 2017; Eskilsson et al., 2018; Saleem et al., 2019].

Despite the failure of many drugs against EGFR alterations, strategies to target EGFR in GBM continue to be investigated, and the targeting of EGFR axis is still considered as valid [Pan et al., 2020]. To overcome the mechanisms of resistance described above, some possible approaches have been described by Saleem et al.; they include a pulsatile drug scheduling, the targeting of specific mutations that co-occur with EGFR mutation/gene amplification (such as cyclin-dependent kinase inhibitor 2A, CDKN2A and PTEN), the combinatory use of inhibitors specific for the compensatory pathways (multitarget therapy), and lastly the poly-pharmacological approach, which means the use of a single drug able to inhibit simultaneously multiple kinases [Saleem et al., 2019].

Vascular endothelial growth factor receptors (VEGFRs)

Vascular endothelial growth factor (VEGF) family consists of five members (VEGFA, VEGFB, VEGFC, VEGFD and placenta growth factor (PlGF)), identified as master regulators of vascular development and of blood and lymphatic vessel function during health and disease in the adult [Koch et al., 2012].

VEGFs act through the vascular endothelial growth factor receptor (VEGFR) family, which includes three RTKs: VEGFR1 (or Fms-like tyrosine kinase 1, Flt-1), VEGFR2 (or kinase insert domain-containing receptor, KDR), and VEGFR3 (or Fms-like tyrosine kinase 4, Flt-4) [Alifieris et al., 2015]. VEGFRs are expressed on vascular endothelial cells and, upon activation, induce endothelial cell migration (VEGFR1), stimulate endothelial cell proliferation, increase vascular permeability and the expression of proangiogenic factors (VEGFR2) and lead to lymphangiogenesis (VEGFR3) [Alifieris et al., 2015]. In addition to angiogenic effects, VEGF is also involved in the suppression of the anti-tumor immune response, by inhibiting the maturation of dendritic cells (DCs) leading to the inactivation of CTLs, and in the induction of the immunosuppressive TME, through the activation of Tregs, TAMs, and MDSCs cells [Tamura et al., 2019].

In the TCGA GBM dataset analyzed by Tilak et al., VEGFR1 has been found not significantly enriched in the CL subtype, minimally mutated in the ME subtype (2.1%) and deleted in all subtypes [Tilak et al., 2021]. Regarding VEGFR2, the expression of the protein has been found significantly upregulated in ME subtype; in addition, mutations were detected in the CL (2.6%) and NE (4.2%) subtypes and deletions were encountered in the PN (28%) and G-CIMP (28.6%) subtypes. Finally, no mutations of VEGFR3 have been observed, but a considerable proportion of G-CIMP samples showed gene deletion (42.9%) [Tilak et al., 2021].

Several VEGF ligands and receptors are regulated by hypoxia, which stimulated their expression during tissue growth both in health (wound healing, embryonic development) and disease (cancer) [Koch et al., 2012]. In terms of tumor angiogenesis, VEGFA (hereafter referred as VEGF) is considered as the most physiologically relevant form; it is able to stimulate endothelial cell survival, invasion and migration into surrounding tissues, proliferation, as well as vascular permeability and inflammation through its primary receptor VEGFR2 [Napione et al., 2017]. High levels of VEGF and its receptors have been detected also in GBM, and the increased angiogenesis and dysfunctional tumor vasculature is attributed mostly to an aberrant VEGFR2 signaling, since the receptor is involved in the regulation of cellular survival, proliferation, migration, and vessel permeability [Tilak et al., 2021]. These features are required by tumor to maintain survival beyond the size of 2 mm [Alifieris et al., 2015]. Thus, the hypoxic environment of GBM triggers the so-called “angiogenic switch” wherein the release of HIF-1α induces the production of VEGF by tumor cells and the tumor-associated stromal and inflammatory cells, leading to the transition from quiescent to active endothelium and to the vascularization of the growing cell mass [Napione et al., 2017; Clavreull et al., 2019; Tilak et al., 2021]. More recently, although VEGFA is still considered as the major pro-

angiogenic factor in GBM, VEGFC has also emerged as an important pro-tumorigenic factor in GBM, by promoting viability and proliferation of GBM cells and by sustaining VEGFR2 activation despite bevacizumab (the anti VEGFA antibody) treatment. Thus, the autocrine VEGFC/VEGFR2 signaling could contribute to bevacizumab resistance [Michaelsen et al., 2018].

Five mechanisms have been identified to be exploited by tumor to increase blood supply: angiogenesis, vessel co-option, intussusception, vascular mimicry, and bone marrow-derived vasculogenesis, as shown in Figure 10 [Clavreul et al., 2019].

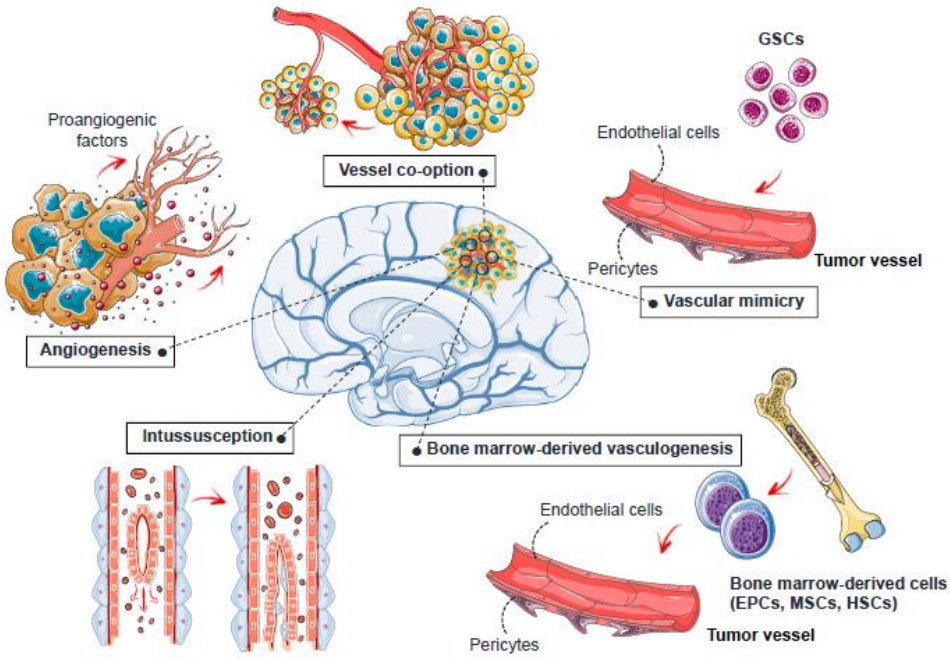

Figure 10. Mechanisms of tumor blood supply in GBM. Abbreviations: EPCs (endothelial progenitor cells); GSCs (glioblastoma stem-like cells); HSCs (hematopoietic stem cells); MSC (mesenchymal stem cells) [Clavreul et al., 2019].

Angiogenesis process results from the disruption of the balance between proangiogenic factors (e.g., VEGF and fibroblast growth factor-2, FGF-2), and antiangiogenic factors (e.g., angiostatin and endostatin) released by the tumor itself or by the surrounding tissues and involves a sequence of coordinated events which lead to the formation of new vessels, see Figure 11 [Nakada et al., 2011; Clavreul et al., 2019]. Briefly, the angiogenic factors released by glioma cells in the hypoxic glioma microenvironment trigger endothelial cell proliferation and migration through the binging to their cognate receptors on endothelial cells; at the same time, the concurrent local degradation and breakdown of ECM paving the way for newly sprouting vessels [Nakada et al., 2011]. In addition, Ang-2 promotes angiogenesis by destabilizing the blood vessels (e.g., by decreasing pericyte

coverage) through the binding to its cognate receptor Tie2 and by sensitizing ECs to proliferation signals mediated by VEGF. Thus, Ang-2 acts as a strong enhancer of sprouting angiogenesis in presence of VEGF, particularly in the early period of tumor progression [Park et al., 2016].

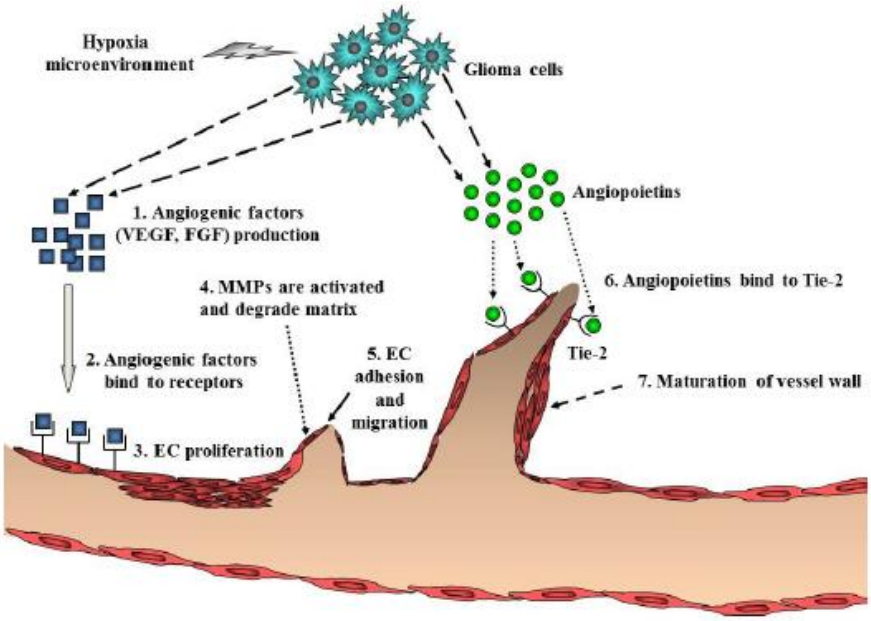

Figure 11. A schematic diagram of angiogenesis process in gliomas [Nakada et al., 2011].

Regarding the other mechanisms of tumor blood supply (Figure 10), vascular co-option involves the infiltration of tumor cells into normal tissue and the adoption of the pre-existing vasculature, vessel intussusception represents the formation of new vessels by the enlargement and bifurcation of existing vessels, and vasculogenic mimicry is a process in which GBM stem-like cells contribute to the formation of tumor blood vessels by differentiating into endothelial cells or pericytes [Clavreul et al., 2019]. Lastly, the bone marrow-derived vasculogenesis involves the recruitment of endothelial progenitor cells (EPCs), mesenchymal stem cells (MSCs), or hematopoietic stem cells (HSCs) to the tumor, their integration into the vessel wall, and their differentiation into endothelial cells [Clavreul et al., 2019].

However, the new tumor vasculature is leaky and circuitous, with a haphazard pattern of interconnection. The endothelial cells lining the new vessels have an irregular, disorganized morphology and are often poorly connected; the pericytes are loosely attached or absent, and the basement membrane may be abnormally thick or entirely absent. These vascular abnormalities reflect into a heterogeneity in tumor blood flow and oxygenation, and, together with the

microenvironment, create fuel for tumor progression and decrease the efficacy of chemotherapy, radiotherapy, and immunotherapy [Clavreul et al., 2019].

As already mentioned before, the tumoral angiogenic response to VEGF is mainly mediated by VEGFR2. Upon the activation of the receptor, several signaling pathways involving different effectors initiate, eventually leading to different endothelial responses (i.e., cell survival and proliferation, vascular permeability, and cell migration), which ultimately allow tumor angiogenesis to take place, Figure 12a-b [Napione et al., 2017].

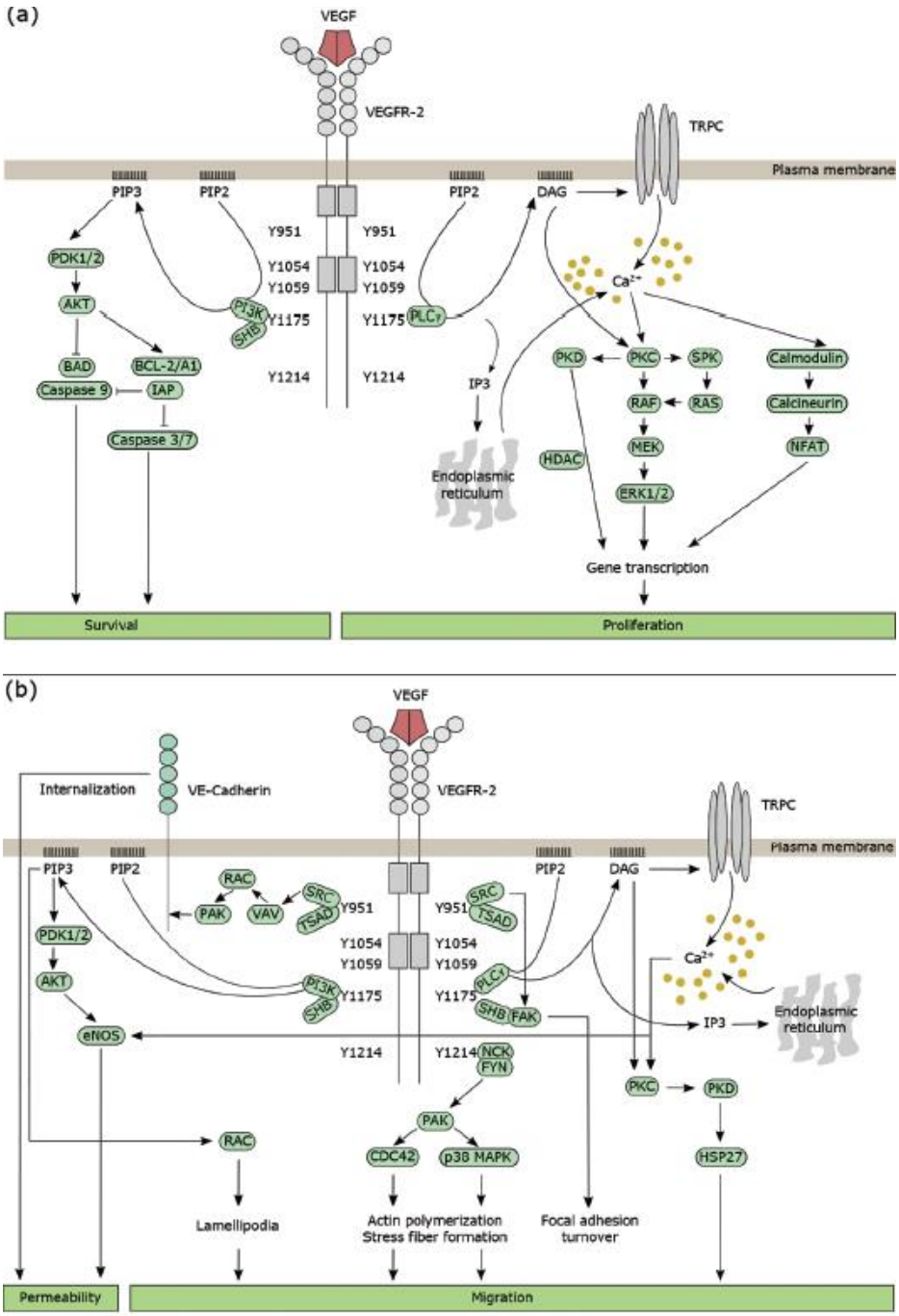

Figure 12. Schematics of signal transduction pathways mediated by VEGF/VEGFR2 [Napione et al., 2017].

The binding of VEGF to VEGFR2 promotes receptor dimerization, allowing trans/autophosphorylation of intracellular tyrosine residues [Napione et al., 2017]. Among the 19 tyrosine residues present in the intracellular domain of VEGFR2, five have been identified as the major phosphorylation sites: Y951, Y1054, Y1059, Y1175 and Y1214. The fist residue is present in the kinase insert domain of the receptor and its phosphorylation serves as a binding site for T cell-specific adaptor (TSAD), also known as VEGFR2-associated protein (VRAP). Due to their presence in the kinase domain activation loop of the receptor, the phosphorylation of the Y1054 and Y1059 residues is critical for receptor catalytic activity. Lastly, the Y1175 and Y1214 residues are located in the carboxy-terminal domain of the receptor. The phosphorylated Y1214 residue has been described to bind the adaptor protein NCK which in turn recruits Fyn kinase, whereas the phosphorylation of Y1175 creates a binding site for several proteins (i.e., PLCγ, p85 subunit of PI3K, the adaptor proteins SHB and SCK), and for this reason it is considered as a critical mediator of VEGFR2 signaling [Napione et al., 2017]. Moreover, VEGFR2 activation and downstream signaling can be regulated also by different mechanisms including the receptor interaction with NRP1, specific integrins and VE-cadherin, and the activity of the protein tyrosine phosphatases (PTPs) such as vascular endothelial PTP (VEPTP), SRC homology 2 domain PTP (SHP2) and PTP1B [Napione et al., 2017].

Despite of the theoretical biologic rationale by which the inhibition of angiogenesis should lead to increased hypoxia, thereby limiting tumor growth or causing tumor regression, treatment with anti-angiogenic agents showed controversial results. It has been demonstrated that increased hypoxia fuels tumor progression by promoting angiogenesis, cancer cell invasion, genetic instability, stem-like phenotype, and many other mechanisms that counteract the potential benefit of an anti-angiogenic therapy [Lu-Emerson et al., 2015; Gacche, 2015; Carmeliet et al., 2011]. Several clinical trials with anti-angiogenic agents support the evidence that normalization of abnormal tumor vessels, rather than “vessel blocking” strategy, can contribute to a better drug delivery due to an increased blood perfusion, and translate in clinical benefits, although they differ significantly between individual patients [Lu-Emerson et al., 2015]. A second benefit of anti-VEGF agents is the reduction in vasogenic brain oedema, a major cause of neurologic morbidity in all patients with GBM. Finally, the application of anti-angiogenic agents may disrupt the link between tumor-vasculature and stem-like GBM cells located in perivascular niches and surrounded by endothelial cells [Lu-Emerson et al., 2015].

Bevacizumab is the most thoroughly studied anti-VEGF biologic agent in GBM. As previously discussed, it has been approved by FDA only for rGBM, wherein it demonstrated survival benefits, whereas its administration in nGBM failed to demonstrate an improvement in OS. However, bevacizumab has also been used in combination with other drugs (e.g., cetuximab, an anti-EGFR antibody, and erlotinib) but results showed response rates and PFS6 (progression-free survival at 6 months) comparable to historical bevacizumab-containing regimens [Lu-Emerson et al., 2015]. In addition to small molecule inhibitors, the other anti-angiogenic strategies are based on the development of biologics targeting the VEGF and VEGFR2, the delivery of nano-vesicles such as SapC-DOPS, (SaponinC-dioleoylphosphatidylserine, Bexion pharmaceuticals) and gene therapy such as VB-111 (ofranergene obadenovec, VBL Therapeutics). Moreover, because of anti-angiogenic therapy may change the TME into an immunological favorable “hot” microenvironment, combinatorial therapies with ICIs are under investigation; furthermore, other immunotherapies such as DC-based immunotherapies, tumor vaccine therapy, and CAR-T cell therapy could be added to improve therapeutic efficacy [Tamura et al., 2019].

Intracellular tyrosine kinases

Upon activation of the receptors, the signal is transmitted intracellularly up to the nucleus through several kinases, including members of Src-family kinases (SFKs).

The SFKs family consists of nine members (Blk, Fgr, Fyn, Hck, Lck, Lyn, Src, Yes, and Yrk) which exhibit the following conserved domain organization: a myristoylated N-terminal segment, the SH3 domain, the SH2 domain, a linker, the tyrosine kinase catalytic domain, and a C-terminal tail [Parsons et al., 2004].

SFKs play key roles in regulating signal transduction pathways involved in cell adhesion, migration, invasion, proliferation, apoptosis, and angiogenesis, by interacting with multiple cell surface receptors (e.g., integrin, EGFR, PDGFR, and VEGFR) [Han et al., 2014].

Increased SFKs activity mediates tumorigenesis and is critical for GBM cell motility, invasion, and angiogenesis. Within the SFKs, Src, Fyn, Yes and Lyn have all been shown to be involved in the GBM-related signaling [Lewis-Tuffin et al., 2015].

The intracellular tyrosine kinase Src has been demonstrated to be involved in the activation of different pathways, including the Ras/Raf/MAPK pathway; the latest is one of the main intracellular

pathways activated in GBM, promotes the regulation of a wide range of intracellular signaling leading to cell survival, proliferation, motility, and angiogenesis, as well as sustains tumor growth by maintaining inflammation and metabolic reprogramming concurring with TME development [Paolillo et al., 2018; Cirotti et al., 2020].

By in vivo GBM knock-down experiments in mice, it has been demonstrated that Yes kinase affects tumor cell biology in a pro-tumorigenic manner, whereas Lyn acts in anti-tumorigenic way [Lewis-Tuffin et al., 2015]. Moreover, Kleber et al. identified the involvement of Yes kinase in the induction of the invasive phenotype of GBM cells. Indeed, after the induction of the expression of CD95 ligand resulting from the tumor interaction with the surrounding brain tissue, the binding of CD95 ligand to CD95 present on GBM cells leads to the recruitment of Yes and the p85 subunit of PI3K; the downstream activation of the glycogen synthase kinase 3-β (GSK3β) pathway finally leads to the expression of MMPs, thus promoting tumor invasion [Kleber et al., 2008].

Regarding Fyn and Src kinases, they have been described by Lu et al. as important players in EGFR and EGFRvIII intracellular signaling [Lu et al., 2009]. Indeed, the authors demonstrated that the expression of the constitutively active form of EGFR (EGFRvIII) resulted in activating phosphorylation and physical association with Src and Fyn, promoting tumor growth and motility in vivo in a mouse model of GBM [Lu et al., 2009].

Lck kinase has been recently demonstrated to be involved in glioma progression at different levels by promoting the migration of GBM cells and tumor growth, and by regulating cancer cells stemness [Zepecki et al., 2019]. In addition, Lck has been demonstrated to be involved in the resistance of glioma stem cells to cisplatin and to fractionated radiations [Bommhardt et al., 2019]. Indeed, a selective increase of Lck activity in glioma cells and an expansion of glioma stem cells have as been detected after fractionated radiation [Bommhardt et al., 2019]. At the same time, the siRNA-mediated knockdown of Lck resulted in a significant suppression of glioma stem cell population expansion, and in the restoration of the sensitivity of glioma cells to cisplatin and etoposide treatment, supporting the hypothesis of the involvement of Lck in the resistance of glioma stem cells to cisplatin and radiations treatment [Bommhardt et al., 2019].

In addition to the tyrosine kinases described above, the HGK (aka MAP4K4) serine/threonine kinase has recently emerged as a relevant kinase for GBM development, specifically as a strong regulator of GBM invasion. HGK expression resulted mostly upregulated by EGFRvIII compared to the wild-type EGFR and the increased HGK activity seems to promote the migration and invasion of GBM

cells through the reduction of the expression of cell-cell adhesion molecule and the direct activation of proteins involved in cytoskeletal rearrangements [Prolo et al., 2019].

CR13626

In vitro pharmacology

The in vitro activity of CR13626 was evaluated at the concentration of 1 µM in a panel of 173 kinases at Eurofins Cerep laboratories (Celle-Lévescault, France) in accordance with Eurofins validation Standard Operating Procedures. Enzyme assays were performed in duplicate under optimized conditions for each enzyme. The following figures summarize the activity of CR13626 against kinases belonging to the same class: the tyrosine kinases belonging to the RTK and CTK (intracellular tyrosine kinases) subfamilies (Figure 13, panels A and B), the serine/threonine kinases belonging to the CMGC, CAMK, AGC, STE and TKL subfamilies (Figure 14, panels A, B, C, D, E) and other kinases (Figure 15). Most of the activity of CR13626 was observed against tyrosine kinases belonging to the receptor tyrosine kinase and intracellular tyrosine kinase subfamilies (Figure 13, panels A-B).

A

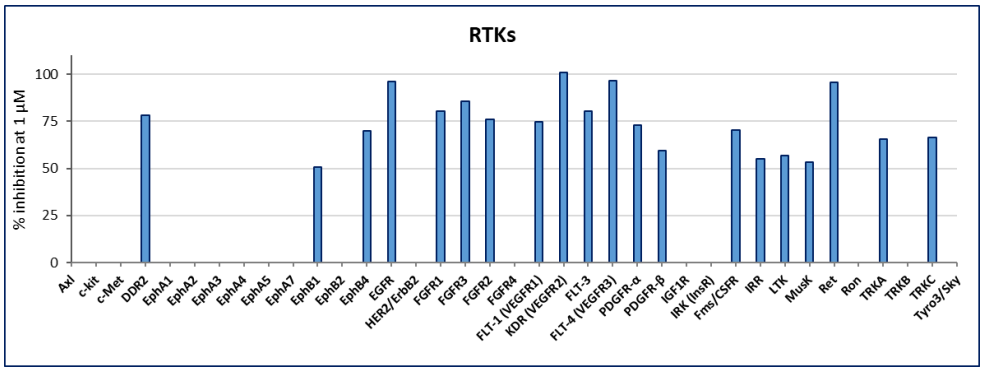

B

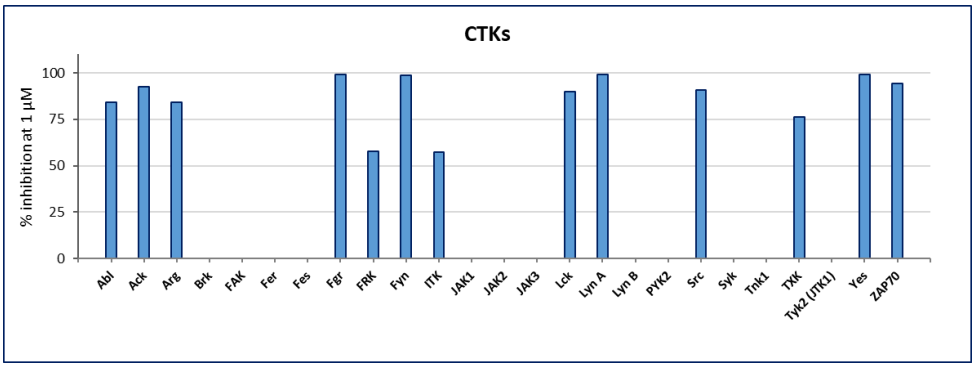

Figure 13. Activity of CR13626 1 µM against tyrosine kinases belonging to the receptor (RTK) (A) and the intracellular (CTK) (B) subfamilies.

A

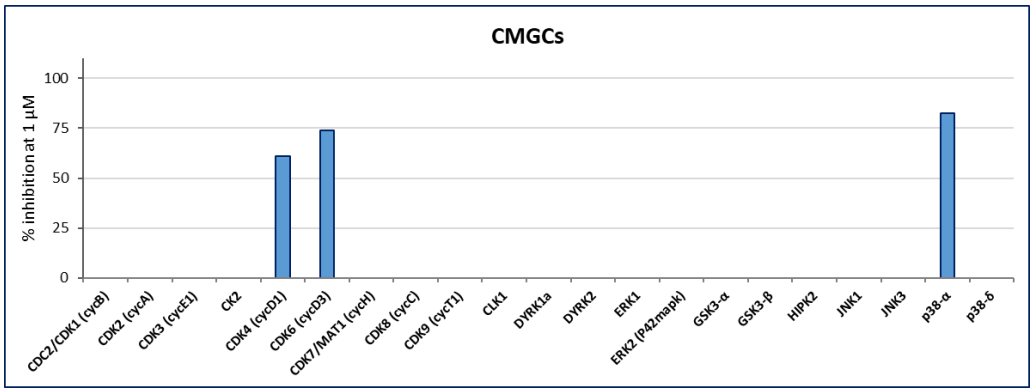
CMGCs
% inhibition at 1 µM
100
75
50
25
0
CDC2/CDK1 (cycB)
CDK2 (cycA)
CDK3 (cycE1)
CK2
CDK4 (cycD1)
CDK6 (cycD3)
CDK7/MAT1 (cycH)
CDK8 (cycC)
CDK9 (cycT1)
CLK1
DYRK1a
DYRK2
ERK1
ERK2 (P42mapk)
GSK3-α
GSK3-β
HIPK2
JNK1
JNK3
p38-α
p38-δ

B

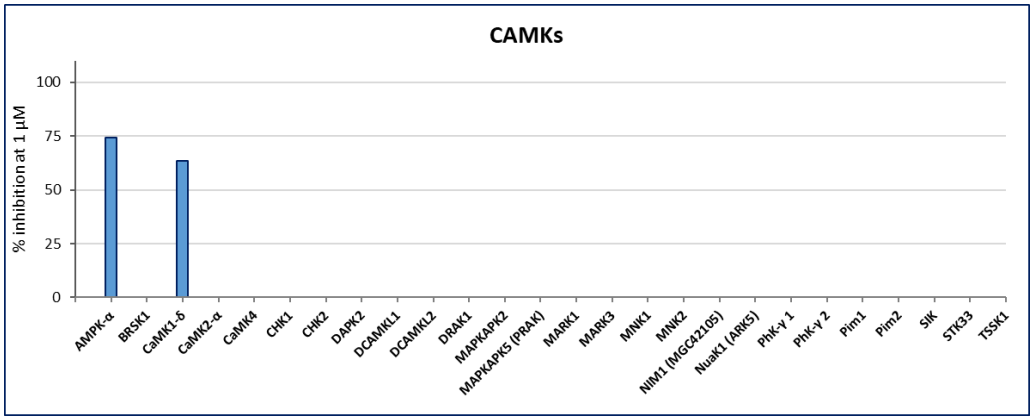
CAMKs
% inhibition at 1 µM
100
75
50
25
0
AMPK-α
BRSK1
CaMK1-δ
CaMK2-α
CaMK4
CHK1
CHK2
DAPK2
DCAMKL1
DCAMKL2
DRAK1
MAPKAPK2
MAPKAPK5 (PRAK)
MARK1
MARK3
MNK1
MNK2
NIM1 (MGC42105)
NuaK1 (ARK5)
Phk-γ 1
Phk-γ 2
Pim1
Pim2
SIK
STK33
TSSK1

C

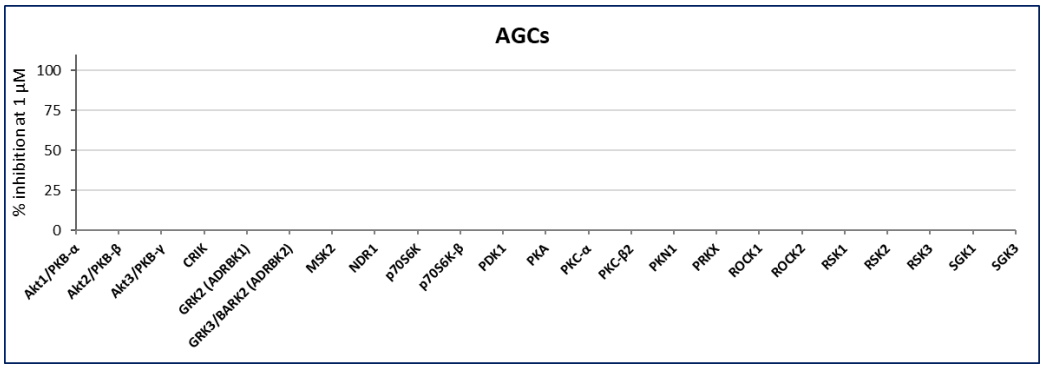
AGCs
% inhibition at 1 µM
100
75
50
25
0
Akt1/PKB-α
Akt2/PKB-β
Akt3/PKB-γ
CRIK
GRK2 (ADRBK1)
GRK3/BARK2 (ADRBK2)
MSK2
NDR1
p70S6K
p70S6K-β
PDK1
PKA
PKC-α
PKC-β2
PKN1
PRKX
ROCK1
ROCK2
RSK1
RSK2
RSK3
SGK1
SGK3

D

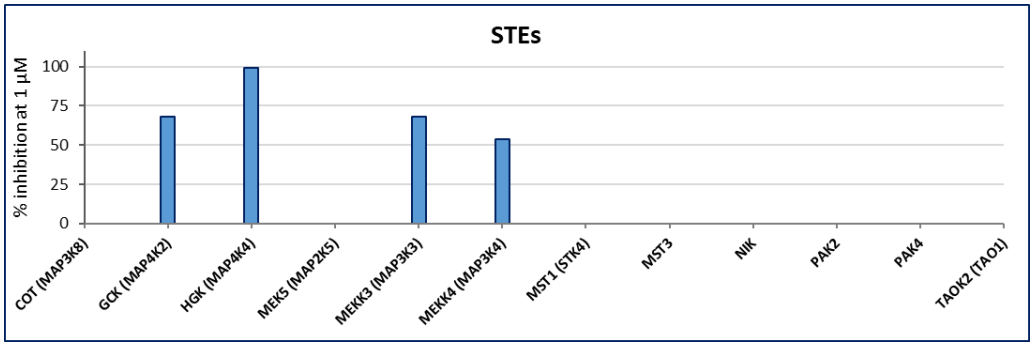
STEs
% inhibition at 1 µM
100
75
50
25
0
COT (MAP3K8)
GCK (MAP4K2)
HGK (MAP4K4)
MEK5 (MAP2K5)
MEKK3 (MAP3K3)
MEKK4 (MAP3K4)
MST1 (STK4)
MST3
NIK
PAK2
PAK4
TAOK2 (TAO1)

E

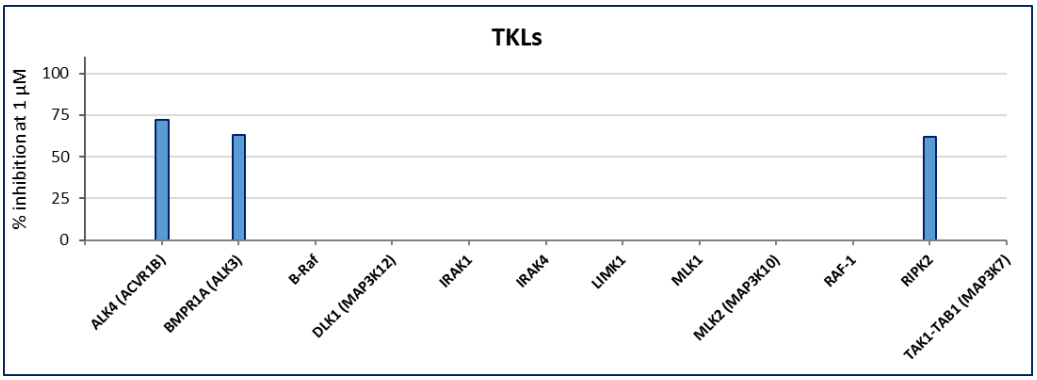

Figure 14. Activity of CR13626 1 µM against Serine/Threonine kinases belonging to the CMGC (A), CAMK (B), AGC (C), STE (D) and TKL (E) subfamilies.

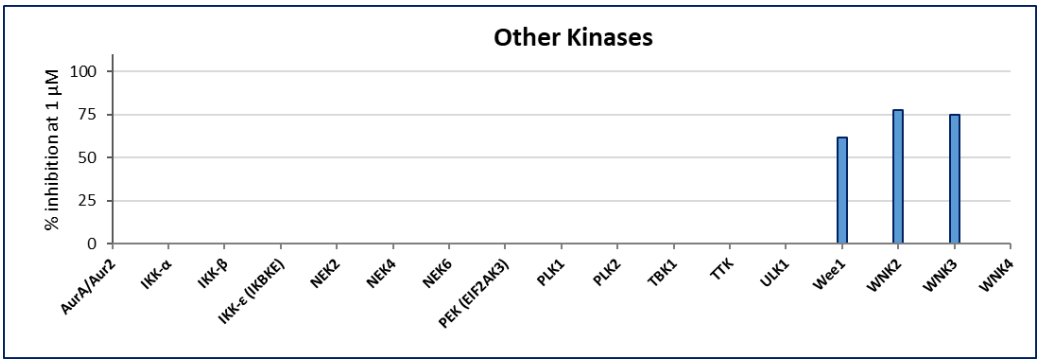

Figure 15. Activity of CR13626 1 µM against other kinases included in the screening panel.

The potency of CR13626 against selected kinases relevant for glioblastoma was then assessed by testing CR13626 in dose response curves in the concentration range of 0.001 - 1 µM of CR13626. The IC_{50} values were determined and reported in Figure 16.

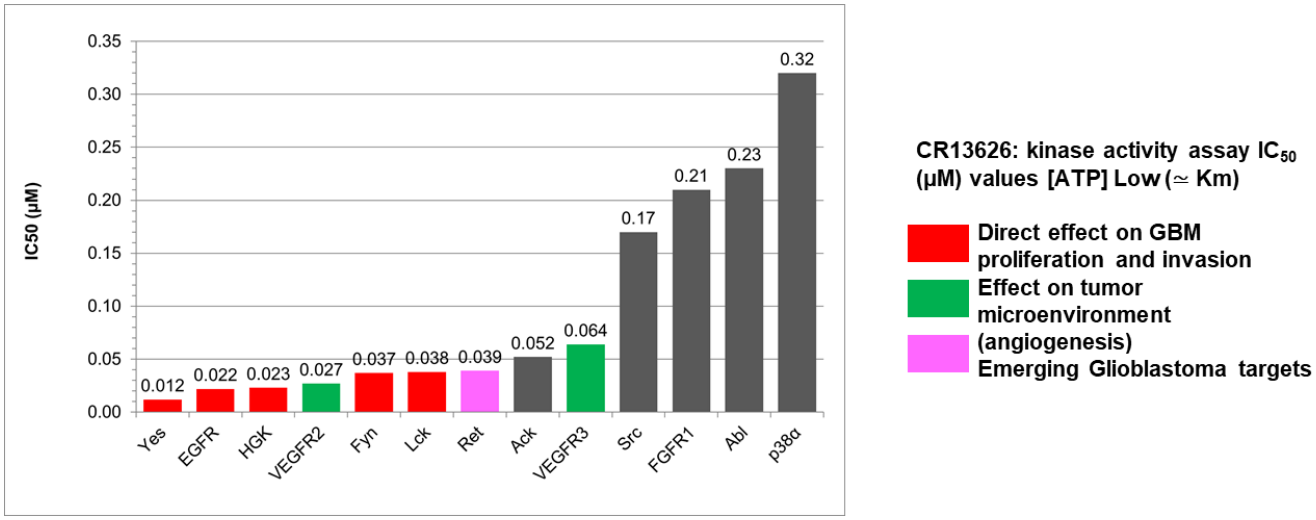

Figure 16. Potency of CR13626 against a set of tyrosine kinases relevant for GBM.

In vitro pharmacokinetic

The CR13626 in vivo permeability across the intestinal tract was evaluated by assessing the in vitro transport rate of CR13626 across the Caco-2 cells monolayer membrane. CR13626 was tested at the concentration of 10 µM and the transports in the apical to basolateral (A→B) and in the basolateral to apical (B→A) directions were determined by applying the compound either to the apical (A) or the basolateral (B) side of the cell monolayer (upper or lower compartment of the insert, respectively). The amount of CR13626 at the basal and apical sides over 1.5 hours of incubation at 37°C was quantified by HPLC-MS/MS. The A→B and B→A apparent permeability (Papp), B→A/ A→B ratio and A→B and B→A mass balances were calculated. According to the results summarized in Table 1, CR13626 could be classified as a medium permeability drug both in the apical-to-basolateral (A→B) and basolateral-to-apical (B→A) directions. Moreover, CR13626 did not result a substrate of P-gp and BCRP multidrug efflux transporters, which are involved in brain tumor drug resistance and represent one of the obstacles that must be overcome by a drug compound to achieve therapeutic concentrations.

Papp (A→B) (cm/s x 10^{-6})	Papp (B→A) (cm/s x 10^{-6})	(B→A)/(A→B) ratio	Efflux	Mass balance A→B (%)	Mass balance B→A (%)
17.5	**5.3**	**0.3**	**NO**	**85**	**76**

Table 1. CR13626 in vitro transport rate evaluation. Papp (apparent permeability); A (apical side), B (basolateral side).

In vivo pharmacokinetic in CD1 mice

The pharmacokinetics and brain exposure of CR13626 after single dose administration were assessed by LC-MS/MS in plasma and brain homogenate tissues of CD1 male mice (Charles River, 29-33 g weight). CR13626 was dissolved in 5% DMSO in phosphate buffer pH 7 (150 mM), 0.1 % Tween 80 and 5% Cremophor EL and the pharmacokinetics of CR13626 after single intravenous (IV) and oral (PO) administration at the dose of 3 mg/kg was evaluated in blood and brain samples collected before dosing and at 0.08 (IV only), 0.25, 0.5, 1, 2, 4, 6, and 24 hours post dosing (3 animals per time point), Figure 17.

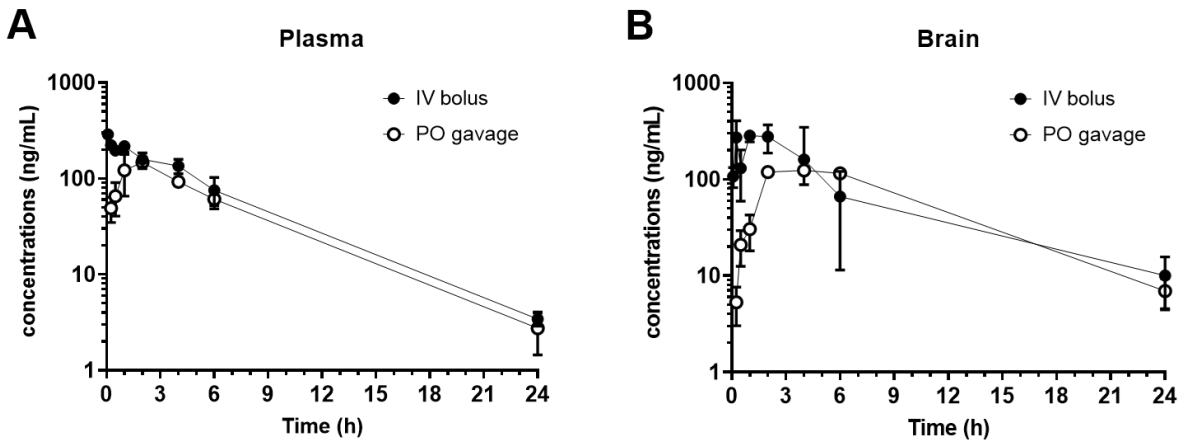

Figure 17. Pharmacokinetic profiles of CR13626 after administration in CD1 mice. Plasma (A) and brain (B) concentration time profile of CR13626 in CD1 mice after single IV and PO administration (3 mg/kg). Blood and brain samples were collected before dosing and at 0.25, 0.5, 1, 2, 4, 6, 24 hours post dose. Each data point represents the mean ± SD of three replicates.

CR13626 showed good oral absolute bioavailability (72%) and relevant brain penetration (brain/plasma ratio of 1.4), as reported in Table 2.

	Plasma					Brain					
CR13626 (3 mg/kg)	**T_{max}** (hours)	**C_{max}** (ng/ml)	**AUC** (ng*h/ml)	**$t_{1/2}$** (hours)	**F**	**T_{max}** (hours)	**C_{max}** (ng/g)	**AUC** (ng*h/g)	**$t_{1/2}$** (hours)	**F**	**B/P ratio**
IV	0.08	-	1643	3.87	-	1	-	1951	NA	-	**1.2**
PO	2	147	1183	3.98	**72%**	2	119	1676	4.8	**86%**	**1.4**

Table 2. CR13626 pharmacokinetic parameters in plasma and brain of CD1 mice treated with 3 mg/kg by the intravenous (IV) or the oral (PO) way. Parameters were estimated by curve fitting of all individual data (n=3 observations per time point). AUC: area under the curve; B/P: Brain/Plasma ratio.

The dose proportionality of CR13626 pharmacokinetics in male CD1 mice (Charles River, 27-28 g weight) was also evaluated after single oral administration in the dose range from 3 to 100 mg/kg (CR13626 suspension in 0.5% HPMC solution, HPMC E4M Premium, Colorcon). Blood and brain samples were collected before dosing and at 0.25, 0.5, 1, 2, 4, 6, 24 hours post dose and analyzed

by LC-MS/MS to determine the CR13626 concentration. Within the dose-range tested, CR13626 showed linear exposure as evidenced in Table 3 (C_{max}/dose and AUC/dose columns), demonstrating that its pharmacokinetics are independent of the administered dose.

	Plasma (P)						Brain (B)						
CR13626 (mg/kg)	**T_{max}** (h)	**C_{max}** (ng/ml)	**AUC** (ng*h/ml)	**$t_{1/2}$** (h)	**C_{max} / dose**	**AUC / dose**	**T_{max}** (h)	**C_{max}** (ng/g)	**AUC** (ng*h/g)	**$t_{1/2}$** (h)	**C_{max} / dose**	**AUC / dose**	**B/P ratio**
3	2	147	1183	3.98	49	394	2	119	1676	4.8	40	559	**1.4**
10	2	597	4352	5.71	60	435	2	895	10523	5.3	90	1052	**2.4**
30	1	1520	14693	3.82	51	490	2	1233	14509	4.9	41	484	**1.0**
100	1	3860	37060	5.95	39	371	4	4182	66832	8.3	42	668	**1.8**

Table 3. Dose-proportionality of CR13626 pharmacokinetics in plasma and brain of CD1 mice treated with ascending oral doses. Parameters were estimated by curve fitting of all individual data (n=3 observations per time point). AUC: area under the curve; B/P: Brain/Plasma ratio.

This data demonstrated the ability of CR13626 to cross the BBB and penetrate the brain, suggesting the potential of CR13626 to reach the tumor and remain at the tumor site. Taking together, such evidence warrants the further development of CR13626 as a potential new drug candidate in GBM.

4. Aims

Glioblastoma multiforme (GBM) is the most common and aggressive type of primary brain neoplasm. The lack of effective treatment options for this disease leads to a dismal prognosis and a poor median survival of patients of 15 months. The first-line treatment options are limited and include surgery, chemotherapy, and the application of alternating electrical fields of low intensity (tumor-treating fields, TTF). Due to the high infiltrative nature of the tumor, recurrence is almost universal. Owing to the aggressive nature of the tumor and the development of drug resistance during the course of disease, the treatment of GBM remains challenging and many efforts are ongoing to find a more effective therapy that provides survival benefit.

CR13626 has emerged as a novel brain permeant small molecule able to inhibit EGFR, VEGR2, Fyn, Yes, Lck, HGK and RET kinases relevant for GBM development.

Thus, my study was aimed at characterizing the in vitro and in vivo activities of CR13626 to investigate its potential for glioblastoma therapy.

The first aim of my study was to evaluate the ability of CR13626 to inhibit the ligand-induced activation EGFR and VEGFR2 receptors in cellular models (i.e., U87MG GBM cells and HUVEC-C cells, respectively) by analyzing the reduction of phosphorylation levels at specific residues of the receptors. The ability of CR136265 to inhibit Fyn kinase, one of the downstream effectors of the above-mentioned receptors, was also evaluated in a selected cellular model (Fyn/Tau co-transfected HEK-293 cells) through the measurement of the Fyn-mediated phosphorylation of Tau by a customized indirect ELISA.

Secondly, I investigated the ability of CR13626 to reduce the formation of new vessel-like structures in a HUVEC-C tube formation assay, as an indication of its antiangiogenic properties, since VEGFR2 is largely involved in promoting angiogenesis process.

Thirdly, I verified the effect of CR13626 on cellular proliferation in different 2D human glioblastoma cell lines (i.e., U87MG, U373, U87MG vIII and T98G cells) harboring some of genetic alterations/mutations present in GBM tumor cells. I also evaluated the activity of CR13626 on HEK-293 cells to assess the effect of the compound on a non-tumoral human cell line and exclude a potential toxicity on healthy cells.

I also investigated the efficacy of CR13626 in reducing cellular proliferation in U87MG cells cultured as 3D spheroids, because they are more representative of the complexity of tumor environment and constitute a more reliable model to assess cellular response to a drug treatment.

Finally, the in vivo antitumor activity of CR13626 was evaluated in an orthotopic xenograft mouse model of GBM based on the injection of U87MG-Luciferase cells in nude mice. The schedule of oral treatment with CR13626 (i.e., 50 mg/kg/daily for ten days) was chosen as a stringent protocol to assess the activity of the compound, if present, avoiding false positive results. In a satellite group of tumor-bearing mice treated with CR13626 (50 mg/kg/daily for 5 days), the plasma and brain concentrations of CR13626 were also determined.

5. Materials and Methods

I hereby declare that part of the following "Materials and Methods" section has been already published in the paper: Galimberti C, Piepoli T, Letari O, Artusi R, Persiani S, Caselli G, Rovati LC. CR13626: a novel oral brain penetrant tyrosine kinase inhibitor that reduces tumor growth and prolongs survival in a mouse model of glioblastoma. Am J Cancer Res. 2021 Jul 15;11(7):3558-3574.

Cell lines and culture conditions

The human glioblastoma cells lines were obtained as follow: U87MG and T98G cell lines were from ATCC, the U373 cell line was from ECACC and the U87 MG vIII cell line was purchased from Celther Polska. Cells were cultured in DMEM medium supplemented with 10% FBS and 1% Pen-Strep (U87MG, T98G and U373) or in MEM medium supplemented with 10% FBS, 1% Pen-Strep, 0.2% Gentamycin and 200 µg/ml G418 (U87 MG vIII) at 37°C with 5% CO_2.

The human embryonic kidney 293 cells (HEK-293, from ATCC) were cultured in DMEM medium supplemented with 10% FBS at 37°C with 5% CO_2. The human umbilical vein endothelial cells (HUVEC-C, from ATCC) were grown in medium F12K + 0.1 mg/ml Heparin + 0.05 mg/ml ECGS (Sigma, #E2759) + 10% FBS at 37°C with 5% CO_2.

Cellular phosphorylation assays

EGF-induced EGFR (Y1068)-phosphorylation

U87MG cells were seeded at $3x10^5$ cells/well in 12w microplates. After 24 hours, starvation was induced overnight in medium DMEM + 0.1% FBS (medium starvation). At the end, cells were treated for 1 hour with CR13626 or reference compound (erlotinib, Sigma, #CDS022564) diluted in medium starvation (DMSO 0.1% final concentration) and then stimulated for 15 min with EGF (Sigma, #E9644, 10 ng/mL final concentration in medium starvation). At the end, cells were lysed in M-PER lysis buffer containing 1x Protease/Phosphatase inhibitors cocktail (Cell Signaling, #5872S) and samples were sonicated. 10 µg of total protein were separated by SDS-PAGE followed by transfer to a PVDF membrane. Membranes were blocked with Blocking buffer (Thermo Scientific #37542) and probed overnight with primary antibodies specific to phospho-EGFR (p-Tyr1068, Cell Signaling, #2234), EGFR (Cell Signaling, #2239) or Actin (ThermoFisher, #MA5-11869). Membranes were washed and protein bands visualized using appropriate HRP-conjugated secondary antibodies and chemiluminescent detection. Densitometric analysis of sample lanes were performed by

ImageQuant TL software (GE Healthcare Life Sciences). Each sample value was normalized by respective Actin and the relative level of protein phosphorylation was determined by normalizing the phospho-protein signal to that of the total protein.

VEGF-induced VEGFR2 (Y1175)-phosphorylation

HUVEC-C cells were seeded at $6x10^4$ cells/well in 24w microplates. After 24 hours, starvation was induced overnight in medium F12K + 0.1 mg/ml Heparin + 0.5% FBS (medium starvation). At the end, cells were treated for 1 hour with CR13626 or reference compound (axitinib, SellekChem, #S1005) diluted in medium starvation (DMSO 0.1% final concentration) and then stimulated for 5 min with VEGF stimuli (Sigma, #V7259, 50 ng/mL final concentration in medium starvation). At the end, cell lysates were obtained as described above. 15 µL of each sample were separated by SDS-PAGE followed by transfer to a PVDF membrane. Membranes were blocked as reported and probed overnight with primary antibodies specific to phospho-VEGFR (p-Tyr1175, Cell Signaling, #2478), VEGFR (Cell Signaling, #9698), phospho-Fyn/Src (p-Tyr416, Cell Signaling, #2101), Fyn (Cell Signaling, #4023) or Actin (ThermoFisher, #MA5-11869). Membranes were washed and protein bands visualized using appropriate HRP-conjugated secondary antibodies and chemiluminescent detection. Densitometric analysis of sample lanes were performed by ImageQuant TL software (GE Healthcare Life Sciences). Each sample value was normalized by respective Actin and the relative level of protein phosphorylation was determined by normalizing the phospho-protein signal to that of the total protein.

Tau phosphorylation upon Fyn activation

HEK-293 cells were seeded at $6x10^5$ cells/well in 12w microplates coated with poly-D-lysine hydrobromide (PDL). The day after, the expression of both FynB and Tau proteins was induced for 24 hours through the co-transfection of cells with the respective encoding vectors by using the Lipofectamine 3000 Transfection Reagent (Life Technologies, # L3000_008). At the end of the incubation, medium was replaced and the treatment with CR13626 or the reference saracatinib (both diluted in medium DMEM+10%FBS, DMSO 0.1% final concentration) was performed for 24 hours. At the end, lysates of cells were then obtained by adding M-PER lysis buffer, sonicated, and stored at -80°C. Phosphorylation of Tau was investigated by a customized indirect-ELISA as follow.

Lysates were diluted in coating buffer (Sigma, #C3041) at the concentration of 30 µg/mL; 3 µg/100 µL/well of total protein were coated overnight at 4°C in a 96w plate (NUNC Maxisorp). At the end, wells were washed 3x in PBST, then blocked in PBS-1% BSA for 1 hour at room temperature with gentle shaking. Wells are then washed 3x in PBST and incubated with the primary antibodies specific to phospho-Tau (p-Tyr18, MediMabs, #MM-0194-P) or anti-total Tau (Sigma Aldrich, #MAB2239) for 2 hours at room temperature with gentle shaking. After 3x washing with PBST, wells were incubated for 1 hour with the HRP-conjugated anti-mouse secondary antibodies (Jackson Immuno Research, #115-035-071) and gentle shacked. At the end, wells were washed 3x in PBST and 100 µL/well of HRP-substrate TMB (3,3',5,5'-tetramethylbenzidine) were added. The colorimetric reaction was stopped by adding sulfuric acid, and the signal was measured at 450 nm by Multiskan FC Microplate Photometer (ThermoFisher Scientific). The effect of the compounds was calculated by using the ratio pospho-Tau/Total-Tau of treated wells compared to controls (not treated cells) and expressed as percentage. The IC_{50} values were calculated by GraphPad Prism Software.

In vitro endothelial cell tube-formation assay

The assay was performed using HUVEC-C cells and the tube formation assay kit (Abcam, #ab204726). Briefly, 50 µL/well of the extracellular matrix (ECM) solution were added to an empty 96w culture plate and incubated for 1 hour at 37°C to allow the solution to form a gel. Then, $2x10^4$ cells/100 µL were seeded to each well, followed by the addition of 25 µL/well of a 100x mix solution containing PMA stimuli (phorbol 12-myristate 13-acetate, Sigma, #P1585, 20 nM final concentration) +/- inhibitors (CR13626, axitinib, erlotinib and vinblastine) in medium F12K + Heparin 0.1 mg/ml + FBS 5% (DMSO 0.1% final concentration). Cells were incubated for 18 hours at 37°C with 5% CO_2 to allow tube formation. At the end, cells were washed once and stained according to the manufacturer's instructions. The formation of vessels-like structures was examined using light microscopy by EVOS microscope.

Cell proliferation assays

2D cultures

The effects of CR13626 on cellular proliferation were investigated in different human GBM cell lines (U87MG, U373, U87MG vIII) as 2D cultures by ViaCount assay (Millipore). $2x10^4$ cells/well were plated in a 24w in DMEM 10%. After 72 hours the cells are treated with the CR13626 for 24, 72h or 7 days, with a medium replacement on day4. At the end of the incubation the analysis was performed according to kit instructions.

3D spheroids

The effects of CR13626 on cellular proliferation were assessed in U87MG 3D spheroids. First, U87MG tumor cells spheroids were grown in MW96 CELLCARRIER SPHEROID ULA-96 plates. 1500 cells/well were seeded in medium containing or not CR13626 and incubated for 72 hours. At the end spheroids were analyzed by the CellTiter Glo 3D Cell Viability assay (Promega), according to kit instructions.

Orthotopic mouse model of GBM

The study was performed at Accelera Srl laboratories (Nerviano, Italy). The protocol A14D6.EXT.16 was approved by the Italian Authorities. Human GBM U87MG cells (source ATCC) were engineered to express the luciferase gene, Luc2 (pGL4, Promega). On the implantation day (Day 0), U87MG-luc cells ($1x10^6$ / 2 µL of PBS), were injected into the brain (right hemisphere) of athymic nude (Hsd:AthymicNude-Foxn1nu) male mice from Charles River aged 5 weeks (23.6-32.2 g weight). Briefly, anesthetized mice (zoletil + xilor 2% anesthesia) were placed under the stereotaxic apparatus, gently fixed with ear bars into the head holder, and then the right coordinates for injection were chosen (+ 0.5 mm anterior and + 2.2 mm lateral, right). A small burr hole was done by a microdrill, and cells were injected at 3 mm depth. The burr hole was closed using bone wax and the wound closed with sterile autoclips. Mice, after surgery were monitored until wakening and complete recovery from anesthesia. Eight days from tumor cell implantation, mice were subjected to the first bioluminescence (BLI) detection. According to the BLI values, animals were randomized and distributed into four experimental groups (8 mice/group). The oral treatment with CR13626 (50

mg/kg/daily suspended in 0.5% HPMC solution, HPMC E4M Premium, Colorcon) or vehicle started on day 9 post implantation and continued for 10 days. Tumor growth was evaluated by in vivo BLI measurements at the end of dosing (day 19) and during follow-up (days 26 and 33).

Survival of animals was also evaluated. Mice were monitored daily for mortality and clinical signs (including body weight). Toxicity was evaluated based on body weight reduction and signs of distress caused by the treatment. Animal survival was assessed using a Kaplan–Meier survival curve and Mantel-Cox test was used to determine differences between groups. The analysis was performed using GraphPad Prism (GraphPad Software Inc.).

Satellite group: six mice intracranially injected with the U87MG-luc cells were treated orally for 5 days with CR13626 (50 mg/kg/daily suspended in 0.5% HPMC solution, HPMC E4M Premium, Colorcon), starting from day 37 post cell injection and sacrificed 3 hours after the last dosing. The determination of CR13626 in plasma and brain samples was assessed by liquid chromatography-tandem mass spectrometry (LC-MS/MS) on an API 4000 Qtrap ESI instrument in the positive ion mode) as follow. 500 µL of blood were taken from retro-orbital plexus under deep anesthesia (2% isoflurane in pure oxygen) and collected in tubes with anticoagulant. Samples were centrifuged and plasma was stored at -80°C. CR13626 was extracted from plasma through a protein precipitation method by adding 200 µL of methanol to 20 µL of plasma in 96-deep well plates (Greiner), followed by mixing and centrifugation for 15 min at 3700 rpm at 4°C. To determine CR13626 concentrations in brain, each mice brain was removed, washed twice in saline solution, dried with blotting paper, weighted, cut in half, and frozen at -80°C. One hemisphere was weighted and homogenized through acoustic disruption (Covaris AFA S2), by adding a volume of acidic solution (formic acid 0.1% in water) corresponding to three times the weight (mL/g) of the hemisphere. Each homogenized-containing tube was processed with 6 repeated cycles of the following two run conditions: 1) 20 sec. 50% duty cycle, 10 intensity, 1000 cycles/burst, and 2) 10 sec. 50% duty cycle, 10 intensity, 100 cycles/burst. Then, 30 µL of the extracted solution were added to 0.23 mL of methanol, mixed, and centrifuged for 5 min at 13500 rpm at 4°C. The supernatant was transferred to a 96-deep well plate (Axygen) and injected into the LC-MS/MS system.

Ethical approval

All procedures performed in studies involving animals were in accordance with the current Italian legislation (legislative Decree March 4th, 2014 n. 26) enforcing the EU Directive 2010/63/EU on the protection of animals for biomedical research. All the studies were approved by Italian authorities.

Statistical Analysis

GraphPad Prism 7 (GraphPad Software, Inc., La Jolla, CA, USA) was used for the data statistical analysis. The effects of CR13626 on U87MG and HEK-293 cellular proliferation were presented as the mean ± SD. The inter-group differences were evaluated by one-way ANOVA. The graph showing the comparison between the effects of CR13626 at 10 µM with those of comparators (i.e., erlotinib and saracatinib) on U87MG human GBM cells at 6-7 days of treatment, was obtained by plotting data expressed as mean ± SEM and the inter-group differences were defined through "Brown-Forsythe and Welch's ANOVA test". The activities of CR13626 on the proliferation of different human GBM cell line (i.e., T98G, U87MG vIII, and U373) were presented as mean ± SD and the inter-group differences were evaluated by one-way ANOVA with Tukey's multiple comparisons test ($p<0.05$ was considered statistically significant). The data showing the effect of CR13626 on the viability of U87MG cells cultured as 3D spheroids were presented as mean ± SEM and the inter-group differences were evaluated by one-way ANOVA. The data showing the comparison between the effect of CR13626 with that of TMZ were expressed as mean ± SD and the inter-group differences were evaluated by one-way ANOVA.

In the in vivo study animals were randomly assigned to each group according to BLI values at day 8 after U87 MG-Luc injection (mean values at randomization of $9x10^6$ ph/s/cm^2/sr). Tumor progression was evaluated through the measurement of BLI at three different data points (day 19, 26 and 33). Individual values were reported as continuous lines and the geometric mean was also included in the graph as black lines (dotted Controls (or Vehicle), continuous CR13626). Animal survival was evaluated using a Kaplan–Meier survival curve and the statistical significance between groups was evaluated by Mantel-Cox test ($p<0.05$ accepted as significant).

6. Results

I hereby declare that part of the following "Results" section has been already published in the paper: Galimberti C, Piepoli T, Letari O, Artusi R, Persiani S, Caselli G, Rovati LC. CR13626: a novel oral brain penetrant tyrosine kinase inhibitor that reduces tumor growth and prolongs survival in a mouse model of glioblastoma. Am J Cancer Res. 2021 Jul 15;11(7):3558-3574.

CR13626 biochemical characterization on selected kinase

Upon the binding of specific ligands to tyrosine kinase receptors, several residues located in the intracellular domain of the receptors were phosphorylated, leading to the activation of receptors and to the recruitment of downstream effectors that mediate signals into the cell and activate specific biological pathways. Given the inhibitory activity of CR13626 towards some RTKs (i.e., EGFR and VEGFR2) and Fyn kinase, the ability of CR13626 to inhibit those enzymes was evaluated in different cellular models.

Effect of CR13626 on ligand-induced phosphorylation of EGFR

The effect of CR13626 on EGFR activation was determined in the human GBM cell line U87MG using erlotinib as standard EGFR inhibitor ([Moyer et al., 1997]). Elevated levels of EGFR phosphorylation at residue Y1068 have been detected in tissue samples of GBMs [Tanaka et al., 2011]. As shown in Figure 18, CR13626 reduced the ligand-induced activation of EGFR receptor at residue Y1068 in a concentration dependent fashion, with an IC_{50} value of 3 µM. The EGFR selective reference inhibitor erlotinib was able to inhibit the ligand-induced phosphorylation of EGFR, as expected (Figure 18).

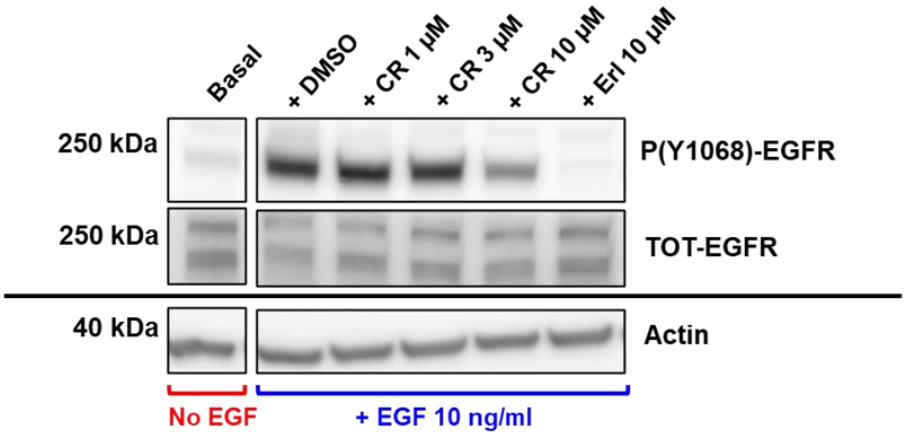

Figure 18. Effect of CR13626 on EGF-induced phosphorylation of EGFR at residue Y1068. Immunoblot analysis of EGFR phosphorylation on tyrosine residue 1068 (P(Y1068)), total EGFR (TOT-EGFR), and Actin (loading control) in human GBM U87MG cell lysates. Cells were serum-starved overnight and then treated with DMSO 0.1% or indicated compounds (CR13626, CR and erlotinib, Erl) for 1 hour. Cells were then stimulated with 10 ng/ml EGF for 15 min.

Effect of CR13626 on ligand-induced phosphorylation of VEGFR2

The effect of CR13626 on VEGFR2 activation was determined in HUVEC-C cells using axitinib as standard VEGFR inhibitor ([Rugo et al., 2005]). CR13626 inhibited the ligand-induced receptor activation at residue Y1175 in a concentration dependent manner, reaching a total signal inhibition at 1 µM (Figure 19, panel A). As expected, axitinib also inhibited the VEGFR2 phosphorylation induced by VEGF, but it did not show any effects on the activation of Fyn/Src, probably due to the presence of collateral pathways (Figure 19, panel A). On the contrary, CR13626 also inhibited the Fyn/Src phosphorylation, suggesting a potential stronger impact on the intracellular signal transmission upon VEGFR2 activation (Figure 19, panel A). The densitometric analysis allowed the determination of the relative optical density for each sample (i.e., each phospho and total sample lines normalized with the respective value of Actin) and the further calculation of the ratio between the phospho and total protein signals. The corresponding ratio values for each condition were used to evaluate the effect of the treatment with CR13626 or axitinib on VEGFR2 and Fyn/Src phosphorylation respect to the basal (i.e., cells which received VEFG stimuli and treated with DMSO 0.1% final only), Figure 19, panel B. The resulting histogram emphasized the results displayed by western blot images and showed a complete inhibition of VEGFR2 phosphorylation at the residue Y1175 after the treatment with both CR13626 and axitinib compounds, whereas only CR13626 was able to reduce the phosphorylation levels at the Y416 residue of Fyn/Src (Figure 19, panel B).

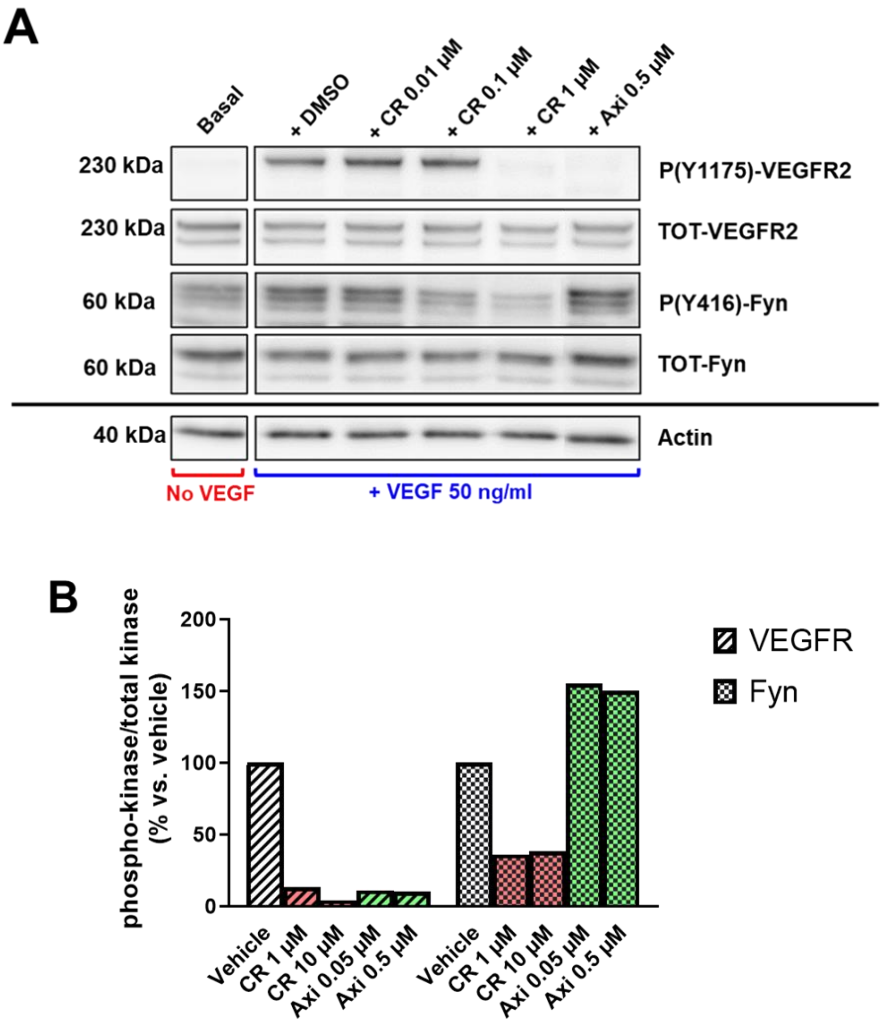

Figure 19. Effect of CR13626 on VEGF-induced phosphorylation of VEGFR2 at residue Y1175. A) Immunoblot analysis of VEGFR2 phosphorylation on tyrosine residue 1175 (P(Y1175)), total VEGFR2 (TOT-VEGFR2), Fyn/Src phosphorylation on tyrosine residue 416 (P(Y416)), total Fyn (TOT-Fyn) and Actin (loading control) in human HUVEC-C cell lysates. Cells were serum-starved overnight and then treated with DMSO 0.1% or indicated compounds (CR13626, CR and axitinib, Axi) for 1 hour. Cells were then stimulated with 50 ng/ml VEGF for 5 min. B) Densitometric analysis of VEGFR2 and Fyn/Src immunoblot images.

Effect of CR13626 on Fyn-mediated phosphorylation of TAU

To better define the potency of CR13626 on Fyn kinase in a cellular model, the Fyn-mediated phosphorylation levels of Tau in Fyn/Tau co-transfected HEK-293 cells was evaluated. Indeed, it has been demonstrated that Fyn kinase is specifically responsible of the phosphorylation of Tau at the tyrosine residue 18 (Y18) and this modification is present in the neurofibrillary tangles in Alzheimer's disease (AD) brain, giving to Fyn a fundamental role during the neurodegenerative process of AD [Lee et al., 2004]. Saracatinib (Src family inhibitor [Hennequin et al., 2006]) was also tested and used as reference inhibitor of Fyn. As represented in Figure 20, after 24h hours of treatment, CR13626

inhibited the phosphorylation of Tau at Y18 residue, with an IC_{50} value of 401 nM, being almost 2-fold more active than the reference saracatinib. The data shown in Figure 20 are derived from the simultaneous nonlinear fitting analysis of several independent experiments performed in duplicate (n = 4 experiments for CR13626 and n = 3 experiments for saracatinib).

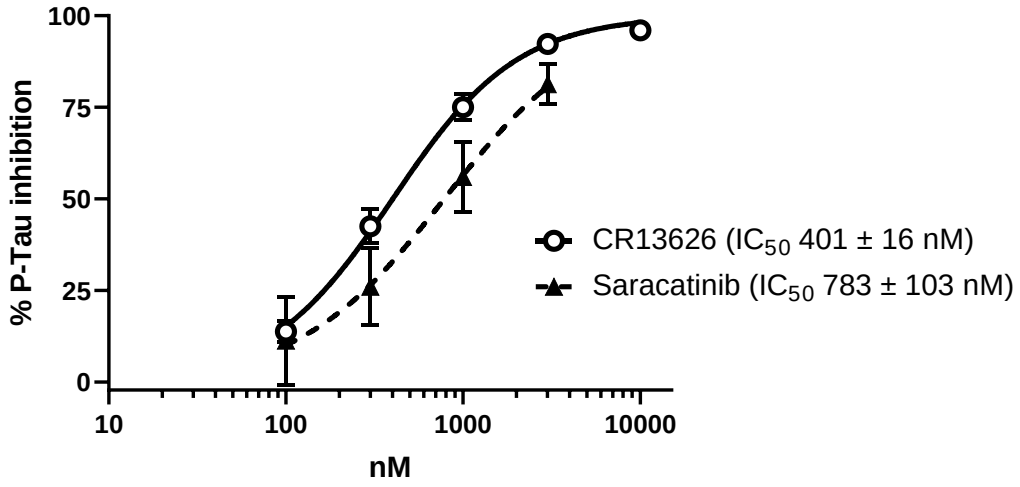

Figure 20. Effect of CR13626 on Fyn-mediated phosphorylation of Tau. A representative graph describing the activity of CR13626 (CR) compared to saracatinib (Sar) on Tau phosphorylation at Y18 residue in Fyn/Tau over-expressing HEK-293 cells. The treatment of cells with CR13626 or saracatinib was performed for 24 hours. Data points are the mean ± SD from 4 (CR13626) and 3 (Saracatinib) independent experiments performed in duplicate.

CR13626 effect on angiogenesis

The ability of CR13626 to reduce the formation of new vessel-like structures was evaluated in a HUVEC-C tube formation assay, as an indication of its antiangiogenic properties (Figure 21). It has been demonstrated that the PMA-induced tube formation is reduced by either inhibiting the VEGF receptor kinase or VEGF knockdown [Xu et al., 2008]. Vinblastine (inhibitor of microtubule formation [Bijman et al., 2006]) and axitinib (VEGFR inhibitor [Rugo et al., 2005]) were used as reference inhibitors, whereas erlotinib (EGFR inhibitor [Moyer et al., 1997]) was included as negative control. CR13626 decreased the PMA-induced tube formation in a dose-dependent manner, indicating a potential effect of the compound on the angiogenic process (Figure 21).

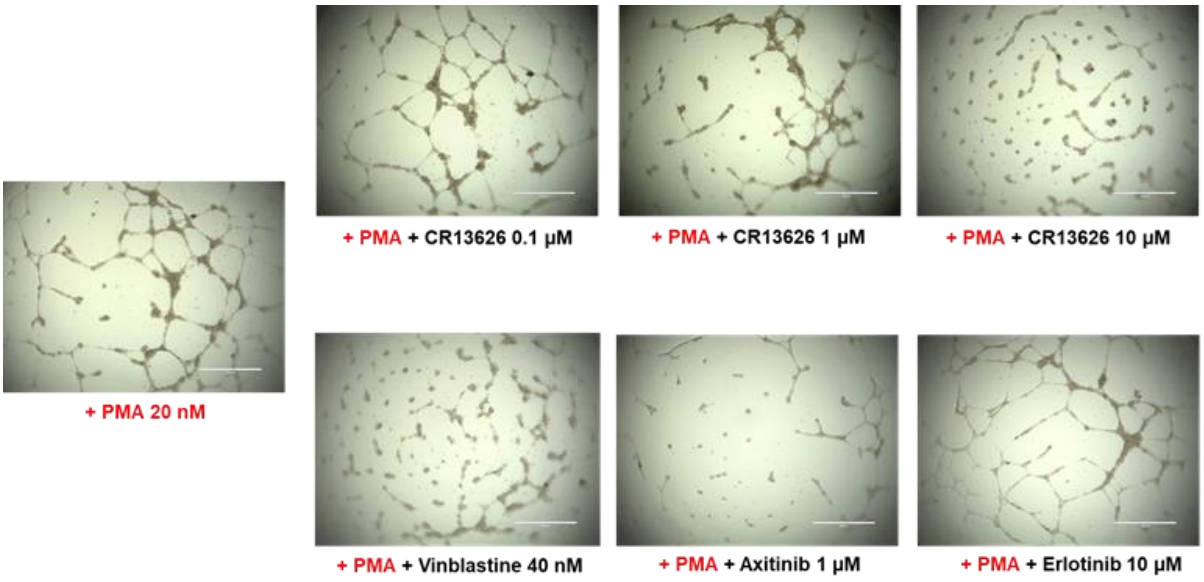

Figure 21. Effect on CR13626 on the formation of tube-like structures induced by PMA. Representative phase-contrast images of HUVEC-C tube formation on ECM after 18 hours of treatment. Scale bar = 1000 µm.

CR13626 activity on proliferation of different cell lines cultured as 2D

Effect of CR13626 on U87MG glioblastoma cells compared to the non-tumoral HEK-293 cells

CR13626 preferentially reduced the proliferation of the U87MG human GBM cells with respect to non-tumoral cells (Figure 22). The 24 hours of treatment with CR13626 1 µM led to more than 50% decrease of the viability of U87MG cells. Conversely, when CR13626 has been tested in the same conditions on the human non-tumoral HEK-293 cells, it did not show any effect on cellular proliferation (Figure 22).

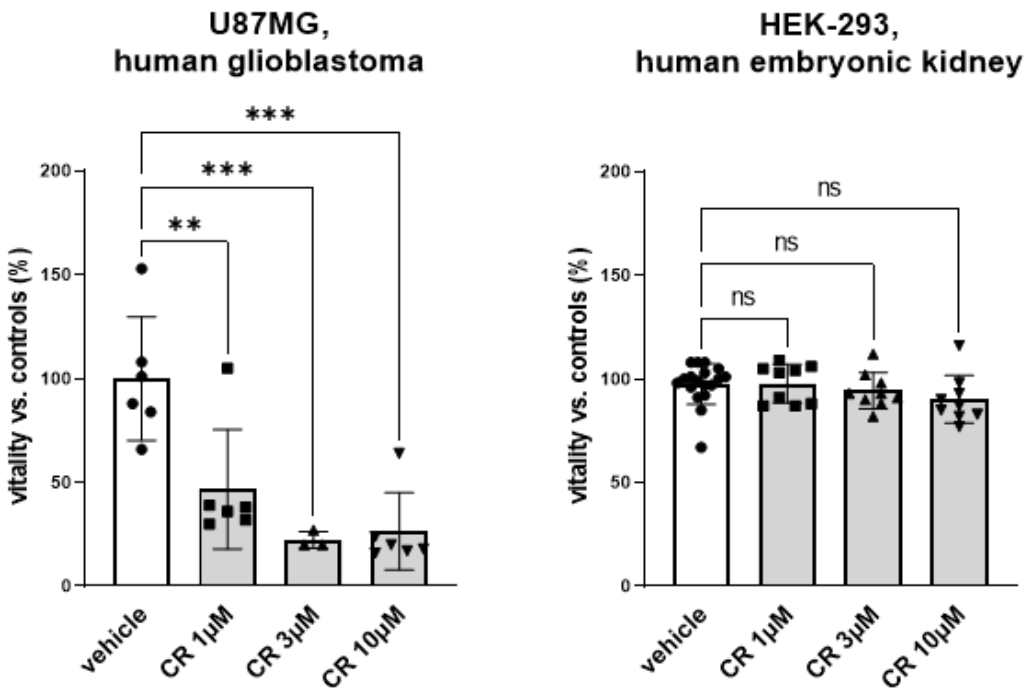

*Figure 22. Effect of CR13626 (CR) on U87MG human GBM cells compared to HEK-293 cells. Percent of residual cell vitality in the presence of CR13626 (single values and mean ± SD), 24 hours of treatment); ** P<0.01; ***P<0.001 by one-way ANOVA.*

Effect of CR13626 on U87MG glioblastoma cells compared to erlotinib and saracatinib

The ability of CR13626 to reduce the proliferation of U87MG cell line was compared to that of erlotinib (EGFR inhibitor [Moyer et al., 1997]) and saracatinib (Src family inhibitor [Hennequin et al., 2006]) after 6-7 days of treatment. CR13626 showed a higher efficacy than erlotinib, while the Src family inhibitor saracatinib resulted inactive (Figure 23).

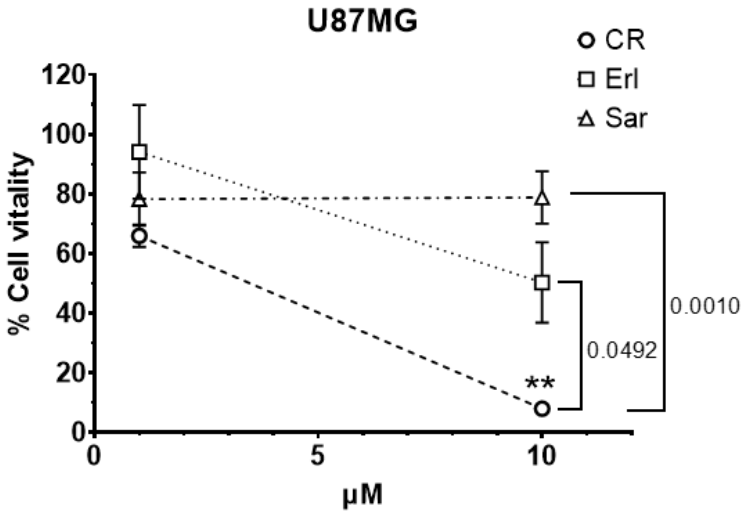

*Figure 23. Effect of CR13626 on U87MG human glioblastoma cells in comparison with erlotinib (Erl) and saracatinib (Sar). Cells were treated for 6-7 days (medium replacement at day 4). Data are expressed as mean ± SEM, n=6; ** p<0.01 vs vehicle (100 % ± 10.5); on the right p values at 10 µM vs. comparators "Brown-Forsythe and Welch's ANOVA test" are indicated.*

Effect of CR13626 on different human glioblastoma cell lines

Since glioblastoma is characterized by a wide cellular heterogeneity, the effect of CR13626 on the proliferation of three more human GBM cell lines commercially available (U373, U87MG vIII and T98G) was also evaluated. Indeed, these cell lines harbor some of the genetic alterations/mutations present in GBM tumor cells.

U373 cells share with U87MG cells the expression of the wild-type form of EGFR but, if the latter has deletions in PTEN and CDKN2A/2B genes, the former holds the amplification of PDGFRα and VEGFR2. Thus, the U87MG and U373 cells differ significantly in their gene expression fingerprints and show phenotypes resembling the neuronal and mesenchymal characters of GBM, respectively [Motaln et al., 2015], even if the neuronal nature of U87MG cells has been recently challenged by Lane et al., 2019. U87MG vIII cells express high levels of the constitutive active mutant form of EGFR (EGFRvIII). This ligand-independently activated form results from the deletion of exon 2-7 in the extracellular domain of the EGF receptor and represents the most frequent deletion occurring in GBM. Wild type EGFR and EGFRvIII elicit differential signaling cascades. It has been demonstrated that EGFR amplification is acquired early by GBM cells, contributing to invasive processes. Then, upon tumor progression, GBM cells acquire EGFRvIII mutation which contributes to the angiogenic switch and a more aggressive tumor growth [Eskilsson et al., 2018]. Finally, T98G are TMZ resistant cell line [Lee et al., 2016].

CR13626 reduced the proliferation of all the cells cited above, being more effective than comparators. Moreover, the effects of CR13626 were maintained also after 7 days of treatment (Figure 24).

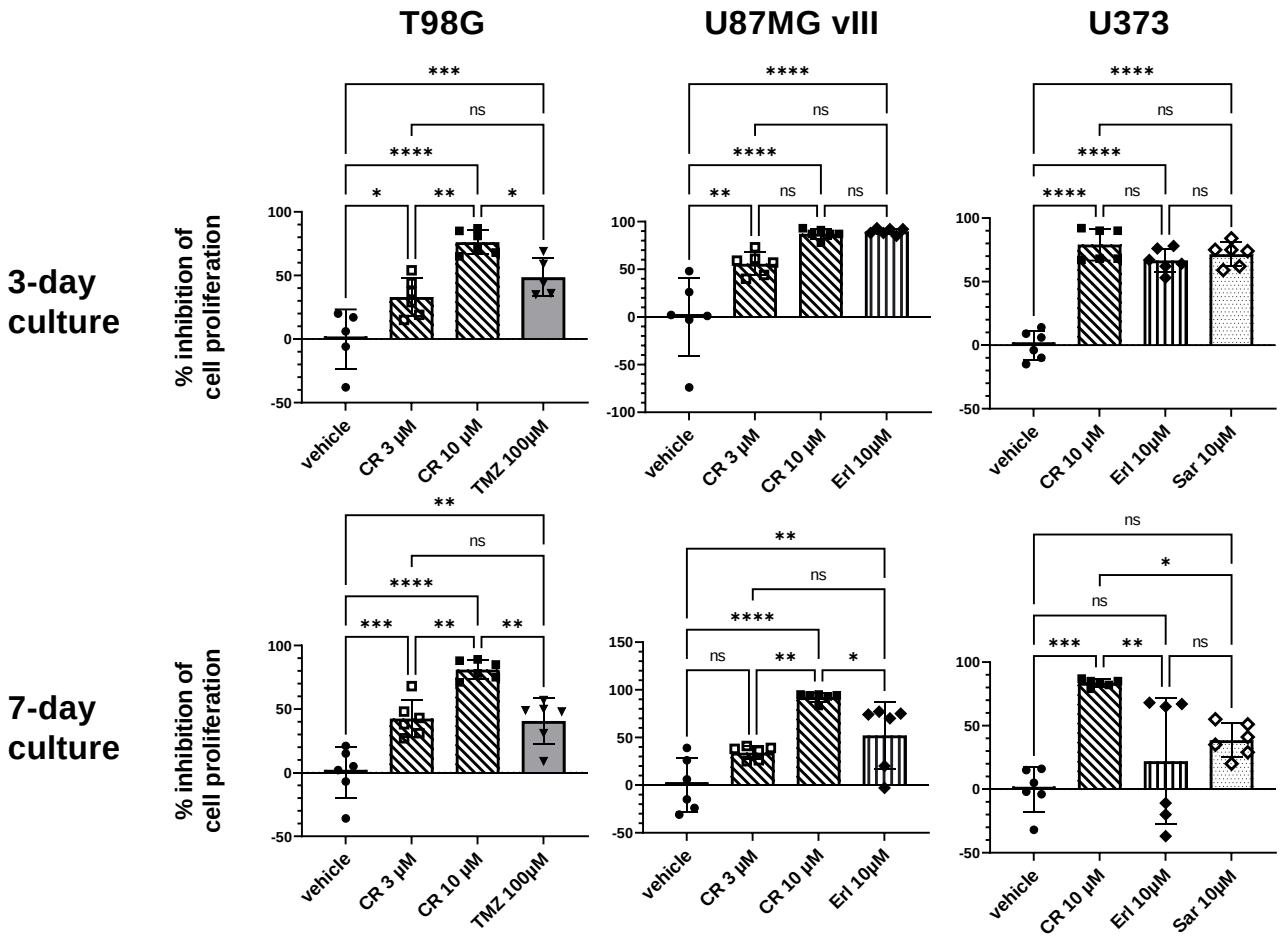

*Figure 24. Effect of CR13626 on different human GBM cell lines commercially available: T98G (TMZ resistant), U87MG vIII (constitutively activated EGFR form, EGFRvIII), and U373 (mesenchymal GBM features). CR13626 was tested in comparison with temozolomide (TMZ), erlotinib (Erl) and saracatinib (Sar). Percent of inhibition of proliferation after 3 or 7 days of treatment. Single values and mean ± SD; ** P<0.01; ***P<0.001 by one-way ANOVA and Tukey test.*

CR13626 activity on proliferation of U87MG cell line cultured as 3D spheroids

Since 3D cell spheroids are more representative of the complexity of tumor environment with respect to 2D cultures, therefore representing a more reliable model to assess cellular response to a drug treatment, the efficacy of CR13626 in reducing cellular proliferation was also evaluated in

U87MG cells cultured as 3D spheroids. After 3 days of treatment, CR13626 decreased the proliferation of U87MG cells in a dose-dependent fashion, showing an GI_{50} value of 4.5 µM (Figure 25, panels A and B).

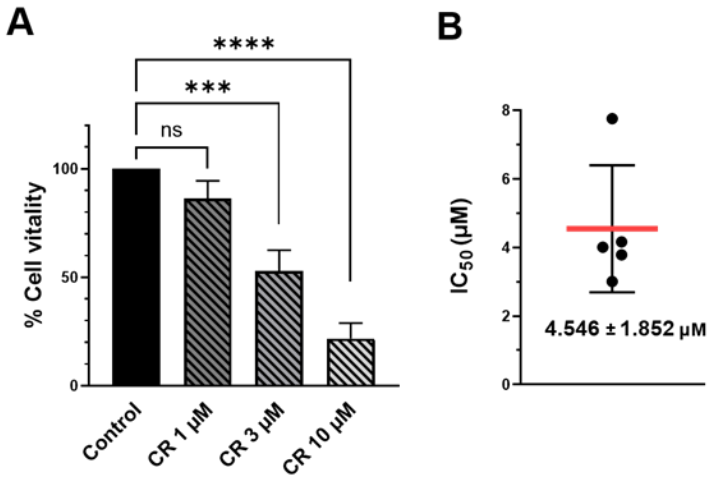

*Figure 25. Effect of CR13626 (CR) on the proliferation of U87MG glioblastoma cell line cultured as 3D spheroids. A) Percent of residual cell vitality of U87MG cells in presence of CR13626 (mean ± SEM of 5 experiments performed with n=5-6 spheroids/condition, 3 days of treatment); ***P<0.001; ****P<0.0001 by one-way ANOVA. B) GI_{50} values, single values and mean ± SD.*

In the same culture conditions, the standard of care TMZ was also able to reduce U87MG spheroids proliferation, even if at higher concentrations with respect to CR13626, Figure 26.

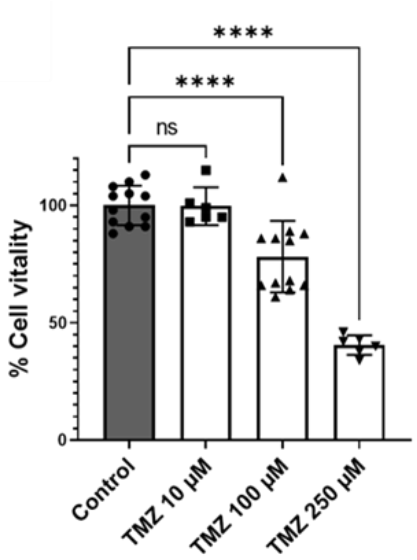

*Figure 26. Effect of temozolomide (TMZ) on the proliferation of U87MG glioblastoma cell line cultured as 3D spheroids. The graph reports the single spheroid values (percent of residual cell vitality in the presence of TMZ, 3 days of treatment) from two combined experiments and the mean ± SD; ****P<0.0001 by one-way ANOVA.*

CR13626 pharmacokinetics in tumor bearing mice

The brain tropism of CR13626 was evaluated in a satellite group of tumor bearing mice (U87MG-Luc mice) treated orally once a day for five consecutive days at the dose of 50 mg/kg, as described in materials and methods. CR13626 plasma and brain tissues concentrations were obtained at 3 hours from the last dose (i.e., the time necessary for CR13626 to reach the maximum brain concentration in CD1 mice, Figure 17). As reported in Table 4, the results confirmed the brain tropism of CR13626, and the exposure observed in CD1 mice (Table 2). Moreover, CR13626 preferentially accumulates in the right brain hemisphere, where the U87MG-Luc cells were injected, and tumor developed (Figure 27). These data confirmed the ability of CR13626 to cross the BBB and penetrate the brain, suggesting the potential of CR13626 to reach the tumor and remain at the tumor site.

Nude Mouse ID (50 mg/kg)	**Plasma (ng/ml)** (at 3h)	**Brain right hemisphere (tumor bearing)**		**Brain left hemisphere (tumor free)**	
		(ng/g)	**Brain/Plasma ratio**	**(ng/g)**	**Brain/Plasma ratio**
4707	698	1020	1.46	1163	1.67
4715	352	2213	6.29	888	2.52
4719	399	852	2.14	881	2.21
4731	536	804	1.5	901	1.68
Mean	496.25	1222.25	2.85	958.25	2.02
SD	155.51	666.96	2.32	136.75	0.42

Table 4. CR13626 concentrations (ng/g) in tumor bearing nude mice. Compound's concentrations (ng/g) and tissue weight (mg) values were measured in right (R) and left (L) brain hemispheres of tumor bearing nude mice (n=4). CR13626 oral treatment was 50 mg/kg/daily/5 days. 3h after the last dose all mice were euthanized, plasma and brain tissues collected, and the two brain hemispheres separated. Samples were analyzed by LC-MS/MS.

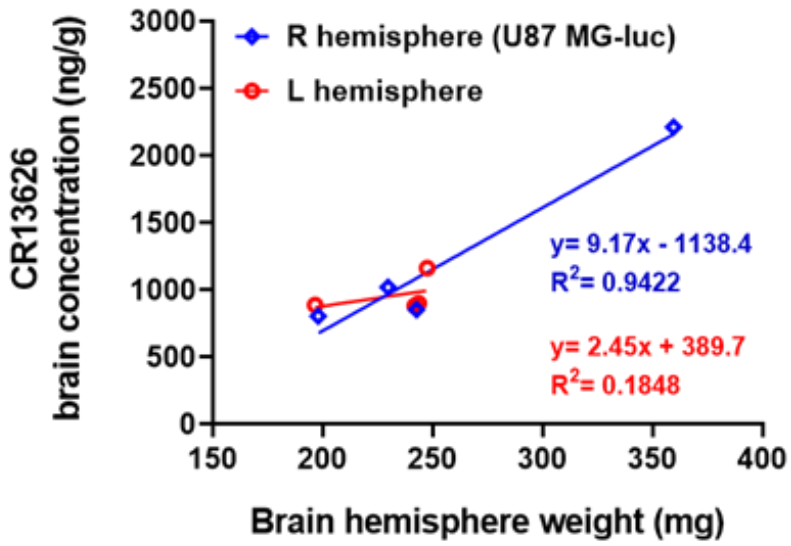

Figure 27. Correlation between CR13626 concentrations (ng/g) and tissue weight (mg) measured in the right (R) and left (L) brain hemispheres of tumor bearing mice (blue and red symbols, respectively) orally treated with the dose of 50 mg/kg/daily/5 days. Brain samples were collected 3 hours after the last dosing.

CR13626 antitumor efficacy in tumor bearing mice

The in vivo antitumor activity of CR13626 was determined in a mouse model of GBM obtained by the orthotopic injection of U87 MG-Luciferase (U87 MG-Luc) GBM cells in nude mice, as described in materials and methods. CR13626 oral treatment started on day 9 post-implantation and continued for 10 days (50 mg/kg/daily). This stringent protocol of treatment was chosen to allow the assessment of the activity of CR13626, if present, avoiding false positive results. Bioluminescence (BLI) measurements showed a time-dependent reduction of tumor growth in the CR13626-treated group, reaching 60% on the last BLI evaluation, 33 days post-implantation (i.e., 15 days after the end of dosing), as illustrated in Figure 28. Due to the high variance, no statistics could be attempted on radiance data.

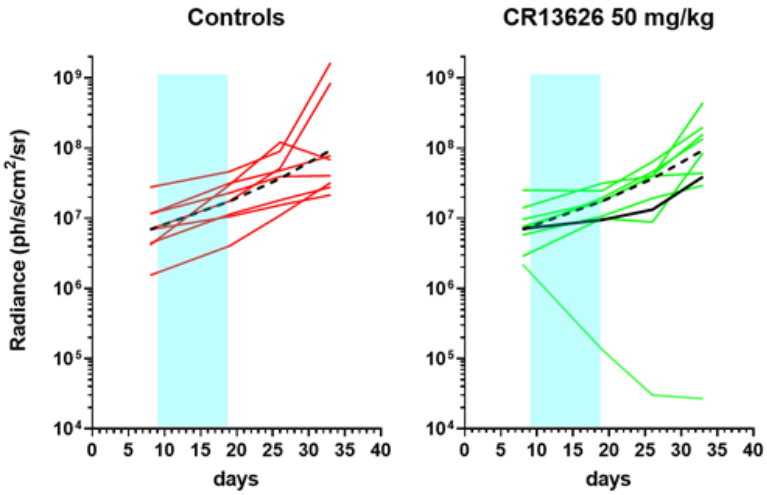

Figure 28. CR13626 effect on tumor growth in a U87MG-Luc mouse model of glioblastoma. Randomization of animals was performed (n=8/group) according to bioluminescence (BLI) values at day 8 after U87 MG-Luc injection (mean values at randomization of $9x10^6$ ph/s/cm2/sr). One day later, animal started oral administration of vehicle (Controls) or CR13626 (50 mg/kg/daily/10 days, shaded area). Tumor progression was evaluated through the measurement of BLI at the end of dosing (day 19) and during follow-up (days 26-33). BLI is expressed as Radiance (ph/s/cm2/sr). Individual values and geometric mean (black line, continuous CR13626, dotted Controls (Vehicle)). Dosing of CR13626 started on day 9 and lasted 10 days only (shaded areas).

After the last BLI measurements, animals were monitored to assess survival. Tumor growth inhibition translated into an increase of 25% of the median survival time of animals treated with CR13626 compared to the vehicle group ($p<0.05$), Figure 29. The observed antitumor effects agreed with the exposure of tumor-bearing mice to CR13626, which was above the TKs in-vitro IC_{50} values.

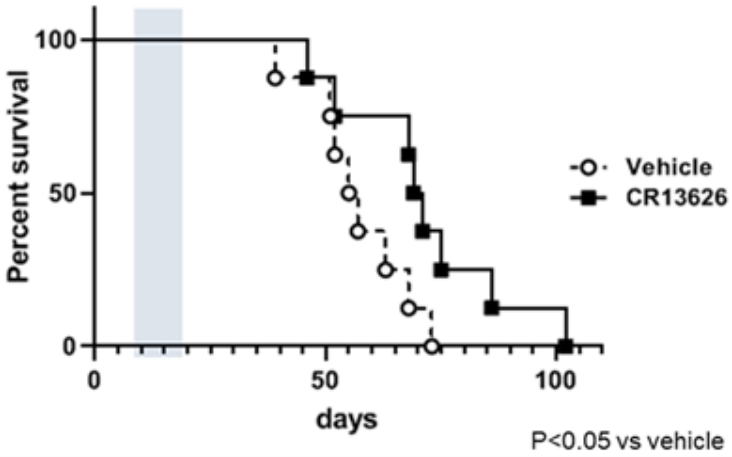

*Figure 29. CR13626 effect on animal survival. Survival curves of CR13626 (50 mg/kg/daily/10 days) vs. vehicle. Animal survival was evaluated using a Kaplan–Meier survival curve; *P<0.05 by Mantel-Cox test. Dosing of CR13626 started on day 9 and lasted 10 days only (shaded area).*

7. Discussion and Conclusions

Discussion

Glioblastoma multiforme is considered as one of the most aggressive and difficult to treat tumor [Tilak et al., 2021]. GBM is the most malignant type of primary brain cancer and represents half of all new diagnoses of gliomas [Paolillo et al., 2018]. To date, there is no cure for GBM; after the first line treatment according to the approved clinical protocol, the recurrence of the tumor is almost universal and the median patient survival is of approximately 15 months from diagnosis, with a five-year survival of 5% [Pearson et al., 2017]. Because of its dismal prognosis and the high unmet clinical needs, many efforts are ongoing to find more effective therapies that provide survival benefit.

Many obstacles have been encountered by investigational agents and several factors have been identified so far as fundamental elements to be considered for the development of new therapeutical agents for GBM.

Firstly, the presence of the BBB represents a physical obstacle to the entrance of therapeutic agents into the brain, and efflux transporters contribute to preventing the accumulation of drugs into the brain [van Tellingen et al., 2015; Ganipineni et al., 2018]. Although in GBM the organization of BBB is affected, by creating the so called BBTB, the disruption of BBB is observed only at primary site of the tumor but not at infiltrative areas, where the intact BBB is maintained, thus limiting the access of therapeutic drugs to tumor cells [Ganipineni et al., 2018]. In addition, the leakage of the dysfunctional BBTB leads to the development of brain edema and to an increased intracranial pressure, which is one of the major clinical complications of GBM [Ganipineni et al., 2018]. Thus, the ability to efficiently cross the BBB and remain into the brain without being substrate of efflux transporters, reaching effective concentrations, are essential prerequisites for new therapeutics. In healthy CD1 mice, CR13626 demonstrated a good oral bioavailability (72%) and a relevant brain penetration when dosed orally, with a brain/ plasma ratio of 1.4, suggesting the potential of CR13626 to reach the tumor and remain at the tumor site. Indeed, the brain tropism of CR13626 was confirmed in a satellite group of tumor bearing mice obtained by the injection of U87MG-Luc cells into the brain of nude mice. In this model, the oral treatment with CR13626 once a day for five consecutive days at the dose of 50 mg/kg confirmed the exposure levels observed in CD1 mice and showed a preferential accumulation of the compound in the right hemisphere, where the tumoral cells were injected and tumor developed. Moreover, CR13626 did not result to be a substrate of P-gp and BCRP multidrug efflux transporters involved in brain tumor drug resistance. This feature gives to CR13626 a higher chance to remain into the brain achieving therapeutic concentrations.

The infiltrative nature of GBM needs large areas to be covered by current local delivery system; at the same time, a lack of selectivity and specificity for tumor cells could limit the efficiency of chemotherapeutics, by exerting toxicity on the surrounding healthy brain tissues [Ganipineni et al., 2018]. In cellular cultures, CR13626 preferentially reduced the proliferation of the U87MG GBM cells with respect to the non-tumoral HEK-293 cells. In particular, 24 hours of treatment with CR13626 1 µM showed more than 50% of viability decrease for U87MG cells, whereas no signs of toxicity were observed in the same conditions on HEK-293 cells.

The high grades of cellular proliferation, invasiveness, cellular atypia, and angiogenesis are also important features of GBM tumors, contributing to the poor prognosis. The pathogenesis of gliomas involves sequential accumulation of genetic alterations and abnormal regulation of growth factor signaling pathways that result in malignant transformation [Alifieris et al., 2015]. Several gene expression profiling studies have highlighted the strong molecular heterogeneity of GBM and have helped to classified GBM into four different subclasses (classical, mesenchymal, proneural and neural subgroups), although a more recent transcriptomic analysis identified only the first three subtypes as tumor specific. Moreover, IDH1/2 mutations have been identified as strong positive prognostic factors for GBM, as well as epigenetic alterations have been recognized to be involved in tumor resistance or in the sensitization to specific treatment (i.e., methylation of the MGMT gene promoter). However, more studies are needed to better understand the complexity of GBM and to provide new elements useful for a more accurate patient segmentation, more specific targeted treatments, and a better design of clinical trials on a molecular basis [El-Khayat et al., 2021]. In 2D cellular cultures, CR13626 was able to reduce the proliferation of the U373, U87MG vIII and T98G cell lines at 3 days of treatment, and the effects were still visible after 7 days of treatment. These commercially available GBM cell lines harbor some of the genetic alterations/mutations present in GBM tumor cells, suggesting a potential broad activity of the compound. U373 cells share with U87MG cells the expression of the wild-type form of EGFR but, if the latter has deletions in PTEN and CDKN2A/2B genes, the former holds the amplification of PDGFRα and VEGFR2. Thus, the U87MG and U373 cells show phenotypes resembling the neuronal and mesenchymal groups of GBM, respectively [Motaln et al., 2015], even if the neuronal nature of U87MG cells has been recently challenged by Lane et al., 2019. On the other hand, U87MG vIII cells express high levels of EGFRvIII, the constitutive active mutant form of EGFR. EGFRvIII represents the most frequent deletion occurring in GBM, contributes to several processes such as angiogenesis and tumor growth, and is involved in the regulation of stemness in glioma stem cells [Eskilsson et al., 2018; Talukdar et

al., 2020]. Finally, T98G cells are TMZ resistant [Lee et al., 2016]. Interestingly, CR13626 resulted also able to reduce in a dose-dependent fashion the proliferation of U87MG cells cultured as 3D spheroids, which are considered a more reliable model to assess cellular response to a drug treatment since they are more representative of the complexity of tumor environment with respect to 2D cultures. However, further analysis in patient derived GBM primary cells could be useful to corroborate these effects and to better define the potential of the compound.

As already mentioned, the high intratumoral heterogeneity gives more chances to GBM to evade therapy and generate resistance to highly selective treatments [Qazi et al., 2017]. GBM cancer stem cells constitute a second layer of GBM heterogeneity and are thought to represent the tumor driving force, due to the multiple roles that they exert in GBM pathology [Neftel et al., 2019; Lathia et al., 2015]. Indeed, the intrinsic plasticity of these cells allows to modulate the cellular state of tumor cells in response to microenvironmental cues, including those induced by drug treatment, creating supportive niches, and promoting tumor growth [Dirkse et al., 2019]. CSCs also stimulate the angiogenesis process through the release of high levels of VEGF, and contribute to vascular structures through transdifferentiation into pericytes, promoting tumor growth [Lathia et al., 2015]. Finally, CSCs are involved in the modulation of the immune system to create an immunosuppressive microenvironment, by inducing Treg, diminishing CTLs activation, and promoting the M2 immunosuppressive phenotype of macrophages [Lathia et al., 2015]. These effects contribute to the creation of the severe immunosuppression which characterizes GBM, leading to define GBM as an immunologically “cold” tumor.

In GBM, tumor’s growth, progression, proliferation, as well as the angiogenesis process, depend largely upon the activity of cell surface membrane RTKs and the activation of their downstream signals [Paolillo et al., 2018]. Whitin the existing 20 classes of RTKs, 12 showed the higher degree of association with GBM tumors according to the TCGA-GBM dataset analyzed by Tilak et al., therefore constituting attractive targets for therapy [Tilak et al., 2021]. Among these, the EGF and VEGF receptors families are the most extensively studied in the past years, because of their strong involvement in tumor growth and angiogenesis process.

Regarding EGFR, because of its ability to activate different pathways in parallel, it can be considered as a hub involved in regulating various cellular processes, including proliferation, migration, differentiation, and induction of angiogenesis through VEGF expression [Alifieris et al.; Oprita et al., 2021]. Despite the failures of many drugs against EGFR alterations, strategies aimed at hitting EGFR

in GBM continue to be investigated, and the targeting of EGFR axis is still considered as valid [Pan et al., 2020]. In U87MG cells CR13626 was able to reduce the ligand-induced activation of EGFR receptor at residue Y1068, which resulted highly phosphorylated in tissue samples of GBMs [Tanaka et al., 2011].

Among the VEGF receptors family, increased levels of VEGFR2, as well as of its ligand VEGF, have been detected in GBM as a consequence of hypoxia [Tilak et al., 2021]. An aberrant VEGFR2 signaling is considered to be significantly involved in the increased angiogenesis and in the dysfunctional tumor vasculature observed in GBM [Tilak et al., 2021]. The impaired new tumor vasculature is leaky and circuitous and leads to a heterogeneity in tumor blood flow and oxygenation, promoting tumor progression and intratumoral edema, which is a major cause of morbidity for GBM patients [Clavreul et al., 2019; Monteiro et al., 2017]. To date, treatment with anti-angiogenic agents showed controversial results; however, many different anti-angiogenic strategies are under investigation, such as the delivery of nano-vesicles, gene therapy, and combinatorial therapies with ICIs. Upon the activation of the receptor, several signaling pathways initiate, through the phosphorylation of intracellular tyrosine residues which recruits specific downstream effectors [Napione et al., 2017]. Particularly, the residue Y1175 is considered as a critical mediator of VEGFR2 signaling because of its ability to recruit several proteins (i.e., PLCγ, p85 subunit of PI3K, the adaptor proteins SHB and SCK) [Napione et al., 2017]. In HUVEC-C cells, CR13626 was able to reduce the phosphorylation of the Y1175 residue induced by VEGF ligand in a concentration dependent fashion. In addition, CR13626 also inhibited the phosphorylation of the downstream effectors Fyn/Src, suggesting a potential stronger impact on the intracellular signal transmission upon VEGFR2 activation. Furthermore, CR13626 showed dose-dependent reduction of new vessel-like structures formation, indicating a potential effect of the compound on the angiogenic process.

In addition to EGFR and VEGFR2, CR13626 demonstrated inhibitory activity also against the RET receptor (IC_{50} value of 39 nM), which has been found overexpressed in several cancers, including glioma [Mulligan, 2019]. Although RET overexpression and fusions are acknowledged mechanisms related to EGFR resistance in many tumors, they have been recently associated also with GBM [Pan et al., 2020, Lin et al., 2016; Leonetti et al., 2019; Zhu et al., 2019; Woo et al., 2020].

RTKs alterations usually coexist with mutations that activate other core intracellular regulatory pathways [Gong et al., 2018]. Three of the most prominently altered RTK pathways in gliomas include the Ras/MAPK, PI3K/Akt/PTEN, and FAK/Src pathways, all of which rely on adaptor proteins

such as Grb2 and Shc to relay the signals from the cell membrane to the downstream effectors [Tilak et al., 2021].

Members of the SFKs family are also involved in the intracellular transmission of the signal. An increased SFKs activity have been found to mediate tumorigenesis and have been demonstrated to be critical for GBM cell motility, invasion, and angiogenesis [Lewis-Tuffin et al., 2015]. CR13626 showed in vitro inhibitory activity against a set of kinases which play a fundamental role in GBM development, allowing the compound to potentially act on several aspects of GBM tumor. Indeed, CR13626 potently inhibited the Fyn, Yes and Lck kinases, all of which belongs to the SFKs family. Fyn and Src have been described as important players in EGFRvIII intracellular signaling, by promoting tumor growth and motility through the physical association with the receptor in a mouse model of GBM [Lu et al., 2009]. CR13626 demonstrated a direct inhibitory activity against Fyn kinase either in a biochemical assay (IC_{50} 37 nM) and in a cellular model obtained through the Fyn/Tau co-transfection of HEK-293 cells, where CR13626 reduced the Fyn-mediated phosphorylation of Tau at the residue Y18. Yes kinase has been demonstrated to affect tumor cell biology in a pro-tumorigenic manner and to be involved in the induction of the invasive phenotype of GBM cells [Lewis-Tuffin et al., 2015; Kleber et al., 2008]. CR13626 showed inhibitory activity against Yes kinase with an IC_{50} of 12 nM. Finally, CR13626 showed inhibitory activity vs Lck (IC_{50} 38 nM), which has been recently found to be involved in the regulation of in glioma progression by promoting the migration of GBM cells and tumor growth, and by regulating cancer cells stemness [Zepecki et al., 2019]. Moreover, it has been demonstrated that Lck kinase contributes also to the resistance of glioma stem cells to cisplatin and to fractionated radiations [Bommhardt et al., 2019]. Interestingly, it has been observed that in small cell lung cancer Lck mediates the signal of c-kit receptor upon its activation by the stem cell factor (SCF) ligand [Krystal et al., 1998], and this interaction seems to be involved also in GBM resistance to TMZ [Zaman et al., 2020].

CR13626 showed inhibitory activity also against the serine/threonine kinase HGK (IC_{50} of 23 nM), which has been identified by Prolo et al. as a strong regulator of GBM invasion, whose expression is mostly upregulated by EGFRvIII compared to the wild-type EGFR [Prolo et al., 2019]. Moreover, the HGK activation downstream the c-MET receptor has been recognized as an emerging driving mechanism for medulloblastoma motility and invasiveness [Santhana et al., 2015; Tripolitsioti et al., 2018], and this mechanism could be also potentially involved in GBM.

The presence of compensatory pathways is one of the causes of the failure of highly selective treatments. Thus, the ability to hit different key players of GBM pathology in parallel could give advantages against these mechanisms. CR13626 could well represent the multikinase inhibitor acting on several targets at once described by Frantz [Frantz, 2005]. Indeed, taking advantages from its pharmacokinetic properties (including brain penetration) and its selectivity against kinases relevant for GBM development, CR13626 could have the potential to act on several fronts of GBM. We hypothesize some mechanisms by which CR13626 could act in GBM, as described in Figure 30. In particular, CR13626 could have effects both on endothelial and GBM tumor cells through the inhibition of VEGFR2, EGFR and the downstream kinase Fyn, leading to a diminished tumor cells proliferation and migration, and counteracting the angiogenesis process. On GBM tumor cells, CR13626 can block the constitutively active form of EGFR receptor (EGFRvIII), the most frequent deletion occurring in GBM. Moreover, the inhibition of Yes kinase could contribute to a less invasive phenotype of GBM. By acting on Lck kinase downstream the activated c-kit receptor, CR13626 could reduce cancer cells stemness and counteract the GBM resistance to TMZ. Furthermore, the inhibition of Fyn and HGK kinases could impair the c-MET receptor signaling pathway, leading to a decreased GBM migration and invasion. Finally, CR13626 could counteract one of the EGFR resistance mechanisms by blocking RET kinase.

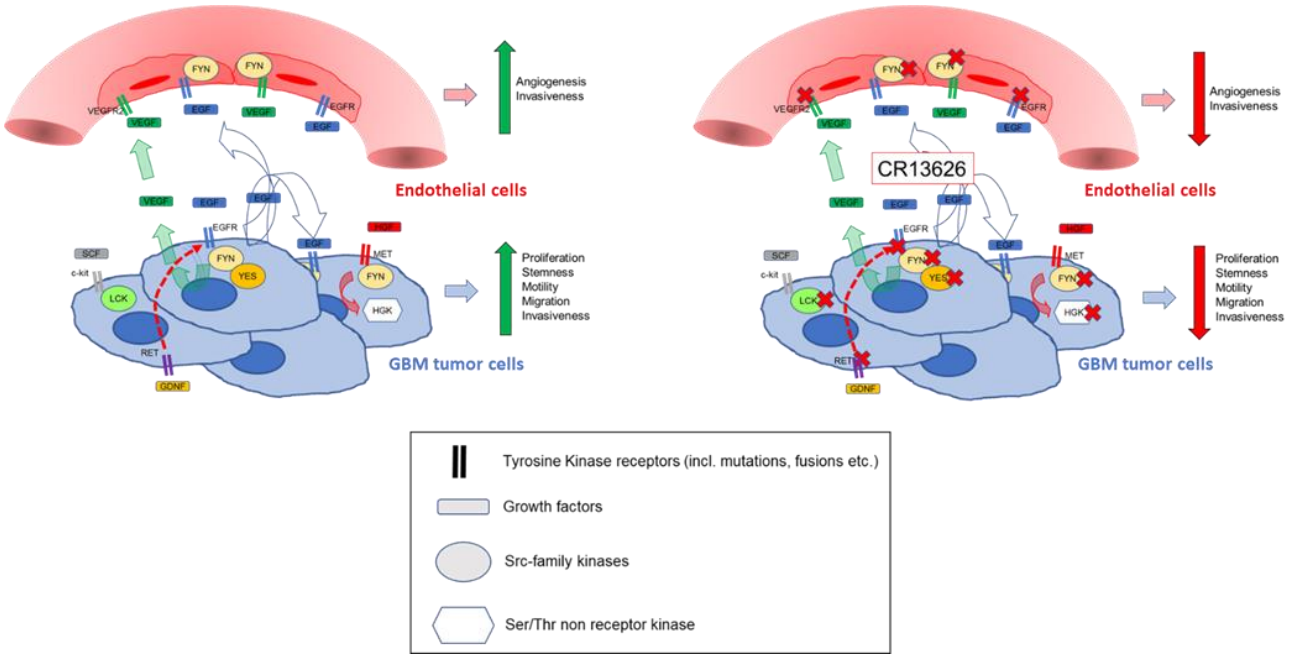

Figure 30. Proposed mechanism by which CR13626 could act in GBM.

In the already mentioned orthotopic xenograft mouse model of GBM (obtained by the injection of U87 MG-Luc GBM cells), the oral treatment with CR13626 for 10 days (50 mg/kg/daily) led to a time-dependent reduction of tumor growth and to an increase of 25% of the median survival time of animals. The observed antitumor effects agreed with the exposure of tumor-bearing mice to CR13626, which was above the TKs in-vitro IC_{50} values.

Taking together, such evidence warrants the further development of CR13626 as a potential new drug candidate in GBM.

Conclusions

In summary, the present work described the tyrosine kinase inhibitor CR13626 as a potential new drug candidate for GBM therapy, because of its combined abilities to efficiently cross the BBB without being a substrate of the multidrug transporters involved in tumor resistance and to potently inhibit several players involved in GBM development and aggressiveness, as summarized in Figure 30. Indeed, CR13626 displayed direct inhibition of EGFR and VEGFR2 receptor tyrosine kinases, which have a fundamental role in promoting cell proliferation, migration, and angiogenesis, and showed inhibitory activity against some of the downstream effectors of these receptors, such as Fyn and Yes, giving a potential stronger impact on the intracellular signal transmission upon receptor activation. By inhibiting Lck kinase, CR13626 could counteract the resistance of glioma stem cells to fractionated radiations; at the same time, CR13626 could indirectly impair the SCF/c-kit pathway, that seems to be involved in GBM resistance to TMZ. Even if not directly active against c-MET receptor, CR13626 could dampen this way by blocking the downstream Fyn and HGK kinases, tackling GBM migration and invasion. Finally, CR13626 could counteract one of the EGFR resistance mechanisms by blocking RET kinase.

8. References

Abedalthagafi M, Barakeh D, Foshay KM. Immunogenetics of glioblastoma: the future of personalized patient management. NPJ Precis Oncol. 2018 Dec 4; 2:27.

Alifieris C, Trafalis DT. Glioblastoma multiforme: Pathogenesis and treatment. Pharmacol Ther. 2015 Aug; 152:63-82.

Anjum K, Shagufta BI, Abbas SQ, Patel S, Khan I, Shah SAA, Akhter N, Hassan SSU. Current status and future therapeutic perspectives of glioblastoma multiforme (GBM) therapy: A review. Biomed Pharmacother. 2017 Aug; 92:681-689.

Azuaje F, Tiemann K, Niclou SP. Therapeutic control and resistance of the EGFR-driven signaling network in glioblastoma. Cell Commun Signal. 2015 Mar 31; 13:23.

Bijman MN, van Nieuw Amerongen GP, Laurens N, van Hinsbergh VW, Boven E. Microtubule-targeting agents inhibit angiogenesis at subtoxic concentrations, a process associated with inhibition of Rac1 and Cdc42 activity and changes in the endothelial cytoskeleton. Mol Cancer Ther. 2006 Sep; 5(9):2348-57.

Bommhardt U, Schraven B, Simeoni L. Beyond TCR Signaling: Emerging Functions of Lck in Cancer and Immunotherapy. Int J Mol Sci. 2019 Jul 16; 20(14):3500.

Cancer Genome Atlas Research Network. Comprehensive genomic characterization defines human glioblastoma genes and core pathways. Nature. 2008 Oct 23; 455(7216):1061-8.

Carmeliet P, Jain RK. Principles and mechanisms of vessel normalization for cancer and other angiogenic diseases. Nat Rev Drug Discov. 2011 Jun; 10(6):417-27.

Cirotti C, Contadini C, Barilà D. SRC Kinase in Glioblastoma News from an Old Acquaintance. Cancers (Basel). 2020 Jun 12; 12(6):1558.

Clavreul A, Pourbaghi-Masouleh M, Roger E, Menei P. Nanocarriers and nonviral methods for delivering antiangiogenic factors for glioblastoma therapy: the story so far. Int J Nanomedicine. 2019 Apr 9; 14:2497-2513.

Cohen MH, Johnson JR, Pazdur R. Food and Drug Administration Drug approval summary: temozolomide plus radiation therapy for the treatment of newly diagnosed glioblastoma multiforme. Clin Cancer Res. 2005 Oct 1; 11(19 Pt 1):6767-71.

Dirkse A, Golebiewska A, Buder T, Nazarov PV, Muller A, Poovathingal S, Brons NHC, Leite S, Sauvageot N, Sarkisjan D, Seyfrid M, Fritah S, Stieber D, Michelucci A, Hertel F, Herold-Mende C, Azuaje F, Skupin A, Bjerkvig R, Deutsch A, Voss-Böhme A, Niclou SP. Stem cell-associated heterogeneity in Glioblastoma results from intrinsic tumor plasticity shaped by the microenvironment. Nat Commun. 2019 Apr 16; 10(1):1787.

El-Khayat SM, Arafat WO. Therapeutic strategies of recurrent glioblastoma and its molecular pathways 'Lock up the beast'. Ecancermedicalscience. 2021 Jan 22; 15:1176.

Eskilsson E, Røsland GV, Solecki G, Wang Q, Harter PN, Graziani G, Verhaak RGW, Winkler F, Bjerkvig R, Miletic H. EGFR heterogeneity and implications for therapeutic intervention in glioblastoma. Neuro Oncol. 2018 May 18; 20(6):743-752.

Frantz S. Drug discovery: playing dirty. Nature. 2005 Oct 13; 437(7061):942-3.

Gacche RN. Compensatory angiogenesis and tumor refractoriness. Oncogenesis. 2015 Jun 1; 4(6):e153.

Ganipineni LP, Danhier F, Préat V. Drug delivery challenges and future of chemotherapeutic nanomedicine for glioblastoma treatment. J Control Release. 2018 Jul 10; 281:42-57.

Gong Y, Dong Y, Cui J, Sun Q, Zhen Z, Gao Y, Su J, Ren H. “Receptor Tyrosine Kinase Interaction with the Tumor Microenvironment in Malignant Progression of Human Glioblastoma” chapter, “Glioma-Contemporary Diagnostic and Therapeutic Approaches” book, edited by Omerhodzic I and Kenan A (IntechOpen), 2018.

Han X, Zhang W, Yang X, Wheeler CG, Langford CP, Wu L, Filippova N, Friedman GK, Ding Q, Fathallah-Shaykh HM, Gillespie GY, Nabors LB. The role of Src family kinases in growth and migration of glioma stem cells. Int J Oncol. 2014 Jul; 45(1):302-10.

Hegi ME, Diserens AC, Gorlia T, Hamou MF, de Tribolet N, Weller M, Kros JM, Hainfellner JA, Mason W, Mariani L, Bromberg JE, Hau P, Mirimanoff RO, Cairncross JG, Janzer RC, Stupp R. MGMT gene silencing and benefit from temozolomide in glioblastoma. N Engl J Med. 2005 Mar 10; 352(10):997-1003.

Hennequin LF, Allen J, Breed J, Curwen J, Fennell M, Green TP, Lambert-van der Brempt C, Morgentin R, Norman RA, Olivier A, Otterbein L, Plé PA, Warin N, Costello G. N-(5-chloro-1,3-benzodioxol-4-yl)-7-[2-(4-methylpiperazin-1-yl)ethoxy]-5- (tetrahydro-2H-pyran-4-yloxy)quinazolin-4-amine, a novel, highly selective, orally available, dual-specific c-Src/Abl kinase inhibitor. J Med Chem. 2006 Nov 2; 49(22):6465-88.

Huang L, Fu L. Mechanisms of resistance to EGFR tyrosine kinase inhibitors. Acta Pharm Sin B. 2015 Sep; 5(5):390-401.

Huang J, Yu J, Tu L, Huang N, Li H, Luo Y. Isocitrate Dehydrogenase Mutations in Glioma: From Basic Discovery to Therapeutics Development. Front Oncol. 2019 Jun 12; 9:506.

Informa Pharma Intelligence, *Datamonitor Healthcare_Glioblastoma (GBM)_Market Spotlight*, 2021.

Khaddour K, Johanns TM, Ansstas G. The Landscape of Novel Therapeutics and Challenges in Glioblastoma Multiforme: Contemporary State and Future Directions. Pharmaceuticals (Basel). 2020 Nov 14; 13(11):389.

Kim M, Costello J. DNA methylation: an epigenetic mark of cellular memory. Exp Mol Med. 2017 Apr 28; 49(4):e322.

Kleber S, Sancho-Martinez I, Wiestler B, Beisel A, Gieffers C, Hill O, Thiemann M, Mueller W, Sykora J, Kuhn A, Schreglmann N, Letellier E, Zuliani C, Klussmann S, Teodorczyk M, Gröne HJ, Ganten TM, Sültmann H, Tüttenberg J, von Deimling A, Regnier-Vigouroux A, Herold-Mende C, Martin-Villalba A. Yes and PI3K bind CD95 to signal invasion of glioblastoma. Cancer Cell. 2008 Mar; 13(3):235-48.

Kleihues P, Ohgaki H. Primary and secondary glioblastomas: from concept to clinical diagnosis. Neuro Oncol. 1999 Jan; 1(1):44-51.

Koch S, Claesson-Welsh L. Signal transduction by vascular endothelial growth factor receptors. Cold Spring Harb Perspect Med. 2012 Jul; 2(7):a006502.

Krystal GW, DeBerry CS, Linnekin D, Litz J. Lck associates with and is activated by Kit in a small cell lung cancer cell line: inhibition of SCF-mediated growth by the Src family kinase inhibitor PP1. Cancer Res. 1998 Oct 15; 58(20):4660-6.

Lane R, Simon T, Vintu M, Solkin B, Koch B, Stewart N, Benstead-Hume G, Pearl FMG, Critchley G, Stebbing J, Giamas G. Cell-derived extracellular vesicles can be used as a biomarker reservoir for glioblastoma tumor subtyping. Commun Biol. 2019 Aug 19; 2:315.

Lathia JD, Mack SC, Mulkearns-Hubert EE, Valentim CL, Rich JN. Cancer stem cells in glioblastoma. Genes Dev. 2015 Jun 15; 29(12):1203-17.

Le Rhun E, Preusser M, Roth P, Reardon DA, van den Bent M, Wen P, Reifenberger G, Weller M. Molecular targeted therapy of glioblastoma. Cancer Treat Rev. 2019 Nov; 80:101896.

Lee G, Thangavel R, Sharma VM, Litersky JM, Bhaskar K, Fang SM, Do LH, Andreadis A, Van Hoesen G, Ksiezak-Reding H. Phosphorylation of tau by fyn: implications for Alzheimer's disease. J Neurosci. 2004 Mar 3; 24(9):2304-12.

Lee SY. Temozolomide resistance in glioblastoma multiforme. Genes Dis. 2016 May 11; 3(3):198-210.

Leonetti A, Sharma S, Minari R, Perego P, Giovannetti E, Tiseo M. Resistance mechanisms to osimertinib in EGFR-mutated non-small cell lung cancer. Br J Cancer. 2019 Oct; 121(9):725-737.

Lewis-Tuffin LJ, Feathers R, Hari P, Durand N, Li Z, Rodriguez FJ, Bakken K, Carlson B, Schroeder M, Sarkaria JN, Anastasiadis PZ. Src family kinases differentially influence glioma growth and motility. Mol Oncol. 2015 Nov; 9(9):1783-98.

Lin C, Lu W, Ren Z, Tang Y, Zhang C, Yang R, Chen Y, Cao W, Wang L, Wang X, Ji T. Elevated RET expression enhances EGFR activation and mediates EGFR inhibitor resistance in head and neck squamous cell carcinoma. Cancer Lett. 2016 Jul 10; 377(1):1-10.

Lloyd R, *Datamonitor Healthcare_Glioblastoma (GBM)_Treatment,* 2017.

Louis DN, Ohgaki H, Wiestler OD, Cavenee WK, Burger PC, Jouvet A, Scheithauer BW, Kleihues P. The 2007 WHO classification of tumours of the central nervous system. Acta Neuropathol. 2007 Aug; 114(2):97-109.

Louis DN, Perry A, Reifenberger G, von Deimling A, Figarella-Branger D, Cavenee WK, Ohgaki H, Wiestler OD, Kleihues P, Ellison DW. The 2016 World Health Organization Classification of Tumors of the Central Nervous System: a summary. Acta Neuropathol. 2016 Jun; 131(6):803-20.

Louis DN, Perry A, Wesseling P, Brat DJ, Cree IA, Figarella-Branger D, Hawkins C, Ng HK, Pfister SM, Reifenberger G, Soffietti R, von Deimling A, Ellison DW. The 2021 WHO Classification of Tumors of the Central Nervous System: a summary. Neuro Oncol. 2021 Aug 2; 23(8):1231-1251.

Lu KV, Zhu S, Cvrljevic A, Huang TT, Sarkaria S, Ahkavan D, Dang J, Dinca EB, Plaisier SB, Oderberg I, Lee Y, Chen Z, Caldwell JS, Xie Y, Loo JA, Seligson D, Chakravari A, Lee FY, Weinmann R, Cloughesy TF, Nelson SF, Bergers G, Graeber T, Furnari FB, James CD, Cavenee WK, Johns TG, Mischel PS. Fyn and SRC are effectors of oncogenic epidermal growth factor receptor signaling in glioblastoma patients. Cancer Res. 2009 Sep 1; 69(17):6889-98.

Lu-Emerson C, Duda DG, Emblem KE, Taylor JW, Gerstner ER, Loeffler JS, Batchelor TT, Jain RK. Lessons from anti-vascular endothelial growth factor and anti-vascular endothelial growth factor receptor trials in patients with glioblastoma. J Clin Oncol. 2015 Apr 1; 33(10):1197-213.

Michaelsen SR, Staberg M, Pedersen H, Jensen KE, Majewski W, Broholm H, Nedergaard MK, Meulengracht C, Urup T, Villingshøj M, Lukacova S, Skjøth-Rasmussen J, Brennum J, Kjær A, Lassen U, Stockhausen MT, Poulsen HS, Hamerlik P. VEGF-C sustains VEGFR2 activation under bevacizumab therapy and promotes glioblastoma maintenance. Neuro Oncol. 2018 Oct 9; 20(11):1462-1474.

Monteiro AR, Hill R, Pilkington GJ, Madureira PA. The Role of Hypoxia in Glioblastoma Invasion. Cells. 2017 Nov 22; 6(4):45.

Motaln H, Koren A, Gruden K, Ramšak Ž, Schichor C, Lah TT. Heterogeneous glioblastoma cell cross-talk promotes phenotype alterations and enhanced drug resistance. Oncotarget. 2015 Dec 1; 6(38):40998-1017.

Moyer JD, Barbacci EG, Iwata KK, Arnold L, Boman B, Cunningham A, DiOrio C, Doty J, Morin MJ, Moyer MP, Neveu M, Pollack VA, Pustilnik LR, Reynolds MM, Sloan D, Theleman A, Miller P. Induction of apoptosis and cell cycle arrest by CP-358,774, an inhibitor of epidermal growth factor receptor tyrosine kinase. Cancer Res. 1997 Nov 1; 57(21):4838-48.

Mulligan LM. GDNF and the RET Receptor in Cancer: New Insights and Therapeutic Potential. Front Physiol. 2019 Jan 7; 9:1873.

Nakada M, Kita D, Watanabe T, Hayashi Y, Teng L, Pyko IV, Hamada J. Aberrant signaling pathways in glioma. Cancers (Basel). 2011 Aug 10; 3(3):3242-78.

Napione L, Alvaro M, Bussolino F. "VEGF-Mediated Signal Transduction in Tumor Angiogenesis" chapter, "Physiologic and Pathologic Angiogenesis - Signaling Mechanisms and Targeted Therapy" book, edited by Dan and Agneta Simionescu (IntechOpen), 2017.

Neftel C, Laffy J, Filbin MG, Hara T, Shore ME, Rahme GJ, Richman AR, Silverbush D, Shaw ML, Hebert CM, Dewitt J, Gritsch S, Perez EM, Gonzalez Castro LN, Lan X, Druck N, Rodman C, Dionne D, Kaplan A, Bertalan MS, Small J, Pelton K, Becker S, Bonal D, Nguyen QD, Servis RL, Fung JM, Mylvaganam R, Mayr L, Gojo J, Haberler C, Geyeregger R, Czech T, Slavc I, Nahed BV, Curry WT, Carter BS, Wakimoto H, Brastianos PK, Batchelor TT, Stemmer-Rachamimov A, Martinez-Lage M, Frosch MP, Stamenkovic I, Riggi N, Rheinbay E, Monje M, Rozenblatt-Rosen O, Cahill DP, Patel AP, Hunter T, Verma IM, Ligon KL, Louis DN, Regev A, Bernstein BE, Tirosh I, Suvà ML. An Integrative Model of Cellular States, Plasticity, and Genetics for Glioblastoma. Cell. 2019 Aug 8; 178(4):835-849.e21.

Oronsky B, Reid TR, Oronsky A, Sandhu N, Knox SJ. A Review of Newly Diagnosed Glioblastoma. Front Oncol. 2021 Feb 5; 10:574012.

Ostrom QT, Patil N, Cioffi G, Waite K, Kruchko C, Barnholtz-Sloan JS. CBTRUS Statistical Report: Primary Brain and Other Central Nervous System Tumors Diagnosed in the United States in 2013-2017. Neuro Oncol. 2020 Oct 30; 22(12 Suppl 2):iv1-iv96.

Ou A, Yung WKA, Majd N. Molecular Mechanisms of Treatment Resistance in Glioblastoma. Int J Mol Sci. 2020 Dec 31; 22(1):351.

Paolillo M, Boselli C, Schinelli S. Glioblastoma under Siege: An Overview of Current Therapeutic Strategies. Brain Sci. 2018 Jan 16; 8(1):15.

Pan PC, Magge RS. Mechanisms of EGFR Resistance in Glioblastoma. Int J Mol Sci. 2020 Nov 11; 21(22):8471.

Park JS, Kim IK, Han S, Park I, Kim C, Bae J, Oh SJ, Lee S, Kim JH, Woo DC, He Y, Augustin HG, Kim I, Lee D, Koh GY. Normalization of Tumor Vessels by Tie2 Activation and Ang2 Inhibition Enhances Drug Delivery and Produces a Favorable Tumor Microenvironment. Cancer Cell. 2016 Dec 12; 30(6):953-967.

Parsons DW, Jones S, Zhang X, Lin JC, Leary RJ, Angenendt P, Mankoo P, Carter H, Siu IM, Gallia GL, Olivi A, McLendon R, Rasheed BA, Keir S, Nikolskaya T, Nikolsky Y, Busam DA, Tekleab H, Diaz LA Jr, Hartigan J, Smith DR, Strausberg RL, Marie SK, Shinjo SM, Yan H, Riggins GJ, Bigner DD, Karchin R, Papadopoulos N, Parmigiani G, Vogelstein B, Velculescu VE, Kinzler KW. An integrated genomic analysis of human glioblastoma multiforme. Science. 2008 Sep 26; 321(5897):1807-12.

Parsons SJ, Parsons JT. Src family kinases, key regulators of signal transduction. Oncogene. 2004 Oct 18; 23(48):7906-9.

Pearson JRD, Regad T. Targeting cellular pathways in glioblastoma multiforme. Signal Transduct Target Ther. 2017 Sep 29; 2:17040.

Prolo LM, Li A, Owen SF, Parker JJ, Foshay K, Nitta RT, Morgens DW, Bolin S, Wilson CM, Vega L JCM, Luo EJ, Nwagbo G, Waziri A, Li G, Reimer RJ, Bassik MC, Grant GA. Targeted genomic CRISPR-Cas9 screen identifies MAP4K4 as essential for glioblastoma invasion. Sci Rep. 2019 Sep 30; 9(1):14020.

Qazi MA, Vora P, Venugopal C, Sidhu SS, Moffat J, Swanton C, Singh SK. Intratumoral heterogeneity: pathways to treatment resistance and relapse in human glioblastoma. Ann Oncol. 2017 Jul 1; 28(7):1448-1456.

Oprita A, Baloi SC, Staicu GA, Alexandru O, Tache DE, Danoiu S, Micu ES, Sevastre AS. Updated Insights on EGFR Signaling Pathways in Glioma. Int J Mol Sci. 2021 Jan 8; 22(2):587.

Reifenberger G, Wirsching HG, Knobbe-Thomsen CB, Weller M. Advances in the molecular genetics of gliomas - implications for classification and therapy. Nat Rev Clin Oncol. 2017 Jul; 14(7):434-452.

Rugo HS, Herbst RS, Liu G, Park JW, Kies MS, Steinfeldt HM, Pithavala YK, Reich SD, Freddo JL, Wilding G. Phase I trial of the oral antiangiogenesis agent AG-013736 in patients with advanced solid tumors: pharmacokinetic and clinical results. J Clin Oncol. 2005 Aug 20; 23(24):5474-83.

Rushing, E.J. WHO classification of tumors of the nervous system: preview of the upcoming 5th edition. memo 14, 188–191 (2021).

Saleem H, Kulsoom Abdul U, Küçükosmanoglu A, Houweling M, Cornelissen FMG, Heiland DH, Hegi ME, Kouwenhoven MCM, Bailey D, Würdinger T, Westerman BA. The TICking clock of EGFR therapy resistance in glioblastoma: Target Independence or target Compensation. Drug Resist Updat. 2019 Mar; 43:29-37.

Santhana Kumar K, Tripolitsioti D, Ma M, Grählert J, Egli KB, Fiaschetti G, Shalaby T, Grotzer MA, Baumgartner M. The Ser/Thr kinase MAP4K4 drives c-Met-induced motility and invasiveness in a cell-based model of SHH medulloblastoma. Springerplus. 2015 Jan 14; 4:19.

Stupp R, Mason WP, van den Bent MJ, Weller M, Fisher B, Taphoorn MJ, Belanger K, Brandes AA, Marosi C, Bogdahn U, Curschmann J, Janzer RC, Ludwin SK, Gorlia T, Allgeier A, Lacombe D, Cairncross JG, Eisenhauer E, Mirimanoff RO; European Organisation for Research and Treatment of Cancer Brain Tumor and Radiotherapy Groups; National Cancer Institute of Canada Clinical Trials Group. Radiotherapy plus concomitant and adjuvant temozolomide for glioblastoma. N Engl J Med. 2005 Mar 10; 352(10):987-96.

Stupp R, Taillibert S, Kanner AA, Kesari S, Steinberg DM, Toms SA, Taylor LP, Lieberman F, Silvani A, Fink KL, Barnett GH, Zhu JJ, Henson JW, Engelhard HH, Chen TC, Tran DD, Sroubek J, Tran ND, Hottinger AF, Landolfi J, Desai R, Caroli M, Kew Y, Honnorat J, Idbaih A, Kirson ED, Weinberg U, Palti Y, Hegi ME, Ram Z. Maintenance Therapy With Tumor-Treating Fields Plus Temozolomide vs Temozolomide Alone for Glioblastoma: A Randomized Clinical Trial. JAMA. 2015 Dec 15; 314(23):2535-43.

Stupp R, Taillibert S, Kanner A, Read W, Steinberg D, Lhermitte B, Toms S, Idbaih A, Ahluwalia MS, Fink K, Di Meco F, Lieberman F, Zhu JJ, Stragliotto G, Tran D, Brem S, Hottinger A, Kirson ED, Lavy-Shahaf G, Weinberg U, Kim CY, Paek SH, Nicholas G, Bruna J, Hirte H, Weller M, Palti Y, Hegi ME, Ram Z. Effect of Tumor-Treating Fields Plus Maintenance Temozolomide vs Maintenance Temozolomide Alone on Survival in Patients With Glioblastoma: A Randomized Clinical Trial. JAMA. 2017 Dec 19; 318(23):2306-2316.

Talukdar S, Emdad L, Das SK, Fisher PB. EGFR: An essential receptor tyrosine kinase-regulator of cancer stem cells. Adv Cancer Res. 2020; 147:161-188.

Tamura R, Tanaka T, Akasaki Y, Murayama Y, Yoshida K, Sasaki H. The role of vascular endothelial growth factor in the hypoxic and immunosuppressive tumor microenvironment: perspectives for therapeutic implications. Med Oncol. 2019 Nov 11; 37(1):2.

Tanaka K, Babic I, Nathanson D, Akhavan D, Guo D, Gini B, Dang J, Zhu S, Yang H, De Jesus J, Amzajerdi AN, Zhang Y, Dibble CC, Dan H, Rinkenbaugh A, Yong WH, Vinters HV, Gera JF, Cavenee WK, Cloughesy TF, Manning BD, Baldwin AS, Mischel PS. Oncogenic EGFR signaling activates an mTORC2-NF-κB pathway that promotes chemotherapy resistance. Cancer Discov. 2011 Nov;1(6):524-38.

Thorne AH, Zanca C, Furnari F. Epidermal growth factor receptor targeting and challenges in glioblastoma. Neuro Oncol. 2016 Jul; 18(7):914-8.

Tilak M, Holborn J, New LA, Lalonde J, Jones N. Receptor Tyrosine Kinase Signaling and Targeting in Glioblastoma Multiforme. Int J Mol Sci. 2021 Feb 12; 22(4):1831.

Tripolitsioti D, Kumar KS, Neve A, Migliavacca J, Capdeville C, Rushing EJ, Ma M, Kijima N, Sharma A, Pruschy M, McComb S, Taylor MD, Grotzer MA, Baumgartner M. MAP4K4 controlled integrin β1 activation and c-Met endocytosis are associated with invasive behavior of medulloblastoma cells. Oncotarget. 2018 May 1; 9(33):23220-23236.

van Tellingen O, Yetkin-Arik B, de Gooijer MC, Wesseling P, Wurdinger T, de Vries HE. Overcoming the blood-brain tumor barrier for effective glioblastoma treatment. Drug Resist Updat. 2015 Mar; 19:1-12.

Verhaak RG, Hoadley KA, Purdom E, Wang V, Qi Y, Wilkerson MD, Miller CR, Ding L, Golub T, Mesirov JP, Alexe G, Lawrence M, O'Kelly M, Tamayo P, Weir BA, Gabriel S, Winckler W, Gupta S, Jakkula L, Feiler HS, Hodgson JG, James CD, Sarkaria JN, Brennan C, Kahn A, Spellman PT, Wilson RK, Speed TP, Gray JW, Meyerson M, Getz G, Perou CM, Hayes DN; Cancer Genome Atlas Research Network. Integrated genomic analysis identifies clinically relevant subtypes of glioblastoma characterized by abnormalities in PDGFRA, IDH1, EGFR, and NF1. Cancer Cell. 2010 Jan 19; 17(1):98-110.

Wang Q, Hu B, Hu X, Kim H, Squatrito M, Scarpace L, deCarvalho AC, Lyu S, Li P, Li Y, Barthel F, Cho HJ, Lin YH, Satani N, Martinez-Ledesma E, Zheng S, Chang E, Sauvé CG, Olar A, Lan ZD, Finocchiaro G, Phillips JJ, Berger MS, Gabrusiewicz KR, Wang G, Eskilsson E, Hu J, Mikkelsen T, DePinho RA, Muller F, Heimberger AB, Sulman EP, Nam DH, Verhaak RGW. Tumor Evolution of Glioma-Intrinsic Gene Expression Subtypes Associates with Immunological Changes in the Microenvironment. Cancer Cell. 2017 Jul 10; 32(1):42-56.e6.

Warta R, Herold-Mende C. Helping EGFR inhibition to block cancer. Nat Neurosci. 2017 Jul 26; 20(8):1035-1037.

Weller M, van den Bent M, Preusser M, Le Rhun E, Tonn JC, Minniti G, Bendszus M, Balana C, Chinot O, Dirven L, French P, Hegi ME, Jakola AS, Platten M, Roth P, Rudà R, Short S, Smits M, Taphoorn MJB, von Deimling A, Westphal M, Soffietti R, Reifenberger G, Wick W. EANO guidelines on the diagnosis and treatment of diffuse gliomas of adulthood. Nat Rev Clin Oncol. 2021 Mar; 18(3):170-186.

Westphal M, Maire CL, Lamszus K. EGFR as a Target for Glioblastoma Treatment: An Unfulfilled Promise. CNS Drugs. 2017 Sep; 31(9):723-735.

Woo HY, Na K, Yoo J, Chang JH, Park YN, Shim HS, Kim SH. Glioblastomas harboring gene fusions detected by next-generation sequencing. Brain Tumor Pathol. 2020 Oct; 37(4):136-144.

Xu H, Czerwinski P, Hortmann M, Sohn HY, Förstermann U, Li H. Protein kinase C alpha promotes angiogenic activity of human endothelial cells via induction of vascular endothelial growth factor. Cardiovasc Res. 2008 May 1; 78(2):349-55.

Yi M, Jiao D, Qin S, Chu Q, Wu K, Li A. Synergistic effect of immune checkpoint blockade and anti-angiogenesis in cancer treatment. Mol Cancer. 2019 Mar 30; 18(1):60.

Zaman N, Dass SS, DU Parcq P, Macmahon S, Gallagher L, Thompson L, Khorashad JS, LimbÄck-Stanic C. The KDR (VEGFR-2) Genetic Polymorphism Q472H and c-KIT Polymorphism M541L Are Associated With More Aggressive Behaviour in Astrocytic Gliomas. Cancer Genomics Proteomics. 2020 Nov-Dec; 17(6):715-727.

Zepecki JP, Snyder KM, Moreno MM, Fajardo E, Fiser A, Ness J, Sarkar A, Toms SA, Tapinos N. Regulation of human glioma cell migration, tumor growth, and stemness gene expression using a Lck targeted inhibitor. Oncogene. 2019 Mar; 38(10):1734-1750.

Zhu VW, Klempner SJ, Ou SI. Receptor Tyrosine Kinase Fusions as an Actionable Resistance Mechanism to EGFR TKIs in EGFR-Mutant Non-Small-Cell Lung Cancer. Trends Cancer. 2019 Nov; 5(11):677-692.